Phosphorus and nitrogen dynamics in urban waters: examining nutrient inputs to watersheds and sediment transformations in diverse lentic ecosystems

A DISSERTATION
SUBMITTED TO THE FACULTY OF THE
UNIVERSITY OF MINNESOTA
BY

Erin M. Mittag

IN PARTIAL FULLFILLMENT OF THE REQUIREMENTS
FOR THE DEGREE OF DOCTOR OF PHILOSOPHY

Dr. Jacques C. Finlay
Dr. Sarah E. Hobbie

December 2024

Acknowledgements

My graduate experience has given me a visceral appreciation of the value of ecological data. Every data point in this dissertation (plus many others that did not fit into the stories presented here) is the product of numerous people's expertise, time, labor, and resources. I am grateful to all who contributed to each project and thank them for making this work possible.

Chapter 2: This research followed from preliminary work by Paliza Shrestha and prior work led by Vini Taguchi. Kathryn Hoffman was instrumental in method development, data collection, and sample analyses with additional support from Grace Neumiller, Poornima Natarajan, Martin du Saire, Mary Marek-Spartz, Anita Krause, and Katie Polik. Additional data were provided by the Washington County Conservation District, Rice Creek Watershed District, and the City of Eagan.

Chapter 3: This research was conducted in collaboration with Sarah (Winnie) Winikoff and Katie Polik. Kathryn Hoffman, Grace Neumiller, Martin du Saire, Mary Marek-Spartz, and Jessie Koehle contributed to data collection or sample analyses.

Chapter 4: This research was conducted in collaboration with Ben Janke, Paula Kalinosky, Rachel King, Larry Baker, Tessa Belo, Christopher Buyarski, Ross Bintner, and Mary Marek-Spartz. We partnered with the cities of Prior Lake, Forest Lake, Minneapolis, and Roseville, Minnesota, to collect street sweeping data. We compiled stormwater data from the Capitol Region Watershed District, South Washington Watershed District, City of St. Paul, and City of Plymouth, and we are grateful to those who collect, compile, and make these data available.

Each project also relied on numerous undergraduate students who were indispensable for sample and data collection. Their perseverance, care, and curiosity—especially when conducting challenging field and laboratory work—made the research not only possible but also joyful. I want to especially thank Tejiri Agbamu, Shray Boyalla, Fish Fischer, Jackson Fuqua, Claire Jaeger Mountain, Kirsten Semmer, and Makenna Tosi.

I am additionally grateful for the funding and support provided by the University of Minnesota Department of Ecology, Evolution and Behavior (EEB), the Moos Graduate Research

Fellowship in Aquatic Biology, and the St. Anthony Falls Laboratory Silberman Fellowship. I would also like to acknowledge my employers and colleagues in the Biology Teaching and Learning Department as well as the Center for Writing for their support of my graduate work as well as my pursuit of professional development outside of ecological research.

When I began graduate school, I anticipated the rigorous and compelling academic work. What I did not fully grasp, however, was how deeply personal and, in many ways, transformative my graduate experience would become. I am immensely grateful for the community that helped prepare me for this journey and those who have supported me over the past eight years.

First, thank you to my graduate advisors, Jacques Finlay and Sarah Hobbie. I benefitted immensely from your individual expertise and efforts, and I am grateful to both of you for your thoughtful guidance, respect of student autonomy, kindness, and patience. I am very fortunate to have had the opportunity to work with and learn from you.

Thank you to the other members of my committee, Chip Small and Jim Cotner, for your support and contributions to this work. Your frank engagement and genuine curiosity were instructive and energizing. I look forward to continuing those conversations.

Thank you to those who helped me with the logistical heft of graduate school and dissertation research: Shelly Rorer, Lisa Wiggins, Kate Berry, Neal Jahren, and Kathryn Hoffman. Your friendly reminders and patience were always appreciated, especially when I forgot about that form, email, and/or task (again, apologies).

I also want to thank the educators and mentors who helped lay the foundation for my graduate work. This includes many of my teachers in the Austin, Minnesota, Public School District, especially Nancy Jones and Kimberly Vesterby. This also includes my professors at St Olaf College, particularly my academic advisor, Charles Umbanhowar Jr., as well as Mike Swift, John Schade, David Booth, and James Farrell. My experiences at the St Croix Watershed Research Station (SCWRS) were invaluable in expanding my understanding of lakes, biogeochemistry, and research while also demonstrating that great science should be fun. I am thankful to everyone at SCWRS but especially Joy Ramstack-Hobbs and Jill Coleman-Wasik for their mentorship during particularly formative years.

My experience as a graduate student was immeasurably enriched by the EEB, Finlay lab, and Hobbie lab communities. I am particularly grateful to the past and present EEB folks who

have worked toward making EEB a productive, supportive, and inclusive department. I want to thank and recognize my 2016 graduate student cohort for grappling with some stark realities and unexpected challenges while continuing to conduct amazing research and being truly wonderful people. To the Finlay and Hobbie labs, I have benefited from your thoughtful engagement with my work as well as the opportunity to learn from and support your science. It has been a privilege to work with you all. I especially want to thank Ben Janke, his expansive knowledge of stormwater, and his trusty truck. I also want to thank Winnie Winikoff, who teaches me something every time we talk and has been an essential thought partner, collaborator, and friend. Finally, I want to recognize Adrienne Keller, who has a knack for inviting herself onto people's paddleboards and then becoming an indispensable and admired source of support and guidance.

I am profoundly grateful for the people who, in both big and small ways, helped me navigate my graduate experience and still feel like me. A full list of those people would be too long and peculiar to include here. However, if you were one of the people who fed me, shared a coffee or gin with me, sorted my mail, reached out first, planned a trip for us, gave me a nickname, invited me to talk and listened with curiosity, learned and expanded my language, offered me purpose, trusted me, indulged in distractions, laughed with me, or walked with me, know that I am deeply grateful for you. Thank you.

Finally, I feel incredibly fortunate to have been able to conduct my dissertation research in my home of Minnesota. First, I was grateful to frequently connect with the landscapes, waters, and people who feel like family. I thank those places that have shaped me—the Cedar River watershed, the oak savannas, the flat fields, the St Croix River, and the city lakes—as well as my wonderful family, friends, and community for much-needed inspiration, perspective, and grounding. Second, I feel privileged to have had the opportunity to deepen my understanding of the place where I am rooted. Not only was I able to explore the ecology of this region's waters, but I also worked to better understand who stewards them, depends on them, does or does not have access to them, knows them, and loves them. Minnesota's waters carry a complex history and hold profound significance for many communities, especially the Dakota people, for whom this region—Mni Sota Makoce—is both the ancestral and contemporary homeland. In working to better understand the meaning of this place, I found the resources and engagement opportunities provided by the Minneapolis-St Paul Long Term Ecological Research Site's

community engagement team, Yo Mama's House, Inc. (https://www.yomamashouse.com), the Bdote memory map (https://bdotememorymap.org), and the Learning from Place: Bdote workshop (https://www.mnhum.org/program/learning-from-place-bdote) to be especially enlightening. I thank the people who created and continue to support such transformative opportunities. Even after 35 years of living and learning in Minnesota, I feel that I am only just starting to know it. I look forward to further deepening my understanding of, relationship with, and service to this place, its waters, and its people.

Abstract

Urbanization substantially alters the distribution and cycling of phosphorus (P) and nitrogen (N), with widespread consequences for aquatic ecosystems and the communities that rely on them. Cities concentrate human activities that generate an excess of P and N, which are then transported via impervious surfaces and stormwater networks to local surface waters. Such excess nutrient loading degrades water quality and contributes to eutrophication in local and downstream ecosystems. This dissertation focuses on three key processes that drive nutrient availability in urban aquatic ecosystems: sediment P mineralization and denitrification in stormwater ponds and shallow lakes, and nutrient inputs to stormwater from urban tree litterfall in the Minneapolis-St Paul metropolitan region. First, I use sediment incubations to demonstrate that the mineralization of organic P, an under-examined process in aquatic research, can be an important mechanism mobilizing bioavailable P from organic-rich sediments common in urban lentic systems. Furthermore, increasing temperatures exacerbated sediment P release, suggesting that warming may further destabilize sediment P. Second, I explored denitrification across diverse urban lentic sites and found reduced denitrification rates in sites with exceptionally high road salt inputs and high concentrations of total P. Road salt salinization drastically alters water column mixing, while high total P is associated with the loss of macrophytes. Both of these factors may reduce N removal capabilities by limiting the availability of reactants for denitrifiers. These findings underscore the differing drivers of urban P and N cycling, which challenge our ability to mitigate the effects of both. To that end, the final component of my research focuses on a possible shared point of management for P and N: litterfall from street trees. Using datasets to estimate nutrient inputs from street tree litterfall at the watershed scale derived from intensive street sweeping, I found that litterfall inputs frequently comprise a substantial fraction of total watershed nutrient exports, especially during the fall and spring and in watersheds with high street canopy cover. Efforts aimed at removing street tree litterfall may therefore meaningfully reduce nutrient loading to urban waters. Taken together, this body of work demonstrates that cities pose unique challenges but also opportunities for maintaining the integrity of surface waters. In an increasingly urban world, continuing to develop our understanding of the dynamic relationships between urbanized landscapes and their waters is essential for maintaining the integrity of surface waters at local and global scales.

Table of Contents

List of Tables

List of Figures

Chapter 1: Introduction

The rapid expansion of cities and their populations makes the study of urban waters critically important. The prevalence of urban waters is increasing as catchments and shorelines are newly or more intensively urbanized. Additional urban waters are created as novel water bodies are constructed for functional or aesthetic purposes (Larson & Grimm, 2012). The fraction of the global population living in cities and relying on urban surface waters is expected to reach 75% by 2050 (Baeumler et al., 2021). Urban surface waters provide essential services like drinking water, food, water retention and flood mitigation, filtration, climate buffering, transportation, recreation, community, and cultural and spiritual meaning. Similarly, urban waters provide critical habitat for the organisms that increasingly live in or interact with cities (Everard & Moggridge, 2012; Grimm et al., 2008). As urbanization heightens the importance of urban surface waters, it also intensifies the threats they face.

Urban surface waters aggregate materials from and reflect conditions in their watersheds, resulting in novel combinations of stressors. They receive pollutants such as coarse particulates, heavy metals, hydrocarbons, pesticides, and road salt (Everard & Moggridge, 2012; Grimm et al., 2008; Novotny et al., 2008). Additionally, they experience higher temperatures compared to their nonurban analogs due to effects of the urban heat island and their connections to high heat capacity infrastructure (Grimm et al., 2008; Kaushal et al., 2010).

One of the most potent threats faced by urban surface waters is eutrophication, driven by excess P and N. Eutrophication is associated with high algal production, an increased risk of toxic algal blooms, persistent bottom water anoxia, fish kills, reduced reliability of drinking water supplies, and overall diminished water quality (Ansari & Gill, 2014). Phosphorus and N enter and move through cities in intersecting yet distinct ways, shaped by each nutrient's inherent properties as well as the urban environment. Broadly, inputs of P and N to cities are linked to fertilizer application, fossil fuel combustion, deposition, and pet waste (Hobbie et al., 2017). A substantial fraction of incoming nutrients are transported with stormwater over impervious surfaces and through extensive drainage networks to receiving surface waters (Hobbie et al., 2017). As a result, surface waters aggregate nutrients from the urban landscape, making surface waters particularly vulnerable to eutrophication while also being important sites of nutrient processing.

Over the last several decades, the study of how cities alter aquatic nutrient cycles has intensified, but our understanding of these concepts is still emerging. Of particular interest is understanding the determinants of P and N availability in urban waters, including the internal processes that remove bioavailable nutrients and mitigate their effects locally and downstream. My dissertation research focuses on nutrient cycles in urban lentic ecosystems—lakes and stormwater ponds—in the Minneapolis-St Paul metropolitan region in east-central Minnesota, USA. Located in the upper Mississippi River basin, this region is water-rich with over 1,000 lakes and 13,000 ponds.

My dissertation research explores three key topics relevant to lentic ecosystem P and N availability and cycling: 1) the role of biological mineralization in mobilizing sediment P across a range of sediment characteristics and in the context of warming, 2) the factors contributing to variation in denitrification rates and efficiencies in sediments across a diversity of urban lentic systems, with a particular focus on capturing the effects of road salt salinization for N removal, and 3) quantifying nutrient inputs from street tree litterfall at the watershed scale to investigate their contributions to and relationships with stormwater P and N. The findings presented here contribute to our understanding of lentic ecosystem nutrient cycling in cities and beyond, highlight critical research needs, and identify opportunities for effective nutrient management.

Works Cited

Ansari, A. A., & Gill, S. S. (Eds.). (2014). *Eutrophication: Causes, Consequences and Control: Volume 2*. Springer Netherlands. https://doi.org/10.1007/978-94-007-7814-6

Baeumler, A., D'Aoust, O., Das, M.B., Gapihan, A., Goga, S., Lakovits, C., Restrepo Cavadid, P., Singh, G., Terraza, H. (2021). *Demographic Trends and Urbanization*. Washington, DC: World Bank. doi:10.1596/978-1-4648-1112-9

Everard, M., & Moggridge, H. L. (2012). Rediscovering the value of urban rivers. *Urban Ecosystems*, *15*(2), 293–314. https://doi.org/10.1007/s11252-011-0174-7

Grimm, N. B., Faeth, S. H., Golubiewski, N. E., Redman, C. L., Wu, J., Bai, X., & Briggs, J. M. (2008). Global Change and the Ecology of Cities. *Science*, *756*. https://doi.org/10.1126/science.1150195

Hobbie, S. E., Finlay, J. C., Janke, B. D., Nidzgorski, D. A., Millet, D. B., & Baker, L. A. (2017). Contrasting nitrogen and phosphorus budgets in urban watersheds and implications for managing urban water pollution. *Proceedings of the National Academy of Sciences*, 1–6. https://doi.org/10.1073/pnas.1618536114

Kaushal, S. S., Likens, G. E., Jaworski, N. A., Pace, M. L., Sides, A. M., Seekell, D., Belt, K. T., Secor, D. H., & Wingate, R. L. (2010). Rising stream and river temperatures in the United States. *Frontiers in Ecology and the Environment*, *8*(9), 461–466. https://doi.org/10.1890/090037

Larson, E. K., & Grimm, N. B. (2012). Small-scale and extensive hydrogeomorphic modification and water redistribution in a desert city and implications for regional nitrogen removal. *Urban Ecosystems*, *15*(1), 71–85. https://doi.org/10.1007/s11252-011-0208-1

Novotny, E. V., Murphy, D., & Stefan, H. G. (2008). Increase of urban lake salinity by road deicing salt. *Science of the Total Environment*, *406*(1–2), 131–144. https://doi.org/10.1016/j.scitotenv.2008.07.037

Chapter 2: Sediment phosphorus release in organic-rich urban lentic ecosystems is linked to microbial metabolism and sensitive to warming

Summary

Sediment phosphorus (P) release hinders stormwater ponds' ability to store P and mitigate downstream eutrophication. Previous work identified that abiotic processes, such as those driven by redox conditions, may not account for all observed P mobilized from pond sediments. We focus on the role of microbially mediated P mineralization, aiming to understand how this understudied process connects to pond characteristics and conditions. Working in the Minneapolis-St. Paul, MN, USA Metropolitan Area, we used anoxic sediment slurry incubations to measure rates of P release, microbial respiration, and acid phosphatase (AP) activity across four temperature treatments (20, 25, 30, 35 C) in 20 stormwater ponds and 5 lakes representing a range of sediment properties hypothesized to influence biotic P mineralization. We found that high rates of P release were accompanied by high rates of microbial respiration and AP activity, all of which were positively related to incubation temperature and sediment organic matter—clear indications of biotic control of P mobilization. Our findings suggest that unmitigated warming in cities and their waterbodies may threaten the stability of sediment P, especially in the organic-rich sediments common in stormwater ponds.

Introduction

Background

Urban stormwater ponds are ubiquitous features in urban landscapes. Initially designed to slow and retain storm flows, these ponds were quickly recognized as potential hot-spots for ecological functions, including mitigating eutrophication of downstream surface waters by retaining phosphorus (P) carried in stormwater (Frost et al., 2019; Williams et al., 2013; Woodcock et al., 2010). Mass balance and monitoring studies confirmed stormwater ponds' potential to trap stormwater P, but considerable variation in whether and how much P ponds retain has motivated research into mechanisms and drivers of stormwater pond P retention (Clary et al., 2020).

Initial research on pond P retention focused on sedimentation of particulate P, a dominant form of P in stormwater and stormwater ponds, but the long-term fate of P in sediments is uncertain. Pond morphologies and flow paths that increase water residence times allow a greater fraction of particulate P to settle to sediments. However, sediment P in ponds, as in lakes, may not be permanently retained (Song et al., 2017; Taguchi et al., 2020). Release of previously deposited sedimentary P, or internal loading can reduce pond retention capacity (Bostrom et al., 1988; Orihel et al., 2017).

The dissolution of Fe-P complexes under anoxic conditions, an abiotic process well-documented in lakes, contributes to internal P loading from sediments in stormwater ponds (Søndergaard et al., 2003). Despite shallow depths, ponds can experience frequent and sustained periods of anoxia that trigger the release of redox-sensitive P (Song et al., 2017; Taguchi et al., 2020). Indeed, anoxia has been linked to higher dissolved water column P concentrations and reduced P retention in ponds. Further, intact sediment core experiments confirm that anoxic conditions promote P flux from stormwater pond sediments (Taguchi et al., 2020). However, there remains a large amount of unexplained variation in P release from sediments in field and laboratory studies, suggesting mechanisms other than Fe-P dissolution and drivers other than anoxia influence sediment P release (Taguchi et al., 2020).

Phosphorus mineralization—the microbially mediated conversion of organic-P into soluble inorganic-P—likely contributes to sediment P release in lentic ecosystems. Biotic P mineralization is frequently a direct result of biotic activity, facilitated by organisms that synthesize enzymes required to hydrolyze P from OM. It is logical, given high rates of microbial activity in sediments, that biotic P mineralization would contribute meaningfully to sediment P mobilization (Bostrom et al., 1988), and prior research supports this. For example, Qian et al. (2011) found that sterilizing sediments reduced rates of P release, and Song et al. (2017) found increases in water column total dissolved P were accompanied by increased phosphatase activity and rapid declines in sediment organic-P. Despite the potential importance of biotic P mineralization, it remains under-represented in the literature relative to other mechanisms of sediment P mobilization (Hupfer & Lewandowski, 2008). Studies that have centered on lentic sediment biotic P mineralization have predominantly been single-lake studies or spanned a narrow range of sediment properties (Li et al., 2018; Liu et al., 2023; Markovic et al., 2019;

Shinohara et al., 2017). Further, very few assessments have incorporated stormwater ponds (*but see* Song et al., 2017; Taguchi et al., 2020). As a result, uncertainties remain regarding the stability of sediment organic-P across site and sediment conditions and what that means for P retention in lentic ecosystems.

Our work addresses this gap by exploring sediment P mobilization alongside microbial and enzymatic activities across a range of sediment characteristics in urban freshwaters, focusing predominantly on stormwater ponds. Not only are ponds important sites of P cycling in urban environments, they are also highly variable in factors expected to influence microbial activity and biotic P mineralization—sediment organic matter (OM) properties and temperature—making them ideal systems for study. Our work does not attempt to directly disentangle abiotic and biotic mechanisms of sediment P release (Bostrom et al., 1988), instead we assess how P release and microbial activity respond to each other as well as temperature and sediment properties that are known to drive biotic activity.

Sediment properties as drivers of sediment P mobilization

Microbial metabolic activities rely on access to necessary substrates. Sediment organic matter (OM) provides electron donors and nutrients necessary for microbial respiration. Thus, sediments rich in OM likely will be able to support higher rates of sediment microbial respiration and sediment P release. Investigating the role of OM is particularly important in stormwater ponds. While pond sediments vary in OM content, with site age being an important determinant, they tend to be rich in OM. Relatedly, organic P forms (organic-P) dominate in stormwater influent, pond water columns, and pond sediments, suggesting that a large fraction of the total-P pool may be susceptible to liberation via biotic mineralization (Frost et al., 2019; Song et al., 2017; Taguchi et al., 2020). Taguchi et al. (2020) found labile organic-P content in sediments to be just as important a predictor of sediment P loss as redox-sensitive P.

It is not only the quantity but also the quality of OM that influences rates of biotic P mineralization: microbial activities respond to the degradability and elemental composition of sediment OM (Bastviken et al., 2003; Davidson & Janssens, 2006; Gudasz et al., 2012). Organic matter quality is expected to vary considerably in stormwater ponds given the diversity of OM sources (e.g., algal, macrophyte, terrestrial) and the degree of processing that OM undergoes prior to reaching sediments (related to site depth, retention time, and upstream conditions in the

stormwater network). Sediments of low quality for microbial decomposition, such as those with high C:N and C:P ratios might be expected to support lower microbial activity and biotic P mineralization rates.

Temperature as a driver of sediment P mobilization

Temperature is a primary regulator of microbial (Gudasz et al., 2012) and enzymatic activity (Shaw & Cleveland, 2020). The effects of temperature on sediment P mobilization are often studied or discussed in the context of redox-sensitive P: warming indirectly mobilizes P by increasing microbial activity and sediment oxygen demand, inducing anoxia in bottom waters and the rapid dissolution of sediment Fe-P (Søndergaard et al., 2003). However, by facilitating higher rates of respiration and enzymatic activities, warming can directly increase sediment P release via biotic mineralization (Jensen & Andersen, 1992; Zhang et al., 2015). Warming's effects on biotic mineralization may be particularly pronounced when sediment OM properties support higher microbial metabolism (Zhang et al., 2015).

The effects of elevated temperatures are increasingly relevant as global climate change and urban heat island effects warm cities and their ecosystems (Grimm et al., 2008). Stormwater ponds are particularly susceptible to experiencing elevated temperatures due to shallow depths, high turbidity, and connections to paved stormwater infrastructure with a high heat capacity (Hester & Bauman, 2013). Therefore, there is a pressing need to better understand the implications of warming for the stability of sediment P in urban lentic ecosystems.

Research on the role of sedimentation and redox-sensitive sediment P has yielded key insights into pond P retention, but has largely ignored the role of biotically mediated mineralization despite suggestions that it may be important. We used anoxic sediment slurry incubations to determine the influence of sediment characteristics (OM content and C:nutrient stoichiometry) and temperature on biotic P mineralization, with a goal of refining our understanding of the mechanisms and drivers of sediment P mobilization. We tested the following hypotheses:

1) If sediment P release is from biotic mineralization, we expected that P release rates would correlate with microbial respiration and AP activity.

2) We expected that sediments with high OM content would support higher rates of microbial respiration and AP activity. If P release is from biotic mineralization, we also expect OM rich sediments to have higher rates of P release.
3) We expected that sediments with higher C:N or C:P ratios, indicating more recalcitrant OM, would have lower microbial and enzyme activity, as well as lower P release rates should biotic mineralization be important. We also expected that OM quality would mediate the effects of OM quantity by weakening the effects of OM content in sediments with higher C:N or C:P ratios.
4) If sediment P release is from biotic mineralization, we expected that P release rates would respond positively to increased incubation temperatures. We further expected that warming would mediate the effects of sediment properties on biotic P mineralization by increasing microbial metabolism and demand for substrates and strengthening the influence of OM quantities or qualities on P release rates.

Methods

Study sites

We selected study sites to capture a gradient of sediment properties, especially sediment organic matter quantity and quality. Our study sites consisted of 19 ponds with permanent standing pools and 5 lakes. Lakes were included in an attempt to extend gradients in sediment organic matter, phosphorus, and redox characteristics. Ponds include natural and constructed stormwater ponds as well as two smaller, lentic water bodies (Almq and BrOk). All sites were located in the Minneapolis-St. Paul, MN, USA Metropolitan Area (Figure 2.1). For each site, we compiled attributes related to site morphology. All site attributes were directly measured or estimated from satellite imagery and are summarized in Table 2.1 (site-specific attributes are included in Table S2.1). Site anoxic factor is an indicator of sediment oxygen exposure. Calculated from site bathymetry and water column oxygen profiles following Janke et al. (2022), it represents the fractional number of days per year where sediments are overlaid by anoxic water (dissolved oxygen < 2 mg/L). When data were available, all dissolved oxygen profiles from June - August were used in calculating the anoxic factor for a more integrated assessment of a site's oxygen

regime. Statistical analyses that included anoxic factor were conducted separately for all sites and for only those sites with extensive monitoring (>2 years of monitoring).

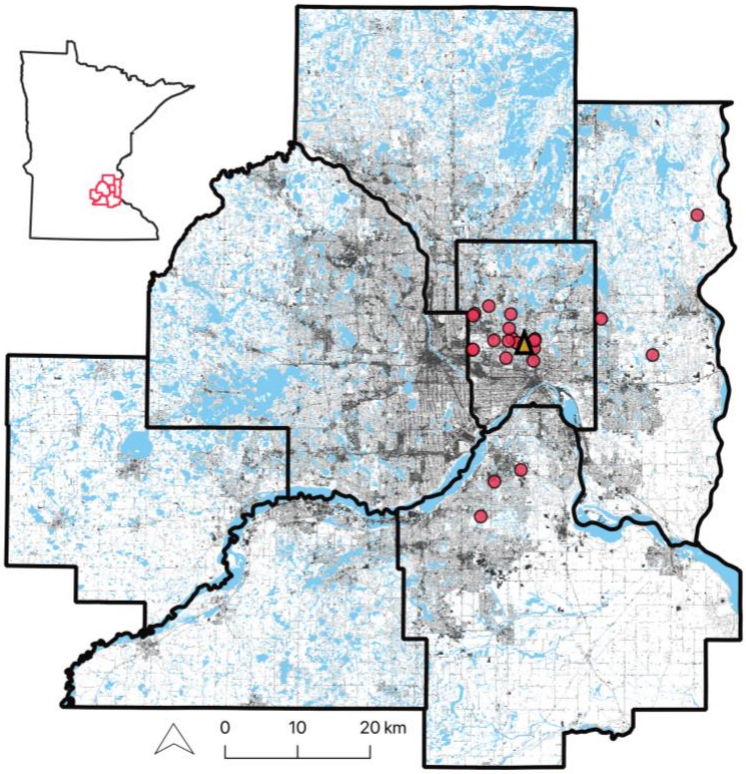

Figure 2.1. Location of study sites
Study sites (points) were located within the Minneapolis-St. Paul metropolitan region, Minnesota, USA. The triangle indicates Lake McCarrons, the source of common water used in sediment phosphorus release incubations.

Sample collection, preparation, and analysis

Sampling events were primarily June – August of 2021 and 2022. Two sampling dates occurred in September 2022 (Table 2.1). At each sampling event, we collected sediment samples, surface water grab samples, and hypolimnion water samples when sites were stratified using a Kemmerer water sampler. We also collected profiles of water temperature, dissolved oxygen, and specific conductance using a Hach portable meter, conductivity cell, and dissolved oxygen sensor.

Table 2.1. Summary of study site physical attributes and key sediment properties.

	Site properties					Sediment properties			
	Size (ac)	Max depth (ft)	Site DO (mg/L)	Site temp (C)	Anoxic factor	OM %	C:N	C:P	Total-P (ug/L)
Mean	36.0	17.1	1.7	19.6	0.3	18	20	187	1397
Median	0.42	5.7	0.1	21.1	0.2	17	18	157	1092
St. Dev	75.5	30.9	3.6	6.0	0.3	11	8	114	1214
Minimum	0.02	0.8	0.0	5.6	0.0	1	10	17	435
Maximum	256.82	140.0	13.4	29.8	1.0	50	47	471	6182

Summary includes lakes and ponds.
DO = bottom water dissolved oxygen at the time of sampling; Site temp = bottom water temperature at the time of sampling; OM = organic matter; C = carbon; N = nitrogen; P = phosphorus; Anoxic factor = index from 0 – 1 with high values indicating more frequent sediment anoxia.

Sediments for P release incubations were collected via an Eckman dredge from the deepest portion of each site. For sites too shallow to dredge or sampled by study partners, a plastic tube (diameter 6 cm) was pressed into the sediment to collect a small sediment core. For both methods, care was taken to save only the surface sediments up to 5 cm. Multiple sediment samples were homogenized (>3 subsamples) to ensure sufficient material for incubations and analyses. Sediments were stored in plastic bags without oxygen, in the dark, and at 4 C. Loss on ignition analyses, used to identify sediment organic matter content, were started on wet sediments within 48 hours (Heiri et al., 2001). At the same time, a sediment subsample was frozen for subsequent assessment of acid phosphatase enzyme activity and another subsample was oven dried at 60 C overnight. Dried sediments were ground and homogenized for analysis of sediment total C and N content, total P, and P fractions. Sediment C and N content were measured using a Costech ECS 4010 CHNSO Elemental Analyzer (Costech Analytical Technologies Inc). These values, along with sediment total P, were used to calculate molar C:N, C:P, and N:P.

Sediment total P and P fractions were extracted from dried sediments following a method adapted from Psenner (1988) and Engstrom (2005). Total P was extracted with H_2O_2 and HCl and treated with sodium metabisulfite before being analyzed for soluble reactive P (SRP) using molybdate colorimetry. For P fractions, serial digestions were used to extract loosely-bound and $CaCO_3$-P (“exchangeable-P”, NH_4Cl extraction), Fe-P ($NaHCO_3$ and $Na_2S_2O_4$ extraction), Al-P (NaOH extraction), and mineral-P (HCl extraction). Labile organic-P was extracted from the Al-

P fraction using $K_2S_2O_8$ (Engstrom, 2005; Psenner 1988). Extracts were analyzed for soluble reactive P (SRP) using molybdate colorimetry. Residual organic-P was calculated as the difference between total P and the sum of all other fractions. Total organic-P is the sum of the labile and residual organic-P fractions. Redox-P is the sum of exchangeable-P and Fe-P.

Water samples were filtered within 24 hours through a pre-ashed 0.45 µm pore-size filter and analyzed for SRP, total dissolved P (TDP), dissolved organic C (DOC), and total dissolved N (TDN). SRP and TDP were analyzed using molybdate colorimetry. DOC and TDN samples were acidified and measured on a Shimadzu TOC-L analyzer equipped with a chemiluminescence detector (TNM-L unit, Shimadzu Corporation).

Sediment P release incubations

Sediment slurry incubations were used to measure the rate of P release and microbial respiration. Incubations were started within 48 hours of sediment collection. Twenty grams of sediment and 120 mL of filtered common water were added to 125 mL glass Wheaton media bottles. We ensured incubated sediments were representative of the collected sample by frequently homogenizing the sediment sample and avoiding anomalous coarse organic material. Sediments were incubated with common water rather than site water to control for differences in starting water chemistry. Common water was collected from near-shore of Lake McCarrons, St. Paul, MN (Figure 2.1), which is known to have low SRP water concentrations. Lake McCarrons water was filtered in the field through a 0.45 µm filter, stored in the dark at 4 C, and used within one week of collection. A subsample of common water was analyzed for SRP, confirming background SRP concentrations were below detection for all incubations.

Incubation bottles were tightly sealed with caps fitted with butyl septa, vigorously shaken, and purged of oxygen by flushing with helium or N_2 gas (used when helium was unavailable). This marked the starting time for each bottle. Establishing anoxia at the onset mimicked site conditions and limited variation due to differences in microbial oxygen consumption. Incubation bottles were kept in the dark until destructively sampled at 2, 24, 48, and 72 hours. An additional 120 hour time point was added for sites with especially low sediment organic matter content (SemNw and PnOak) to account for potentially lower reaction rates. Bottles destructively sampled at 2 hours were incubated at 20 C. We applied a temperature treatment to all other time points, incubating bottles at either 20, 25, 30, or 35 C. Each time point

and temperature had three bottle replicates. The 25 C temperature treatment was dropped for sites with insufficient sediment (Almq, BrOk, PnOak, ResCircW, TRckN). Statistical analyses were performed with and without the 25 C treatment, and missing observations did not meaningfully affect findings.

To sample sediment incubations, bottles were first vigorously shaken to equilibrate the headspace with the sediment slurry. Headspace gas samples were collected through the septa and stored in crimped and evacuated Agilent gas vials. Gas samples were analyzed on a gas chromatograph for O_2, CO_2 and CH_4. Any incubation bottles with headspace O_2 greater than 5%, which may reflect a compromised incubation seal, were omitted from the data. Incubation water was allowed to settle for at most one hour before decanting into centrifuge tubes and centrifuging at 4000 RMP. The supernatant was filtered through a 0.45 µm filter and stored frozen until samples were analyzed for SRP using molybdate colorimetry.

To calculate rates of P release and microbial respiration, we ultimately used only the final (72 or, when available, 120 hour) time point for each site, as SRP concentrations in bottles sampled at earlier times were often below the detection limit. The few SRP concentrations below detection at the final time point were replaced with half the detection limit for rate calculations. Rates of P release and microbial respiration were calculated for each bottle as the mass of P (µg/gram dry sediment) or the sum of CO_2-C and CH_4-C (µg/gram dry sediment) divided by the sampling time for each (hours), respectively. Bottle replicates were averaged to produce final estimates of P release rates (P-rate) and microbial respiration rate (Resp-rate).

Acid phosphatase enzyme activity assays

We performed acid phosphatase (AP) enzyme fluorimetric assays on thawed wet sediments following a microplate method outlined in Marx et al. (2001). Sediments were amended with 4-Methylumbelliferyl Phosphate substrates and buffered to pH 6.8, similar to the pH measured in sediment incubations. To correspond with sediment incubations, we applied a temperature treatment (20, 25, 30, and 35 C) to enzyme assays. We incubated one microplate, containing eight replicate sample wells, at each temperature treatment for each study site. Each microplate was incubated at the assigned temperature for two hours and then read at 365 nm excitation and 450 nm emission on a microplate reader. Only sites sampled in 2022 were

analyzed for AP activity. The addition of substrates means AP activity represents potential activity under conditions when substrates are readily available.

Calculating temperature sensitivity

How P-rate, Resp-rate, and AP activity responded to incubation temperature varied across sites, appearing linear in some instances and exponential in others. We fit regression models to untransformed and log-transformed rates to assess linear and exponential relationships with temperature, comparing model fits using coefficients of determination. For P-rate, we fit these models to untransformed and log-transformed rates using Akritas–Theil–Sen nonparametric regression (Helsel & Helsel, 2012; Julian & Helsel, 2023). This method allowed for a more accurate incorporation of below detection values and is applicable to small datasets (Helsel & Helsel, 2012). This method produces a slope, intercept, measures of model fit (Kendall's tau), and tests of significance. Regression slopes from linear model fits were used as expressions of linear temperature sensitivity. Regression slopes from exponential model fits were used to calculate *Q10* temperature sensitivity for P-rate, Resp-rate, and AP activity at each site following van 't Hoff:

$$Q_{10} = e^{\beta \times 10} \qquad \text{eq. 1}$$

where *Q10* is the temperature sensitivity, e is Euler's number, and β is the slope from the exponential model relating rate to incubation temperature (Davidson & Janssens, 2006).

Statistical analyses

We used bivariate (BV) mixed-effects regression analyses to assess relationships between P-rate, Resp-rate, and AP activity, pooling all temperature treatments and including site as a random intercept to account for non-independence of observations (Pinheiro et al., 2021). We also included an incubation temperature interaction term to assess whether temperature mediates relationships between measured processes.

We used multivariate (MV) mixed-effects regression and the nlme R package to identify proximate drivers of P-rate, Resp-rate, and AP activity (Pinheiro et al., 2021). All three response variables were log-transformed to meet model assumptions, and all models included site as a random intercept. Incubation temperature was included as a main effect and in interactions with sediment properties. Candidate predictors were sediment and site properties hypothesized to be

important or those that emerged as important in BV regression (results not shown). If two candidate predictors were highly correlated (Pearson's correlation coefficient > 0.7), we chose the predictor more strongly correlated with the response variable in BV regressions or the variable that was collinear with the fewest other predictors. Candidate variables that were considered but omitted were sediment total-P, total organic-P, residual organic-P, C content, and N content, as well as P fractions expressed as percent of total-P. To assess whether the effects of individual predictors differed with warming, we included interactive terms between sediment properties and incubation temperature. Main effects included as continuous variables in the initial full model were: incubation temperature, sediment %OM, C:N, C:P, labile organic-P, redox-P, anoxic factor, and site dissolved oxygen concentration, with interactions between incubation temperature and all main effects.

We used two methods to identify optimum models for each response variable: manual backwards selection following Zuur (2009) and Fieberg (2024) using maximum likelihood ratio tests and AICc to identify an optimum model, and 2) automatic model selection (Bartoń, 2022). Both methods arrived at the same set of significant predictors in the optimum model. We report the output from the automatic model selection here. Variables included in all final models had variance inflation factors below three.

Finally, we further tested relationships among site characteristics and temperature by relating site linear temperature sensitivity and *Q10* values to sediment properties using BV linear regression (R Core Team, 2021). As these were bivariate analyses, we could test all predictors of interest regardless of colinearity: sediment %OM, total organic-P, labile organic-P, redox-P, C:N ratio, and C:P ratio as well as site anoxic factor, dissolved oxygen concentration, and temperature at the time of sampling. For all statistical models, we checked assumptions and performed log-transformations of response and predictor variables to meet model assumptions. Unless otherwise noted, the threshold for significance was p-value < 0.05. All statistical analyses were performed in R (R Core Team, 2021).

Results

Sediment incubation findings

Most incubations measured at the final time point showed SRP accumulation in incubation water, indicating sediment P release. The average rate of sediment P release ranged from <0.01 to 0.14 µg/g/hour at 20C (mean 0.03; sd 0.04; Figure 2.2). Increasing incubation temperature significantly increased P-rate in 20 of 24 sites (Figure S2.1). At 35 C, P-rate ranged from <0.01 to 0.62 µg/g/hour (mean 0.13; sd 0.16). Of the four sites where temperature had no significant effect on P-rate, Alam and CentPark had lower (though not the lowest) P-rate across temperature treatments (< 0.02 µg/g/hr), TRckS had an inconsistent response to temperature, and SemOld had slightly higher rates with incidences of elevated P-rate at lower temperatures (Figures 2.2, S2.1). Of those that showed a significant effect of warming, temperature increased P-rate linearly in nine sites and exponentially in ten sites. The differences in goodness of fit between linear and exponential models were minimal (mean difference in adj-R^2 0.06). As a result, we use only the linear temperature response values for P. P temperature sensitivity values ranged from 0 - 37.4 ng P/g/hr/degree C.

The accumulation of gaseous CO_2 and CH_4 in incubation headspace indicated active microbial respiration in all incubations. Average respiration rates varied across sites and temperature treatments from 0.02 - 0.87 µg/g/hour at 20 C (mean 0.29; sd 0.2) to 0.07 - 5.4 µg/g/hour at 35 C (mean 1.1; sd 1.1). Increased incubation temperature significantly increased microbial respiration in all but one site (Almq), and all but two sites increased exponentially with temperature (Figure S2.2). Resp-rate *Q10* ranged from 1.2 - 3.5 (mean 2.4, sd 0.7).

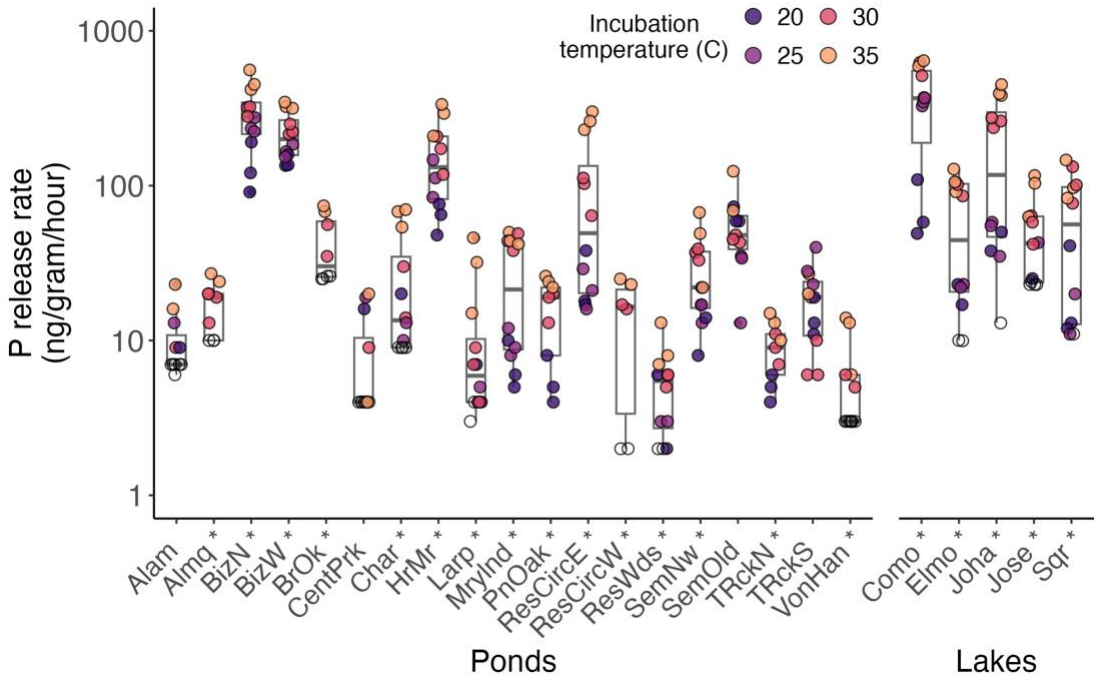

Figure 2.2. Phosphorus release rates under four temperature treatments in all study sites Rates of sediment phosphorus (P) release, measured as the accumulation of soluble reactive P in sediment incubations. All temperature treatments and bottle replicates are shown. Asterisks indicate sites where rates of P release were significantly higher with elevated incubation temperature. Open symbols indicate samples whose soluble reactive P concentrations were below instrument detection. Data are displayed on a log-10 scale.

Acid phosphatase activity measured 44.9 - 491.4 nmol/g/hour at 20 C (mean 173.3; sd 119.1) and 126.1 - 792.6 nmol/g/hour at 35 C (mean 372.1; sd 199.2). Warming significantly increased AP activity in all but one site (TRckN). Exponential relationships between AP activity and temperature out performed linear relationships in only three sites with many sites showing a dip in AP activity from 20 C to 25 C (Figure S2.3). The differences in goodness of fit between linear and exponential models were minimal (mean difference in adj-R^2 0.08). As a result, we use only the linear temperature response values for AP, which ranged from 3 - 26 nmols/g/hr/degree C.

Sediment P release rates had significant positive relationships with microbial respiration (marg-R^2 0.34; figure 2.3a) and AP activity (marg-R^2 0.58 ; figure 2.3b). Resp-rate and AP activity were also positively correlated (marg-R^2 0.38 ; figure 2.3c). None of these relationships were mediated by warming, as temperature interaction terms were not significant (results not

shown). There were also no relationships between temperature sensitivity estimates of P-rate, Resp-rate, and AP activity (results not shown).

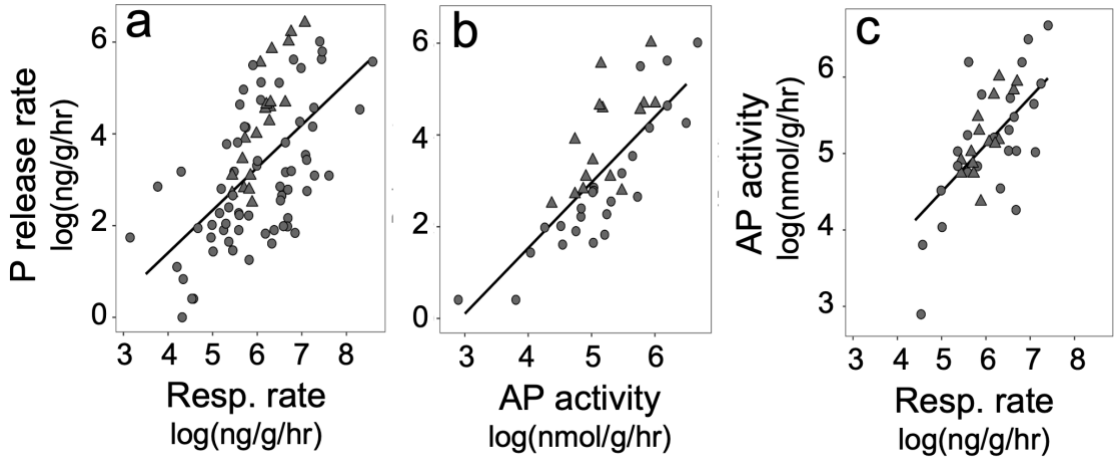

Figure 2.3. Relationships between measured sediment processes
Sediment phosphorus (P) release rate vs. a) microbial respiration rate ("Resp. rate"; marginal R^2 = 0.34; conditional R^2 = 0.83) and b) acid phosphatase (AP) enzyme activity (marginal R^2 = 0.58; conditional R^2 = 0.85). c) AP activity vs. Resp. rate (marginal R^2 = 0.38; conditional R^2 = 0.65). Each point represents the average of incubation replicates. Circles indicate study sites designated as ponds, triangles indicate lakes. Models include all temperature treatments and "site" as a random intercept. All slopes were significantly different from zero (p-value < 0.05).

Sediment properties

Study sites represented a gradient of sediment organic matter quantity (~1 – 50%), molar carbon:nitrogen (C:N 10 – 47), carbon:phosphorus (C:P 17 – 471), and sediment total-P (~ 435 – 6180 mg/kg). There was considerable variation in sediment P fractions (Figure 2.4), with the total organic-P pool comprising between 22 - 62% (mean 50%; sd 10%). Labile organic-P tended to comprise a smaller fraction of total-P (range ~0 - 26%, mean 7%, sd 8%) compared to residual organic-P (range 14 - 62%, mean 40%, sd 14%). Redox-P, composed almost entirely of Fe-P, ranged from 7 - 41% of total-P (mean 15%, sd 7%). The exchangeable-P fraction was less than 7% of total-P (mean 1.5%) in all sites.

Lakes were included to aid in broadening the ranges of sediment properties, but there were few significant differences in measured sediment properties between ponds and lakes. Ponds contained significantly greater fractions of mineral-P and smaller fractions of residual organic-P relative to lakes (t-test; p-value < 0.05; Figure 2.4). Sediment C:N was slightly higher in ponds compared to lakes (t-test, p-value < 0.1) due, in part, to significantly lower N content in pond sediments (t-test, p-value < 0.05).

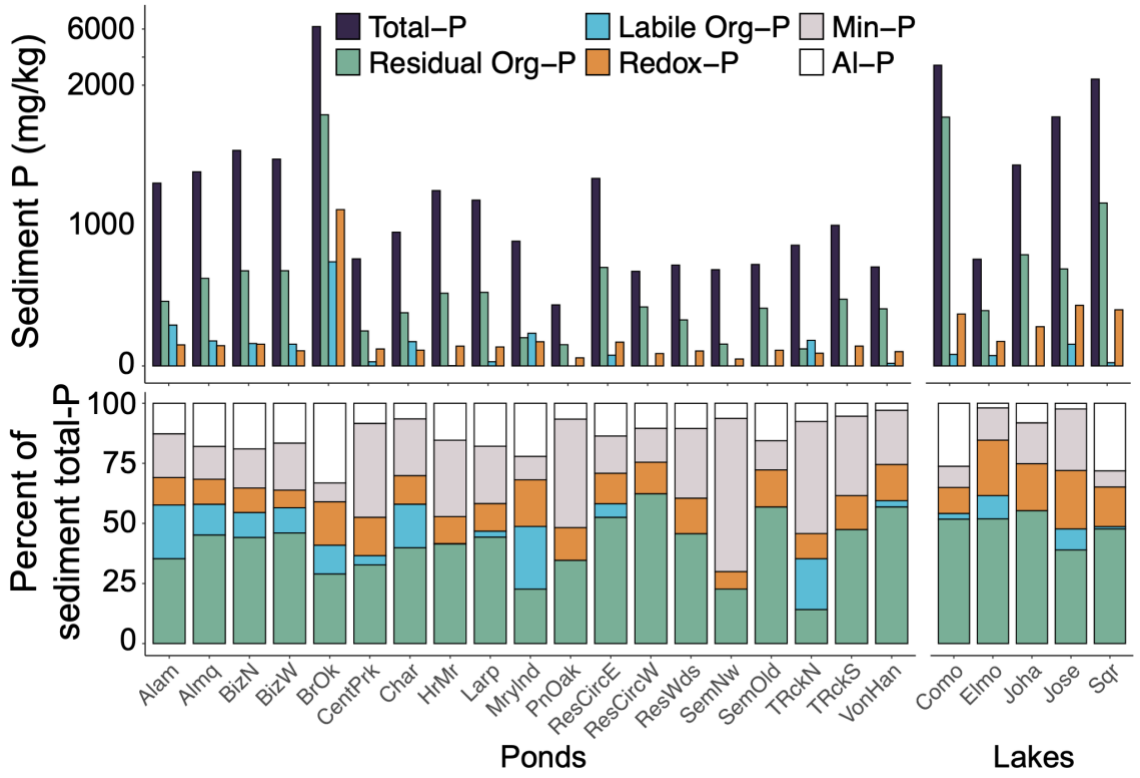

Figure 2.4. Sediment phosphorus fractions
Top: Concentrations of total sediment phosphorus (Total-P) and key sediment P fractions for each site. The upper portion of the y-axis is compressed. From left to right, the order of bars is: Total-P, residual org-P, labile org-P, and redox-P.
Bottom: Sediment P fractions as percent of sediment total P for each site. From bottom to top, the order of bar sections is: residual org-P, labile org-P, redox-P, min-P, and al-P. When only four sections are present, the labile organic-P fraction was zero.
"Org" indicates an organic fraction sensitive to mineralization, with residual org-P assumed to be less accessible to microorganisms than labile org-P. The sum of labile org-P and residual org-P represents total organic-P. "Redox-P" is the sum of loosely-bound P, P bound to calcium carbonate, and iron-bound P, and is sensitive to changes in redox conditions. "Al-P" is aluminum-bound P; "Min-P" is mineral-bound P.

Sediment properties as drivers of measured processes and temperature sensitivities

Multivariate modeling of all study sites revealed that P-rate responded positively to incubation temperature and sediment %OM and negatively to anoxic factor (Table 2.2; Figure 2.5). There were five other models within two AICc units and all included similar significant effects of incubation temperature and %OM. When models included only sites where estimates of anoxic factor incorporated two or more years of summer monitoring, the significant negative effect of anoxic factor persisted (results not shown). Results from MV models that included only ponds were highly similar to those for all sites (Table 2.2).

Table 2.2. Parameter estimates from the optimum multivariate mixed model for phosphorus (P) release rate, microbial respiration rate, and acid phosphatase activity.

	Parameter estimates											
	Incu. Temp	Sed. %OM	AF	Sed. C:N	Sed. lab. org-P	Sed. redox-P	%OM x temp	AF x temp	C:N x temp	n	Marg. R^2	Cond. R^2
All sites												
P release rate*	**0.09**	**0.08**	**-2.36**					0.06		85	0.45	0.90
Respiration rate*	**0.05**	**0.04**		-0.02					**0.002**	85	0.46	0.93
AP activity*	**0.06**	**0.03**			0.003					38	0.48	0.76
Only ponds												
P release rate*	**0.08**	**0.12**	**-2.72**					0.06		65	0.55	0.89
Respiration rate*	**0.07**	0.02				**0.01**	0.001			65	0.69	0.94
AP activity*	**0.05**	**0.10**								23	0.75	0.80

Modeling was performed using all sites and only ponds. Bold values significant at $p < 0.05$. Candidate variables that did not appear in any optimum model are not listed but are described in the text. Asterisks indicate variables log transformed prior to modeling. Number of observations included in each model (n), marginal (Marg.) R^2, and conditional (Cond.) R^2 values are listed. Incu. temp = incubation temperature (C); Sed. %OM = sediment percent organic matter; AF = Anoxic factor; Sed. C:N = sediment molar carbon to nitrogen ratio; Sed. lab. org-P = sediment labile organic-P; "x temp" indicates an interaction with incubation temperature.

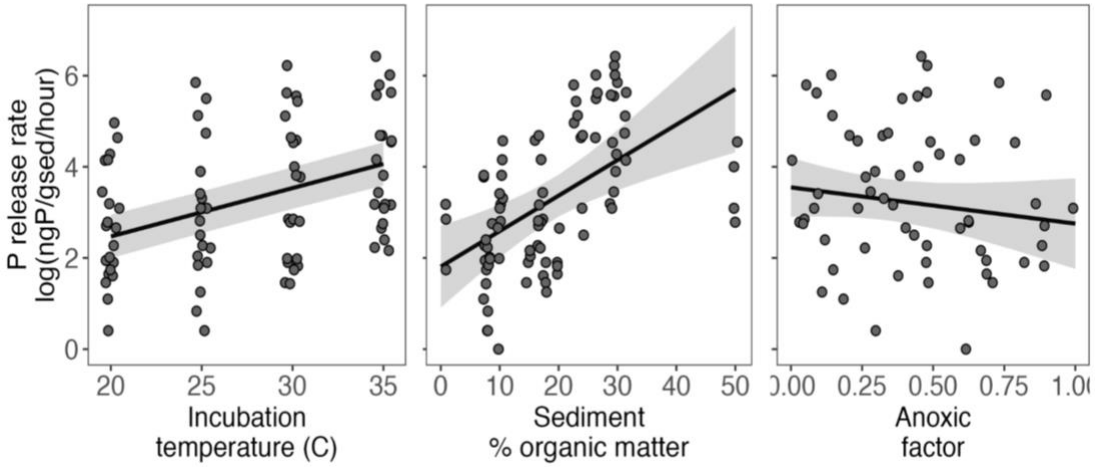

Figure 2.5. Drivers of phosphorus release rates in sediment incubations
Sediment phosphorus (P) release rates vs. each of the three significant predictors ($p < 0.05$) that appeared in the optimum multivariate model. Shading represents the 95% confidence interval. Models included observations from all sites (i.e., lakes and ponds) with site as a random intercept. Model output can be viewed in table 2.

Sediment oxygen exposure may mediate P-rate temperature sensitivity as a positive interaction between incubation temperature and anoxic factor emerged as important in MV

models (Table 2.2). Comparing P-rate temperature sensitivity (i.e., the linear slope between P release rate and incubation temperature) to sediment properties showed that P-rate was more sensitive to warming in sediments rich in OM and organic-P and sediments with higher redox-P (Table 2.3; Figure 2.6). The proportions of total sediment P in organic and redox-sensitive forms were not significant predictors of P temperature sensitivity (Table 2.3).

Table 2.3. The mediating effects of site and sediment properties on the temperature sensitivity for phosphorus (P) release rates, microbial respiration rates (Resp.), and acid phosphatase activity (AP).

		Temperature sensitivity		
		P*	Resp.*	AP*
Site	Anoxic factor			
	Site DO			
	Site water temp	-0.10	-0.08	
Sediment	% OM	**0.36**		
	C:N		**0.25**	-0.22
	C:P*	0.07		
	Total org-P*	**0.20**		**0.40**
	Labile org-P*	**0.15**		0.22
	Redox-P*	**0.12**	**0.22**	
	% total org-P			
	% labile org-P			
	% redox-P			

P and AP temperature sensitivity are the slopes from linear relationships with incubation temperature. Resp. temperature response is *Q10*. Values are coefficients of determination (adj-R2) from bivariate regression models. Negative values indicate a negative relationship. Bold values indicate p-value < 0.05; unbolded values indicate p-value < 0.1. Asterisks indicate log transformed variables. DO: dissolved oxygen; temp: temperature; OM: organic matter; C: carbon; N: nitrogen; org: organic

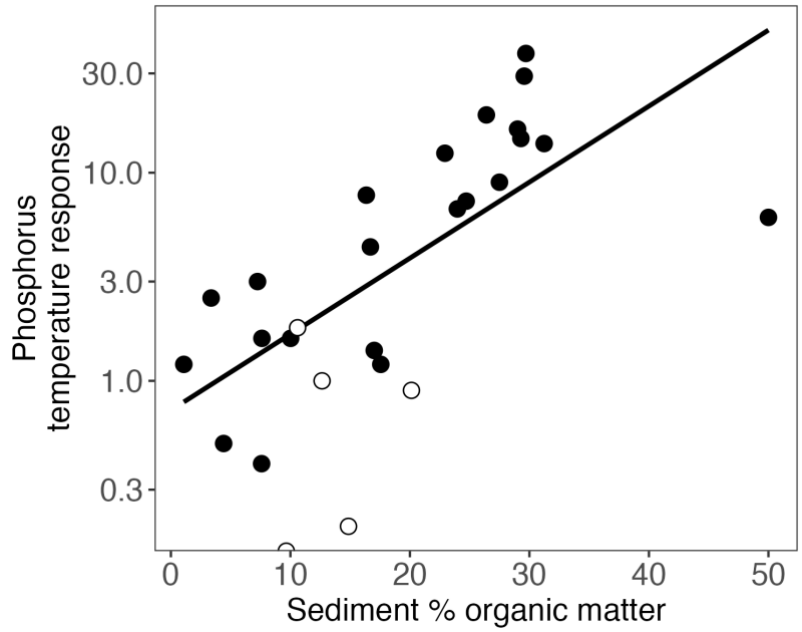

Figure 2.6. Phosphorus temperature sensitivity vs. sediment percent organic matter. Phosphorus temperature sensitivity is the slope of the linear relationship between phosphorus release rates and incubation temperature. Open symbols represent sites where incubation temperature had no significant effect on P release rate. Model adj-R^2 = 0.36, trendline significant at $p < 0.05$.

Sediments varied in the degree to which P release rates, microbial respiration, and AP activities responded to warming. When comparing P-tempR (the slope of the linear relationship between P release rate and incubation temperature) to sediment properties using BV regression, we saw similar results to those described for rates above. In sediments with greater OM and total organic-P, warming led to greater increases in P release rates.

The optimum MV model for Resp-rate included significant positive effects of incubation temperature, sediment %OM, and a sediment C:N x incubation temperature interaction, whereby higher C:N sediments were more sensitive to warming (Table 2.2; Figure S2.4). These were the only significant predictors in all models within two AICc units of the optimum model. When focusing on pond sites, which tended to have higher sediment C:N ratios, the C:N and temperature interaction was eliminated. Anoxic factor did not appear in any Resp-rate top models. BV regression analyses of Resp-rate temperature sensitivity confirmed the positive effect of C:N (Table 2.3).

The optimum model of AP activity included significant positive effects of incubation temperature and sediment %OM (Table 2.2; Figure S2.5). Anoxic factor did not appear as a

predictor of AP activity in any models. AP was more sensitive to increased temperature in sediments high in organic-P (Table 2.3).

Discussion

We expected that if biotic mineralization contributes to the sediment P mobilization, rates of dissolved P accumulation in incubations would 1) be positively related to microbial respiration and AP activity, 2) increase in sediments rich in OM, 3) decrease when sediment C:nutrient ratios were high, and 4) increase with temperature. Additionally, we expected that temperature would mediate relationships between measured processes and interact with sediment properties to shape P mobilization. We found sufficient support for these hypotheses (namely, 1, 2, and 4) to conclude that biotic P mineralization and its drivers contribute meaningfully to sediment P mobilization.

Sediment P mobilization was associated with microbial and enzymatic activity

Phosphorus release rate was positively correlated with Resp-rate and AP activity in sediment incubations, supporting an association of P mobilization with microbial metabolism. These findings align with the few other studies that have compared sediment P mobilization and respiration [Liikanen et al. (2002) in a boreal lake, Taguchi et al. (2020) in MSP stormwater ponds] and P mobilization and phosphatase activity [ZhiJiang et al. (2012) in subtropical wetlands]. The associations between measured processes were independent of incubation temperature, suggesting that these relationships exist even without warming.

Some of the variation in observed relationships between P-rate and Resp-rate and P-rate and AP activity was likely driven by differences in P immobilization. A fraction of freed P can be immobilized in microbial biomass and would not be captured by measurements of P in incubation water. Whether freed P is immobilized or released to the environment depends on microbial metabolic demands. Building on the work of McGill and Cole (1981), McConnell et al. (2020) outlines that biotic P mineralization may be driven by a need for P, C, or both. When P is exclusively limiting, biotic P and C mineralization are decoupled, and P is hydrolyzed from OM without the simultaneous respiration of C. The positive relationship between P-rate and, especially, AP activity with Resp-rate confirms coupled biotic P and C mineralization in

sediment incubations. What remains uncertain is the extent that biotic P mineralization is driven by a microbial demand for P.

Measurable AP activity in study sediments may indicate P limitation. Indeed, numerous studies have found that phosphatase activities decrease when bioavailable P increases (Fujita et al., 2017; Hill et al., 2010; Jansson et al., 1988). However, phosphatase synthesis and biotic P mineralization can be driven exclusively by a need to acquire C as dephosphorylation appears to greatly aid C acquisition from OM (McConnell et al., 2020). Consequently, some studies report that biotic P mineralization and phosphatase activity proceed even when bioavailable P is abundant (Allison & Vitousek, 2005). We similarly saw no effect of site bioavailable P concentrations on P-rates, Resp-rates, or AP activities. That said, the use of common water in incubations could negate any effect of site P availability, and the relatively short duration of incubations compared to the reported halflife of phosphatases would challenge our ability to see an influence of newly freed P on P mobilization (Jansson et al., 1988). While we expect that biotic C- and P-driven mineralization co-occur in study sediments, a thorough investigation is beyond the scope of this work. Understanding the metabolic demands driving biotic P mineralization, including how biotic P mineralization responds to P availability, has implications for internal P loading in lentic ecosystems and should be the focus of future research.

Sediment properties as drivers of measured processes

Sediment OM quantity (as %OM) was among the best predictors for P-rates and AP activities in MV modeling. The importance of sediment %OM was only surpassed by incubation temperature in Resp-rate models. Organic matter provides necessary electrons or reactants for microbial metabolism and the synthesis of phosphatase enzymes. The clear importance of OM quantity further supports coupled biotic mineralization of P and C in our sites. Contrary to our expectations, the effects of OM quantity on measured processes were not affected by sediment C:nutrient ratios nor did sediment C:nutrient ratios independently influence measured processes. However, sediment C:N interacted with temperature to affect microbial respiration, discussed in depth below.

Concentrations of sediment P fractions likely have implications for the relative importance of P mobilization mechanisms: sediments high in organic-P may be susceptible to biotic mineralization while redox-induced dissolution may be important when redox-P

dominates. However, our ability to assess the isolated or relative influence of each P fraction was complicated by strong correlations among them. For example, Spearman's correlation coefficient for redox-P and total organic-P was 0.9. It was no surprise, then, that we observed similarly positive effects of total organic-P and redox-P concentrations on P-rates and Resp-rates in BV analyses ($p < 0.05$). Taguchi et al. (2020) also found similarly positive correlations of redox-P and labile organic-P concentrations with sediment P release rates. In MV modeling, we saw no clear indications that any P fractions were primary drivers of measured processes. These findings emphasize that concentrations of individual sediment P factions may not be useful indicators of dominant sediment P mobilization processes (Søndergaard et al., 2003).

There were indications that sediments from sites with greater oxygen exposure (i.e., low anoxic factor) experienced higher P-rates, though effects were slight. Incubations were anoxic, so this relationship may reflect ways that site redox conditions alter sediment properties. For example, sediments with more frequent or recent oxygen exposure may have a larger pool of Fe-P that could rapidly dissociate under incubation anoxia. Oxygen exposure can also facilitate the downward migration of P into sediments, which could increase the initial P concentrations in homogenized sediment samples (Wang et al., 2022). Nonetheless, we did not see any significant relationships between measured sediment properties and site anoxic factor or bottom water oxygen concentrations. Site oxygen exposure could also affect P-rates by altering microbial abundance or structure (Zhang et al., 2015). Similarly, the starting concentration of phosphatase enzymes may be higher in sediments with frequent or recent oxygen exposure due to higher aerobic metabolism, though no measures of oxygen correlated with AP activities in our study. These potential indirect effects of oxygen exposure on P mobilization would augment the well-established, direct effects that oxygen has on internal P loading.

We did not vary redox conditions in sediment incubations, so it is unknown how changes in oxygen would directly alter the rates and relationships observed. The introduction of oxygen to sediments could increase microbial activity, potentially increasing hydrolysis of organic-P (Bastviken et al., 2003). Conversely, aerobic respiration may be accompanied by a greater demand for P, increasing P immobilization relative to biotic mineralization (Bastviken et al., 2003; McConnell et al., 2020). Additionally, the oxidation of Fe(II) to Fe(III) could increase the capacity of sediments to bind P, reducing the fraction of hydrolyzed P released to porewaters

(Jensen & Andersen, 1992). In fact, Likaanen (2002) observed negligible sediment P release from lake sediment cores under oxic conditions even when subjected to increased temperature, attributing the finding to sediment binding capacity. We did not measure the binding capacity of study sediments, but we expect that the adsorption of freed P to sediments could contribute additional variation to the relationships between rates of P release and microbial respiration, though binding capacity is expected to be low in anoxic incubations.

Warming increases P release rates

Increased incubation temperature significantly increased P release rates, further supporting that P mobilization is microbially-mediated in study sediments (Bostrom et al., 1988). Warming increases P mobilization via biotic mineralization by increasing microbial metabolism and demand for C and/or P, thereby increasing phosphatase synthesis. Warming also increases biotic P mineralization by increasing phosphatase activity (Davidson & Janssens, 2006). These mechanisms are supported by the observed significant increases in Resp-rates and AP activities with higher incubation temperature.

Warming enhanced rates of all measured processes but did not alter the relationships among them. We expected that higher incubation temperature would increase microbial and enzymatic activities, enhancing the role of biotic mineralization for P release and strengthening P-rate relationships with Resp-rate and AP activity. Instead, P release is associated with microbial and enzymatic processes even at lower temperatures (Liikanen et al., 2002); P release via biotic mineralization does not depend on warming.

Comparing temperatures sensitivities reported here and elsewhere reveals similarities and a need for more research, particularly in stormwater ponds. Our Resp-rate *Q10* values (mean 2.4; sd 0.7; range 1.2 - 3.5) aligned with those reported from similar temperatures in boreal lake sediments (mean 2.3; sd 0.4; Liikanen et al. (2002)), streambed sediments (range 0.1 - 4.0; Comer-Warner et al. (2018)), and sediments from tropical freshwaters (single reported value of 2.5). Gudsaz et al. (2012), found that the effect of warming from 0 to 27 C on log-transformed biotic C mineralization rates across 219 lakes was 0.036, which is similar to the effect of temperature on log-transformed Resp-rates in our MV models: 0.05.

Very few studies have estimated the temperature sensitivity of AP activity or biotic P mineralization in aquatic ecosystems and, to our knowledge, none have included stormwater

ponds. Hui et al. (2013) estimated AP *Q10* to be 1.7 using phosphatase kinetic information from a wide range of ecosystems. Liikanen et al. (2002), measuring P release in anoxic intact sediment cores from a boreal lake, reported an average *Q10* of 2.9 (sd 0.5). Referencing the work of Kamp-Nielsen (1975), Jensen and Andersen (1992) report *Q10* values for aerobic sediment P release of 4-12 and 2-3 under anaerobic conditions. We do not report *Q10* for P-rate or AP activity, as relationships between P-rate and temperature across sites were not consistently exponential. P-rate temperature sensitivities in our study did tend to be higher and more variable than those estimated for microbial respiration. This finding is consistent with those reported in Jensen and Andersen (1992), who attributed high P temperature sensitivities relative to losses from the inorganic Fe-P pool as microbial respiration depleted oxygen in sediment cores. Our incubations were purged of oxygen at the onset in an effort to reduce this effect, but this indirect effect of temperature on sediment P release could be factor in our incubations, as well. Additional assessments into P release temperature sensitivity are needed.

Our findings indicate that warming reduces the stability of sediment organic-P, increases biotic mineralization, and may further exacerbate internal and downstream eutrophication. We estimated that one degree of warming increased P release rates under anoxic conditions by 9%, with a large amount of site-to-site variation. We expect that some of this variation was driven by differences in sediment properties, though our findings show few clear patterns.

Interactions between temperature and sediment properties

Rates of phosphorus release were more sensitive to warming in sediments rich in organic matter. This pattern was driven primarily by those sediments with greater than 20% OM with the exception of one site (Jose) that has high %OM but comparatively less organic P. As described above, sediments with higher OM are able to support higher rates of microbial activities and P release. The lack of relationship between Resp-rate temperature sensitivity and sediment %OM, however, could suggest some decoupling of P and C with warming.

Indicators of OM quality—sediment C:N and C:P—were not significant main effects in P-rate, Resp-rate, or AP activity in MV models but may be important mediators of the effects of warming. The degradability of OM substrates is a known regulator of microbial respiration temperature sensitivity (Gudasz et al., 2012; Jane & Rose, 2018). The carbon quality temperature hypothesis states that because more recalcitrant OM has a higher activation energy, it will

respond more strongly to increased temperature (Fierer et al., 2005; Q. Wang et al., 2019; Wen et al., 2024). In support of this, we found that Resp-rates in sediments with higher C:N ratios (often an indication of low OM degradability (Gudasz et al., 2012)) were significantly more sensitive to increased incubation temperature and an interaction between incubation temperature and C:N was a significant predictor of Resp-rate. The effects of C:N on Resp-rate temperature sensitivity did not transfer to P-rate or AP activity or were not captured with elemental ratios. Additional measurements of sediment OM quality and its effects on biotic P mineralization are needed, particularly in stormwater ponds where OM characteristics are highly variable.

The effects of warming on P release rates may change as a warming event persists due to changes in substrate availability (McConnell et al., 2020). As warming increases microbial metabolism, P may become more limiting and immobilization may exceed biotic mineralization. Critical questions remain regarding how substrate availability and temperature interact to determine biotic P mineralization contributions to internal P loading and should be the focus of future study.

Conclusions & implications for management

Biotic mineralization is not the only mechanism of P release in our incubations or site sediments. There is no question as to the importance of redox-sensitive P for internal loading in lentic ecosystems (Ding et al., 2016), and anoxia would facilitate the release of redox-P in our incubations. Further, some sediment P may be lost due to diffusion or desorption, particularly in homogenized sediments, though sediment exchangeable-P content was low (all <7%; mean 1.5%). Differentiating the mechanisms of internal P loading is a persistent challenge (Hupfer & Lewandowski, 2008), and we are not able to quantify the relative contributions of each. Instead, the relationships we observed between P release rates and microbial and enzymatic activities, sediment OM, and temperature make it clear that biotic mineralization contributes meaningfully to P release under anoxic conditions and add to our understanding of the conditions that affect the stability of sediment P. Our findings add to a growing body of evidence that internal P loading is not only driven by redox conditions but also by complex factors that affect microbial metabolism. This understanding is critical for the management of excess P in urban freshwaters.

Efforts to promote P retention in stormwater pond and lentic ecosystem sediments should consider the role of biotic P mineralization. Fortunately, some common strategies used to stabilize redox-sensitive P may also be effective for reducing P loading from biotic mineralization. Strategies that increase sediment P-binding capacity (e.g., iron or aluminum amendments or designing and managing ponds to promote aerobic conditions) can prevent the transport of P mobilized by any mechanism to overlying water. Similarly, particular attention should be paid to sites where high OM content can support higher rates of microbial activities that drive biotic P mineralization as well as the reducing conditions needed for the dissolution of Fe-P. What is gained by more explicitly considering biotic mineralization as a key component of sediment P release is an emphasis on the role of temperature. Efforts to mitigate warming in urban water bodies—including designing stormflow networks to reduce contact between stormwater and high heat capacity paved surfaces or addressing the pressing problem of warming in cities more broadly—would help prevent any stimulatory effects of elevated temperatures on sediment P loading and improve the ability of urban sediments to retain P. Further, as water bodies in cities and beyond experience more frequent and prolonged periods of warming, additional research into how elevated temperatures alter the stability of sediment P within the context of other global change factors, such as excess nutrient loading, is of critical importance.

Works cited

Allison, S. D., & Vitousek, P. M. (2005). Responses of extracellular enzymes to simple and complex nutrient inputs. *Soil Biology and Biochemistry*, *37*(5), 937–944. https://doi.org/10.1016/j.soilbio.2004.09.014

Bartoń, K. (2022). *MuMIn: Multi-Model Inference.* (Version 1.46.0) [R]. https://CRAN.R-project.org/package=MuMIn

Bastviken, D., Olsson, M., & Tranvik, L. (2003). Simultaneous Measurements of Organic Carbon Mineralization and Bacterial Production in Oxic and Anoxic Lake Sediments. *Microbial Ecology*, *46*, 73–82. https://doi.org/10.1007/s00248-002-1061-9

Bostrom, B., Andersen, J. M., Fleischer, S., & Jansson, M. (1988). Exchange of phosphorus across the sediment-water interface. *Hydrobiologia*, *170*, 229–244.

Clary, J., Jones, J., Leisenring, M., Hobson, P., & Strecker, E. (2020). *International Stormwater BMP Database: 2020 Summary Statistics*. The Water Research Foundation.

Comer-Warner, S. A., Romeijn, P., Gooddy, D. C., Ullah, S., Kettridge, N., Marchant, B., Hannah, D. M., & Krause, S. (2018). Thermal sensitivity of CO2 and CH4 emissions varies with streambed sediment properties. *Nature Communications*, *9*(1), 2803. https://doi.org/10.1038/s41467-018-04756-x

Davidson, E. A., & Janssens, I. A. (2006). Temperature sensitivity of soil carbon decomposition and feedbacks to climate change. *Nature*, *440*(7081), 165–173. https://doi.org/10.1038/nature04514

Ding, S., Wang, Y., Wang, D., Li, Y. Y., Gong, M., & Zhang, C. (2016). In situ, high-resolution evidence for iron-coupled mobilization of phosphorus in sediments. *Scientific Reports*, *6*(1), 24341. https://doi.org/10.1038/srep24341

Engstrom, D.R., (2005). Long-term Changes in Iron and Phosphorus Sedimentation in Vadnais Lake, Minnesota, Resulting from Ferric Chloride Addition and Hypolimnetic Aeration. *Lake and Reservoir Management, 21*(1), 95-105. http://www.tandfonline.com/doi/abs/10.1080/07438140509354417

Fieberg, J. (2024). *Statistics for Ecologists: A Frequentist and Bayesian Treatment of Modern Regression Models*. University of Minnesota Libraries Publishing. https://doi.org/10.24926/9781959870029

Fierer, N., Craine, J. M., McLauchlan, K., & Schimel, J. P. (2005). Litter quality and the temperature sensitivity of decomposition. *Ecology*, *86*(2), 320–326. https://doi.org/10.1890/04-1254

Frost, P. C., Prater, C., Scott, A. B., Song, K., & Xenopoulos, M. A. (2019). Mobility and Bioavailability of Sediment Phosphorus in Urban Stormwater Ponds Water Resources Research. *Water Resources Research, 55*(5), 3680-3688. https://doi.org/10.1029/2018WR023419

Fujita, K., Kunito, T., Moro, H., Toda, H., Otsuka, S., & Nagaoka, K. (2017). Microbial resource allocation for phosphatase synthesis reflects the availability of inorganic phosphorus across various soils. *Biogeochemistry*, *136*(3), 325–339. https://doi.org/10.1007/s10533-017-0398-6

Grimm, N. B., Faeth, S. H., Golubiewski, N. E., Redman, C. L., Wu, J., Bai, X., & Briggs, J. M. (2008). Global Change and the Ecology of Cities. *Science*, *319*(5864), 756-760. https://doi.org/10.1126/science.1150195

Gudasz, C., Bastviken, D., Premke, K., Steger, K., & Tranvik, L. J. (2012). Constrained microbial processing of allochthonous organic carbon in boreal lake sediments. *Limnology and Oceanography*, *57*(1), 163–175. https://doi.org/10.4319/lo.2012.57.1.0163

Heiri, O., Lotter, A. F., & Lemcke, G. (2001). Loss on ignition as a method for estimating organic and carbonate content in sediments: Reproducibility and comparability of results. *Journal of Paleolimnology*, *25*, 101–110.

Helsel, D. R., & Helsel, D. R. (2012). *Statistics for censored environmental data using Minitab and R* (2nd ed). Wiley.

Hester, E. T., & Bauman, K. S. (2013). Stream and Retention Pond Thermal Response to Heated Summer Runoff From Urban Impervious Surfaces[1]. *JAWRA Journal of the American Water Resources Association*, *49*(2), 328–342. https://doi.org/10.1111/jawr.12019

Hill, B. H., Elonen, C. M., Jicha, T. M., Bolgrien, D. W., & Moffett, M. F. (2010). Sediment microbial enzyme activity as an indicator of nutrient limitation in the great rivers of the Upper Mississippi River basin. *Biogeochemistry*, *97*, 195–209. https://doi.org/10.1007/s10533-009-9366-0

Hui, D., Mayes, M. A., & Wang, G. (2013). Kinetic parameters of phosphatase: A quantitative synthesis. *Soil Biology and Biochemistry*, *65*, 105–113. https://doi.org/10.1016/j.soilbio.2013.05.017

Hupfer, M., & Lewandowski, J. (2008). Oxygen Controls the Phosphorus Release from Lake Sediments – a Long-Lasting Paradigm in Limnology. *International Review of Hydrobiology*, *95*(4-5), 415–432. https://doi.org/10.1002/iroh.200711054

Janke, B.D., Finlay, J.C., Taguchi, V.C., & Gulliver, J.S. (2022). Hydrologic processes regulate nutrient retention in stormwater detention ponds. *Science of the Total Environment*, *823823*, 153722. https://doi.org/10.1016/j.scitotenv.2022.153722

Jane, S. F., & Rose, K. C. (2018). Carbon quality regulates the temperature dependence of aquatic ecosystem respiration. *Freshwater Biology*, *63*(11), 1407–1419. https://doi.org/10.1111/fwb.13168

Jansson, M., Olsson, H., & Pettersson, K. (1988). Phosphatases; origin, characteristics and function in lakes. *Hydrobiologia*, *170*, 157–175.

Jensen, H. S., & Andersen, F. O. (1992). Importance of temperature, nitrate, and pH for phosphate release from aerobic sediments of four shallow, eutrophic lakes. *Limnology and Oceanography*, *37*(3), 577–589. https://doi.org/10.4319/lo.1992.37.3.0577

Julian, P., & Helsel, D. (2023). *NADA2: Data Analysis for Censored Environmental Data.* (Version 1.1.3) [R]. https://CRAN.R-project.org/package=NADA2

Kamp-Nielsen, L. (1975). A kinetic approach to the aerobic sediment-water exchange of phosphorus in Lake Esrom. *Ecological Modelling*, *1*(2), 153–160. https://doi.org/10.1016/0304-3800(75)90030-7

Li, J., Zhang, Y., & Katsev, S. (2018). Phosphorus recycling in deeply oxygenated sediments in Lake Superior controlled by organic matter mineralization. *Limnology and Oceanography*, *63*(3), 1372–1385. https://doi.org/10.1002/lno.10778

Liikanen, A., Murtoniemi, T., Tanskanen, H., Martikainen, P. J., & Väisänen, T. (2002). Effects of temperature and oxygen availability on greenhouse gas and nutrient dynamics in sediment of a eutrophic mid-boreal lake. *Biogeochemistry, 59*, 269–286.

Liu, C., Shen, Q., Gu, X., Zhang, L., Han, C., & Wang, Z. (2023). Burial or mineralization: Origins and fates of organic matter in the water–suspended particulate matter–sediment of macrophyte- and algae-dominated areas in Lake Taihu. *Water Research*, *243*, 120414. https://doi.org/10.1016/j.watres.2023.120414

Markovic, S., Liang, A., Watson, S. B., Guo, J., Mugalingam, S., Arhonditsis, G., Morley, A., & Dittrich, M. (2019). Biogeochemical mechanisms controlling phosphorus diagenesis and internal loading in a remediated hard water eutrophic embayment. *Chemical Geology*, *514*, 122–137. https://doi.org/10.1016/j.chemgeo.2019.03.031

Marx, M.-C., Wood, M., & Jarvis, S. C. (2001). A microplate reader method for enzymes in soil. *Soil Biology and Biogeochemistry, 33*, 1633–1640.

McConnell, C. A., Kaye, J. P., & Kemanian, A. R. (2020). Reviews and syntheses: Ironing out wrinkles in the soil phosphorus cycling paradigm. *Biogeosciences*, *17*(21), 5309–5333. https://doi.org/10.5194/bg-17-5309-2020

McGill, W. B., & Cole, C. V. (1981). Comparative aspects of cycling of organic C, N, S and P through soil organic matter. *Geoderma*, *26*(4), 267–286. https://doi.org/10.1016/0016-7061(81)90024-0

Orihel, D. M., Baulch, H. M., Casson, N. J., North, R. L., Parsons, C. T., Seckar, D. C. M., & Venkiteswaran, J. J. (2017). Internal phosphorus loading in Canadian fresh waters: A critical review and data analysis. *Canadian Journal of Fisheries and Aquatic Sciences*, *74*(12), 2005–2029. https://doi.org/10.1139/cjfas-2016-0500

Pinheiro, J., Bates, D., DebRoy, S., & Sarkar, D. (2021). *nlme: Linear and Nonlinear Mixed Effects Models* (Version 3.1.153) [R]. R Core Team. https://CRAN.R-project.org/package=nlme

Psenner, R., Pettersson, K., & Bostrom, B. (1988). Fractionation of phosphorus in suspended matter and sediment. *International Journal of Limnology, 22*, 219–228.

Qian, Y., Liang, X., Chen, Y., Lou, L., Cui, X., Tang, J., Li, P., & Cao, R. (2011). Significance of biological effects on phosphorus transformation processes at the water–sediment interface under different environmental conditions. *Ecological Engineering*, *37*(6), 816–825. https://doi.org/10.1016/j.ecoleng.2010.12.005

R Core Team. (2021). *R: A language and environment for statistical computing* (Version 4.1.2) [R]. R Foundation for Statistical Computing. https://www.R-project.org/

Shaw, A. N., & Cleveland, C. C. (2020). The effects of temperature on soil phosphorus availability and phosphatase enzyme activities: A cross-ecosystem study from the tropics to the Arctic. *Biogeochemistry*, *151*(2–3), 113–125. https://doi.org/10.1007/s10533-020-00710-6

Shinohara, R., Hiroki, M., Kohzu, A., Imai, A., Inoue, T., Furusato, E., Komatsu, K., Satou, T., Tomioka, N., Shimotori, K., & Miura, S. (2017). Role of organic phosphorus in sediment in a shallow eutrophic lake. *Water Resources Research*, *53*(8), 7175–7189. https://doi.org/10.1002/2017WR020486

Søndergaard, M., Jensen, J. P., & Jeppesen, E. (2003). Role of sediment and internal loading of phosphorus in shallow lakes. *Hydrobiologia*, *506*, 135–145.

Song, K., Winters, C., Xenopoulos, M. A., Marsalek, J., & Frost, P. C. (2017). Phosphorus cycling in urban aquatic ecosystems: Connecting biological processes and water chemistry to sediment P fractions in urban stormwater management ponds. *Biogeochemistry*, *132*(1), 203–212. https://doi.org/10.1007/s10533-017-0293-1

Taguchi, V. J., Olsen, T. A., Natarajan, P., Janke, B. D., Gulliver, J. S., Finlay, J. C., & Stefan, H. G. (2020). Internal loading in stormwater ponds as a phosphorus source to downstream waters. *Limnology and Oceanography Letters*, 322–330. https://doi.org/10.1002/lol2.10155

Wang, Q., Zhao, X., Chen, L., Yang, Q., Chen, S., & Zhang, W. (2019). Global synthesis of temperature sensitivity of soil organic carbon decomposition: Latitudinal patterns and mechanisms. *Functional Ecology*, *33*(3), 514–523. https://doi.org/10.1111/1365-2435.13256

Wang, Z., Wang, C., Jiang, H., & Liu, H. (2022). Higher dissolved oxygen levels promote downward migration of phosphorus in the sediment profile: Implications for lake restoration. *Chemosphere*, *301*, 134705. https://doi.org/10.1016/j.chemosphere.2022.134705

Wen, S., Hu, A., Jiang, S., Han, L., Jang, K., Tanentzap, A. J., Zhong, J., & Wang, J. (2024). Temperature sensitivity of organic carbon decomposition in lake sediments is mediated by chemodiversity. *Global Change Biology*, *30*(2), e17158. https://doi.org/10.1111/gcb.17158

Williams, C. J., Frost, P. C., & Xenopoulos, M. A. (2013). Beyond best management practices: Pelagic biogeochemical dynamics in urban stormwater ponds. *Ecological Applications*, *23*(6), 1384–1395. https://doi.org/10.1890/12-0825.1

Woodcock, T. S., Monaghan, M. C., & Alexander, K. E. (2010). Ecosystem Characteristics and Summer Secondary Production in Stormwater Ponds and Reference Wetlands. *Wetlands*, *30*(3), 461–474. https://doi.org/10.1007/s13157-010-0057-3

Zhang, Z., Wang, H., Zhou, J., Li, H., He, Z., Van Nostrand, J. D., Wang, Z., & Xu, X. (2015). Redox potential and microbial functional gene diversity in wetland sediments under simulated warming conditions: Implications for phosphorus mobilization. *Hydrobiologia*, *743*, 221–235. https://doi.org/10.1007/s10750-014-2039-6

ZhiJian, Z., ZhaoDe, W., Holden, J., XinHua, X., Hang, W., JingHua, R., & Xin, X. (2012). The release of phosphorus from sediment into water in subtropical wetlands: A warming microcosm experiment. *Hydrological Processes*, *26*(1), 15–26. https://doi.org/10.1002/hyp.8105

Zuur, A. F., Ieno, E. N., Walker, N., Saveliev, A. A., & Smith, G. M. (2009). *Mixed effects models and extensions in ecology with R*. Springer New York. https://doi.org/10.1007/978-0-387-87458-6

Chapter 3: Denitrification rates and efficiencies in urban lentic systems are linked to trophic status and sediment oxygen exposure

Summary

Denitrification (DeN) in small lentic ecosystems like stormwater ponds and lakes is expected to contribute meaningfully to nitrogen (N) removal in urban watersheds, ameliorating the effects of excess N locally and downstream. However, the site characteristics that promote high DeN rates and efficiencies, defined as the release of inert dinitrogen gas over the potent greenhouse gas nitrous oxide (N_2O), are presently unclear. We used amended and unamended DeN enzyme assays with and without acetylene to measure rates of DeN and N_2O production, respectively, from 22 stormwater ponds and lakes in the Minneapolis-St. Paul metropolitan region, Minnesota, USA. Ponds and lakes were selected to vary in factors that we hypothesized would influence DeN, including sediment oxygen exposure, nitrate concentrations, and chloride inputs. DeN and N_2O production measured in assays unamended with carbon and nitrate, representing background rates, were negligible in nearly all sediments. Rates of DeN in assays amended with carbon and nitrate, representing potentials, were highly variable (0.5 – 47 mg N m^{-2} hr^{-1}), as were rates of N_2O production (0.1 – 24 mg N m-2 hr -1) and the proportion of DeN products as N_2O (N_2O yield; 2 – 79%). Large lakes (> 45 ha) had significantly higher amended rates of DeN compared to small lakes (> 5 ha) and ponds (< 5 ha). Amended total DeN and N_2O rates were also significantly higher in sediments collected from the edge of water bodies (depth ≤ 30 cm) compared to deeper center habitats (depth range 60 – 1000+ cm). Comparisons to sediment and site properties revealed that amended DeN rates were significantly higher in sites with lower concentrations of total phosphorus and reduced road salt inputs. Amended DeN was less efficient (i.e., more N_2O was produced as a fraction of total DeN) when dissolved oxygen concentrations in overlying water were high. While a large amount of variation in amended DeN rates, N_2O production, and N_2O yields remained unexplained in our study (>70%), our findings suggest that variables that broadly reflect sediment oxygen exposure and reactant availability alter the ability of urban sediments to remove N.

Introduction

Background

Cities are highly altered, dynamic ecosystems that challenge our ability to adequately characterize their key nutrient flows. Of particular interest is nitrogen (N), whose distribution and cycling has been dramatically modified by anthropogenic activities with consequences for human and ecological well being (Galloway et al., 2008). Much of the anthropogenic N in cities enters stormwater where it can be transported to surface waters (Hobbie et al., 2017). In excess, N can contribute to the eutrophication of urban waters in both inland and coastal regions (Bratt et al., 2020; Elser et al., 2007). At the same time, urban waters may be able to remove some excess N via denitrification, thereby mitigating its effects locally and downstream.

Denitrification is the sequential reduction of nitrate (NO_3^-) to gaseous nitric oxide (NO), nitrous oxide (N_2O), and dinitrogen (N_2), which can then be released to the atmosphere (Davidson & Seitzinger, 2006). Each step requires specific enzymes synthesized by a diverse set of microorganisms as part of anaerobic metabolism with organic carbon (C) as a common electron donor. While the release of any gaseous denitrification products removes bioavailable N from ecosystems (thereby contributing to N "retention") and ameliorates the effects of excess N, the form in which it is released has environmental implications. The production of inert N_2 is highly preferred; in many ways, it represents a reversal of the rampant anthropogenic creation of reactive N that contributes substantially to excess N in global ecosystems (Galloway et al., 2008). In contrast, tropospheric N_2O is a powerful greenhouse gas, and high rates of its release may have negative implications for global climate (Ravishankara et al., 2009). In addition, stratospheric N_2O can be photo-oxidized to NOx and contribute to ozone destruction. Decades of research in soils and sediments has revealed denitrification to be widespread but highly heterogeneous, occurring whenever and wherever requirements are met (Bernhardt et al., 2017; Davidson & Seitzinger, 2006; Piña-Ochoa & Álvarez-Cobelas, 2006). Compared to total denitrification, fewer studies have considered the relative proportion of denitrification products ("denitrification efficiency").

The sediments of urban shallow lakes and stormwater ponds may be hot-spots of N removal via denitrification. Sediments in small aquatic ecosystems tend to contain abundant denitrification reactants N and C, support abundant and diverse denitrifier communities, and

sustain necessary reducing conditions (Bernhardt et al., 2008; Hall et al., 2016; S. Seitzinger et al., 2006). Indeed, rates of potential denitrification or emissions of denitrification products in urban sediments and stormwater infrastructure tend to be greater than or comparable to sediments in nonurban systems (Bauduin et al., 2024; Beaulieu et al., 2011; Bettez & Groffman, 2012; Blaszczak et al., 2018; Ginger et al., 2017). Despite a broad ability to support denitrification, considerable unexplained variation in DeN rates and efficiencies in urban sediments remains (Blaszczak et al., 2018). Urban water bodies are shaped by interacting human and non-human processes in ways that may inhibit or promote denitrification rates and efficiencies. Understanding the drivers of DeN within urban water bodies is critical for understanding urban N cycling.

Controls on denitrification in urban lentic ecosystems

The amount of available reactants regulates denitrification rates and efficiencies. Urban lentic waters can receive abundant N and C from their catchments, especially if they are integrated into the stormwater network (Finlay et al., 2024). Nutrient-rich inputs can also encourage internal primary production, which supplies autochthonous labile C that can enhance denitrification (Fork & Heffernan, 2014). An abundance of reactants in urban waters may facilitate high total DeN rates, but may decrease efficiency. Prior work has found that incomplete denitrification is more likely to occur when NO_3^- is abundant as it is more energetically favorable to reduce NO_3^- over N_2O, especially if the ratio of NO_3^- to labile C is high (Beaulieu et al., 2011; Firestone et al., 1979; G. Wang et al., 2021; Weier et al., 1993). When rates of denitrification are sufficiently high, N_2O may accumulate faster than it can be reduced leading to N_2O release. Relatedly, NO_3^- may directly inhibit the activity of the N_2O-reductase enzymes responsible for reducing N_2O to N_2 (Bakken et al., 2012).

Stratification and mixing regimes in lentic ecosystems regulate denitrification rates and efficiencies through effects on reactant availability. In deep, seasonally stratified lentic ecosystems, denitrification rates in hypolimnetic sediments can slow as bottom water NO_3^- and labile C become depleted (Deemer et al., 2011). Mixing replenishes reactants from upper layers to sediments. In shallow systems, it is assumed that reactants are less likely to become depleted due, in part, to frequent mixing and shorter diffusion distances. That said, prolonged stratification has been observed even in relatively shallow urban ponds due to site morphology

and sheltering, high salt concentrations in northern regions, and organic-rich sediments with high sediment oxygen demand (Song et al., 2013). As a result, reactants in sediments of shallow water bodies may become limiting as they do in deeper systems.

Sediment redox conditions are an important driver of denitrification rates and efficiencies (Rysgaard et al., 1994). Reducing conditions are required for denitrification, and the presence of oxygen rapidly inhibits denitrifying enzymes and shifts the microbial community to aerobic metabolism (Bakken et al., 2012). That said, environments that support oxidizing and reducing conditions in close proximity can have especially high rates of denitrification due to coupled nitrification-denitrification. In sediment pore waters, microbial metabolism rapidly depletes oxygen while oxygenated overlying waters and/or macrophyte roots can replenish oxygen and create interstitial sites able to support aerobic activities, including nitrification (Benelli et al., 2020). As a result, aerobic re-mineralization of ammonium and nitrification convert organic N to NO_3^-, which can be rapidly denitrified. Even when denitrification is uncoupled from nitrification (e.g., in sediments with persistent overlying hypoxia), the ability to nitrify may be important for replenishing NO_3^- as it increases the fraction of total system N available to be denitrified. We expect a system's capacity to convert organic-N into NO_3^- to be especially important in our study sites as a majority of incoming N is in organic forms (Janke et al., 2017). Therefore, sediments that are exposed to oxygen may have higher rates of denitrification. At the same time, coupled nitrification-denitrification may result in greater N_2O yield because of high NO_3^- availability, as described above. Additionally, compared to the other denitrifying enzymes, N_2O-reductases are especially sensitive to oxygen (Bakken et al., 2012). The dynamic oxygen conditions in interstitial porewaters overlaid by oxic waters may be sufficient to prevent the reduction of N_2O to N_2.

A final component that may shape denitrification rates and efficiencies in urban lentic sediments in northern cities is salinization. Anthropogenic salinization is a global phenomenon with context-specific causes and consequences (Herbert et al., 2015). Inland waters in northern climates are experiencing salinization due to the widespread use of road salts (Dugan et al., 2017). Hundreds of thousands of tonnes of road salt are distributed on roads, sidewalks, and parking lots each winter to maintain safe and efficient transportation in winter and are washed into local lakes and streams with snow melt. For example, there is ample evidence that the use of

road salt is driving surface water salinization and elevated Cl^- in the Minneapolis-St Paul metropolitan region (MSP; Novotny et al. 2008). Stormwater pond monitoring in MSP has found that peak Cl^- concentrations range from background levels to over ~20 mg/L (unpublished data) with variation driven by the fraction of paved surfaces in a catchment. Prior work assessing the effect of salinization on N cycling is dominated by studies of estuaries and coastal wetlands (notable exceptions include (Kim & Koretsky, 2013; Laverman et al., 2007; Robert Hamersley et al., 2009). This literature reports conflicting results regarding the mechanisms and system-level effects of salinization on N cycling and N removal (Herbert et al., 2015; Mosier & Francis, 2010; Rysgaard et al., 1999; S. P. Seitzinger et al., 1984). Road salt inputs could represent a substantial, novel stressor to inland denitrifiers and may directly inhibit their function (Wang et al., 2014). High salt inputs may also reduce denitrification reactant availability as salinization strengthens water column density gradients, stratification and anoxia (Novotny et al., 2008), potentially limiting reactant delivery via mixing and nitrification. Additionally, elevated concentrations of Na^+ ions may interrupt NO_3^- production via nitrification by displacing NH_4^+ from sediments (Duan & Kaushal, 2015).

Sediments in small lentic ecosystems can support high rates of denitrification, suggesting that shallow lakes and stormwater ponds may be important for alleviating excess N within and downstream of cities. However, we expect that variation in reactant availability—driven by redox conditions, mixing, and salinity, among others—likely alter denitrification rates and efficiencies. We used denitrification enzyme assays to measure rates of total denitrification and N_2O production. By relating DeN and N_2O production to site characteristics, we aimed to explore patterns in potential (i.e., amended) DeN rates and efficiencies in dynamic urban lentic ecosystems. Our focus on amended incubations means we assessed how site conditions structure denitrifier communities and dictate their ability to perform DeN and remove N. We expected higher total denitrification rates to be associated with 1) high NO_3^- concentrations, 2) higher dissolved oxygen concentrations, which promote coupled nitrification-denitrification, and 3) lower salinity, measured as specific conductance. We further expected greater N_2O yield under 4) high NO_3^- concentrations and 5) higher dissolved oxygen concentrations.

Methods

Study sites

Study sites were located in the Minneapolis-St. Paul metropolitan region (MSP) in central Minnesota, USA (Figure 3.1). We sampled 14 ponds with permanently wet pools (< 5 ha), seven small lakes (5 – 45 ha), and four larger (> 45 ha) lakes. Site designations were based on surface area and informed by Richardson et al. (2022). Sites were selected to capture a range of sediment oxygen exposure, nitrate concentrations, and chloride inputs (Table 3.1). For each site, we classified the mixing regime based on knowledge of the site and prior monitoring of water column temperature, dissolved oxygen, and conductivity. Thirteen of the sites seasonally stratify and 12 are polymictic.

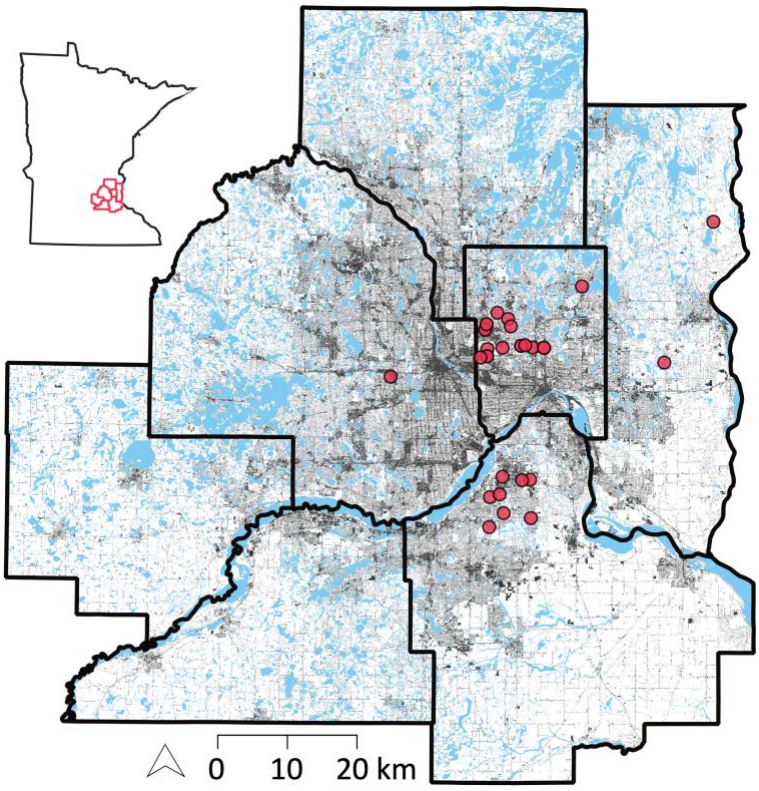

Figure 3.1. Location of study sites
Study sites (points) were located within the Minneapolis-St. Paul metropolitan region, Minnesota (inset), USA.

Sampling events occurred between September 5 and October 6 in 2019 and August 22 and October 5 in 2022 (Table S3.1). Five sites were sampled in both years. In MSP, these

sampling dates span the transition from summer to autumn. From mid-August to mid-October, both years saw large changes in temperature with daily highs ranging from 2 and 3 to 30 and 32 degrees C in 2019 and 2022, respectively. Compared to 2019, 2022 was overall slightly warmer and substantially drier. Between April 1 and November 1, air temperatures in 2022 averaged 16 compared to 15 degrees F in 2019. Total precipitation was 41 cm in 2022 compared to 86 cm in 2019, deviating from 1991–2020 climate normals by -11 and +7 cm, respectively (MN DNR).

Table 3.1. Summary statistics of key sediment and site properties.

	Surface area ha	Sample depth cm	Ave TP µg/L	Cond. µS/cm	Est. Cl^- µg/L	DO µg/L	NO_3^- µg/L
Edge & center n = 37							
Mean	16	420	88	1869	625	2901	182
Median	1	220	63	413	121	1115	8
Stdev	30	763	79	5145	1780	3272	728
Min	0	30	12	153	31	0	0
Max	104	4267	342	30600	10566	9900	4191
Edge, n = 9							
Mean	-	30	-	309	85	5214	232
Median	-	30	-	325	90	5500	23
Stdev	-	0	-	196	68	3224	534
Min	-	30	-	153	31	2200	0
Max	-	30	-	744	235	9900	1531
Center, n = 32							
Mean	-	537	-	2326	783	2046	180
Median	-	232	-	555	170	400	6
Stdev	-	837	-	5809	2010	2889	794
Min	-	60	-	217	53	0	0
Max	-	4267	-	30600	10566	9300	4191

Edge sediments are all estimated to have a depth of 30 cm. Surface area and average total phosphorus concentrations (Ave TP) are site-level variables and are not summarized for individual sample locations. The remaining variables reflect conditions overlying sediments at the time of sampling and were measured from surface waters for edge sediments and bottom waters for center sediments. Specific conductance (Cond.) was used to estimate chloride concentrations (Est. Cl^-). DO indicates dissolved oxygen and NO_3^- indicates nitrate concentrations. *n* refers to the number of observations.

Field and laboratory methods

During each sampling event, we measured dissolved oxygen, specific conductance, and temperature profiles using a Hach portable meter, conductivity cell, and dissolved oxygen sensor. The deepest profile reading was used as the sample depth. Conductivity reflects the

concentration of all dissolved ions present but has been demonstrated to be a reliable indicator of chloride concentrations in MSP waters, especially at higher conductivity values (Herb, 2017). To facilitate comparisons with other studies, we used the conductivity-chloride linear relationships developed for MSP stormwater ponds (Herb, 2017) to estimate chloride concentrations (reported as "est. Cl^-").

We collected surface water grab samples and deep water samples using a Van Dorn sampler. We collected sediments from the deepest region of all sites ("center") using an Eckman dredge. To characterize within-site variation and extend the gradient of sediment oxygen conditions, nearshore ("edge") sediments were collected from sites sampled in 2019. Edge sediments were less than 30 cm deep and were sampled by pressing a polycarbonate tube into the sediment. For both sediment collection methods, care was taken to preserve only the top 5 cm of the sediment profile. From each sample location, we collected and consolidated at least three sediment samples to ensure sufficient material for incubations and that sediments were representative of each site.

Unfiltered water samples were stored at 4 C for use in denitrification incubations. Subsamples for water chemistry were filtered through a pre-ashed 0.45 µm GF/F filter within 24 hours of collection. Filtered samples for NO_3^- and NH_4^+ were stored frozen until thawed and analyzed on a SmartChem 170 discrete analyzer by the cadmium reduction and phenol hypochlorite methods, respectively. NO_3^- values above zero but below the detection limit of 10 µg/L were replaced with one half the detection limit (5 µg/L). Sediments were stored in sealed plastic baggies without oxygen in the dark at 4 C. Within 24 hours of sediment collection, we started loss on ignition on sediment subsamples to characterize bulk density and organic matter content (Heiri et al., 2001). Total phosphorus (TP) was included as an indicator of site trophic status. We averaged summer surface water TP concentrations collected during prior summer monitoring (June – August) between 2016 and 2022. TP is the sum of total dissolved P and particulate P quantified on a whole water sample using a persulfate digestion and analyzed colorimetrically. A summary of key site characteristics is in Table 3.1, and site-specific values are in Table S3.1.

Denitrification enzyme assays

We chose to measure denitrification using denitrification enzyme assays (DEA). The widespread use of DEA in lentic ecosystems facilitates comparisons with the denitrification literature where urban systems remain underrepresented. Additionally, DEA allows for the rapid assessment and high replication necessary to reveal patterns within our highly variable and dynamic study system. Further, the well-documented limitations of this method do not hinder its usefulness in assessing patterns across conditions, which was our primary goal (Dodds et al., 2017; Groffman et al., 2006).

We used DEA with and without acetylene to measure total denitrification rates and rates of N_2O production, respectively. Measuring the final denitrification product, N_2, is notoriously challenging as high atmospheric concentrations can readily contaminate samples (Groffman et al., 2006). Acetylene blocks the activity of enzymes that perform the final step of denitrification, resulting in the release of easily measured N_2O instead of N_2 gas. Therefore, incubations treated with acetylene represent total denitrification (DeN) as all denitrification products are released as N_2O. Incubations not treated with acetylene represent only N_2O production as the fraction of denitrification products converted to N_2 remains unmeasured. We note that nitrification may also produce N_2O: ammonia oxidation, facilitated by ammonia monooxygenase enzymes, can produce byproducts that are then converted to N_2O via chemodenitrification (Wrage et al., 2001). Both the acetylene treatment and the anoxic conditions maintained in all incubations would inhibit this enzyme (Dodds et al., 2017). Therefore, we do not expect this pathway to be a meaningful source of N_2O in our incubations.

We crossed the acetylene treatment with a carbon + N amendment treatment. Incubations amended with carbon and N (160 µL of 2M glucose and 160 µL of 1.8M potassium nitrate) represent potential denitrification rates when these reactants are were limiting, and thus reflect the upper bound of rates as determined by the influence of site conditions on the denitrifier abundance and activity. Incubations without amendments represent rates of denitrification and N_2O production under ambient substrate availability. Importantly, all incubations were treated with chloramphenicol (160 µL of 0.77 M) to prevent the denitrifier community from synthesizing new enzymes in response to incubation conditions (Dodds et al., 2017).

Incubations were performed within 48 hours of sediment collection. We combined 40 g of homogenized sediment and 40 mL of unfiltered overlying water (surface water for edge sediments and mixed sites, bottom water for center sediments) into 125 mL Wheaton media bottles sealed with caps fitted with butyl septa. Incubations were flushed with helium or N_2 gas to establish anoxic conditions. Incubation anoxia removes the effect of differences in sediment oxygen demand and ensures all N_2O production is via denitrification. Incubation bottles were kept in the dark at room temperature (~20 C) and agitated throughout the incubation period. Prior to samping, bottles were shaken vigorously to equilibrate sediment slurries with the headspace. Incubation headspace was sampled through the septa at 20 minutes and 3 hours. Gas samples were stored in sealed, evacuated agilent gas vials and analyzed on a gas chromatograph for N_2O and O_2. Headspace O_2 was measured as an indicator of the quality of the incubation bottle and gas vial seal and sample integrity. Headspace O_2 averaged 0.29% (median 0.21%). No bottles met the method criterion (O_2 > 5%) to be omitted from the analysis.

Denitrification and N_2O rates were calculated as the difference between the second and first time point divided by the time elapsed. All bottle replicates were averaged. N_2O yield, or the proportion of denitrification products as N_2O, was estimated as the average rate of N_2O produced divided by the average total denitrification rate.

Data analyses

We first related total-DeN to rates of N_2O production using a mixed effects bivariate (BV) model. We compared total-DeN to N_2O yields qualitatively as the non-independence of these variables made regression analysis inappropriate. We also used BV mixed effects models to assess how DeN rate, rate of N_2O production, and N_2O yields differed by sample location (edge vs. center), site type (pond, small lake, and large lake) and mixing regime (stratified vs. polymictic). In the case of site type, where the number of categories exceeded two, we conducted pairwise comparisons using the "emmeans" R package, which accounts for the increased probability of a type I error associated with multiple pairwise comparisons (Fieberg, 2024; Lenth, 2024). Additionally, we compared the water and sediment properties between edge and center sediments using BV mixed effects models using the full data set as well the subset of sites with both center and edge observations.

We performed mixed effects multivariate (MV) modeling to assess the importance of key site characteristics on DeN rate, rate of N_2O production, and N_2O yield. Models included all years and sample locations and only observations without missing values. We selected predictor variables based on prior knowledge of drivers of denitrification, ensuring predictors were not highly correlated (Pearson correlation coefficient < 0.7). The candidate predictors were: water temperature, dissolved oxygen, specific conductance, NO_3^-, NH_4^+, and TP. Following Zuur (2009) and Fieberg (2024), we used manual backwards selection, maximum likelihood ratio tests, and AICc to identify the optimum model for each response variable. We additionally used automatic model selection (Bartoń, 2022). Both methods arrived at the same optimum model. We report the output from the automatic model selection here. Variables included in all final models had variance inflation factors below three. To prevent model overfitting we limited the number of final predictors to 10% of the number of observations. We repeated the MV analyses for only center sediments.

Measured NO_3^- concentrations ranged widely, and over 60% of observations were below detection. To facilitate an assessment of NO_3^- effects, we separated the below detection (< 10 µg/L) and exceptionally high NO_3^- values (> 500 µg/L) into low and high categories, respectively, with the remaining observations classified as medium NO_3^- concentrations (10 – 50 µg/L). We performed BV mixed effects modeling for all measured response variables with NO_3^- classification as a categorical predictor.

We incorporated "site" as a random intercept in all models to account for non-independent observations. We explored the inclusion of year in MV models as an additional random effect to account for variation due to climatic differences between 2019 and 2022. Models fit with a random intercept for site and year did not perform better (difference in AICc > 4) than models fit with only site as a random effect, so year was excluded. We did not include year as a fixed effect in MV models as any effect of year alone due to climatic differences would be confounded by differences in sampling methods between years (e.g., only ponds were sampled in 2019; no edge sediments were sampled in 2022). Additionally, we explored the inclusion of "day of year" in MV models as a fixed effect to assess whether sampling date accounted for any variation in response variables. Day of year never emerged as a significant or meaningful predictor in optimum models or those within 2 AICc units and was excluded from

initial full models. Further, day of year was not significantly correlated with any response variables in BV analyses (results not shown).

Results

Patterns of denitrification

Amended total denitrification rates were highly variable, ranging from 0.5 to 47 mg N m^{-2} hr^{-1} (mean 12, sd 12; Table 3.2). Rates of amended N_2O production (as mg N m^{-2} hr^{-1}) ranged from 0.1 to 23.8 (mean 4.7, sd 5.6). On average, amended N_2O yield was 33% but was also highly variable (sd 23%; range 2 – 79%). Rates of amended DeN were positively related to amended N_2O production accounting for 78% of the variation in amended N_2O rates (Figure 3.2). Amended N_2O yield did not appear to change with changes in amended total DeN rates, though these variables were not independent so no statistical analyses were performed (Figure 3.2).

Table 3.2. Summary of total denitrification rates, rates of N_2O production, and N_2O yields on a per area basis.

Amend-ment	Variable	Sample location	n	Mean	Median	Stnd Dev	Min	Max
C+N	Total-DeN	All	39	11.68	8.27	12.04	0.54	47.23
		Center	30	8.43	4.18	10.35	0.54	47.23
		Edge	9	22.50	26.42	11.32	5.86	38.80
C+N	N2O-rate	All	31	4.69	3.18	5.60	0.01	23.83
		Center	22	3.34	1.64	5.33	0.01	23.83
		Edge	9	8.01	7.04	5.04	2.65	18.88
C+N	N2O-yield	All	31	0.33	0.32	0.23	0.02	0.79
		Center	22	0.31	0.28	0.26	0.02	0.79
		Edge	9	0.38	0.38	0.14	0.18	0.60
None	Total-DeN	All	39	1.253	0.001	6.102	0.000	36.422
		Center	30	1.220	0.001	6.648	0.000	36.422
		Edge	9	1.361	0.000	4.075	0.000	12.228
None	N2O-rate	All	31	0.063	0.004	0.316	0.000	1.764
		Center	22	0.007	0.005	0.011	0.000	0.048
		Edge	9	0.201	0.003	0.586	0.001	1.764
None	N2O-yield	All	31	0.07	0.00	0.21	0.00	0.89
		Center	22	0.08	0.00	0.24	0.00	0.89
		Edge	9	0.05	0.00	0.09	0.00	0.23

Total denitrification rates (Total-DeN) and N_2O rates (N_2O-rate) are expressed on a per area basis (mg N m^{-2} hr^{-1}). N_2O yields (N_2O-yield) are the proportion of Total-DeN products released as N_2O, calculated as N_2O-rate divided by Total-DeN. Summaries of amended (C+N) and unamended incubations are shown. Summaries were performed on all observations as well as each sample location: sediments collected from the center of each site and sediments collected along the edge (≤ 30 cm deep). Values expressed on a per mass basis can be found in Table S3.2.

With the exception of one site that had very high ambient nitrate concentrations, unamended incubations showed very little DeN (max 0.08 mg N m^{-2} hr^{-1}) or N_2O production (max 0.05 mg N m^{-2} hr^{-1}). The outlier site was a stormwater pond sampled two years after construction (2019 Bell Pond; table S3.1). This site had an unamended DeN rate of 36.4 mg N m^{-2} hr^{-1} in center sediments, comparable to the highest rates measured in amended incubations. This was likely due to elevated nitrate in 2019 following construction likely due to extensive landscape disturbance around the pond (4191 µg/L NO_3^--N), more than six times greater than the next site's value (609 µg/L NO_3^--N) and more than three orders of magnitude greater than the median NO_3^- concentration in our data. Unamended total DeN in this site's edge sediments were also high at 12.2 mg N m^{-2} hr^{-1}. Interestingly, unamended N_2O production at this site was not correspondingly high with no measurable N_2O in center sediments and 1.8 mg N m^{-2} hr^{-1} in edge sediments. Resampling center sediments in the Bell pond in 2022 revealed far lower unamended DeN (< 0.01 mg N m^{-2} hr^{-1}) and no change in N_2O, as well as lower NO_3^- concentrations (4.9 µg/L NO_3^--N). Given the unusually high NO_3^- concentrations, the 2019 observations from this site were removed from all statistical analyses except a BV analysis using binned NO_3^-. Additionally, given overall very low rates in unamended incubations, the following results reported and discussed are from amended incubations.

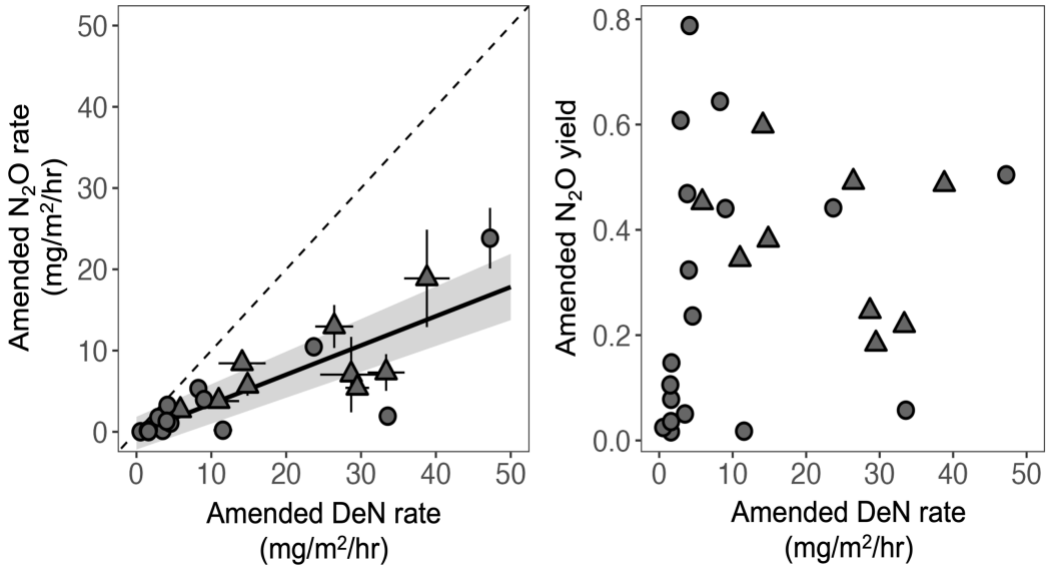

Figure 3.2. N_2O rate and yield compared to total denitrification (DeN) rate.
Left) Rates were measured via denitrification enzyme assays amended with carbon and nitrogen. Points and bars represent the averages and standard deviations of incubation replicates. Circles indicate center

sediments, triangles represent edge sediments (≤ 30 cm deep). The solid trendline captures mixed effects model output (conditional and marginal $R^2 = 0.78$) and was significantly different from zero ($p < 0.05$); line shading represents the 95% confidence interval. A dashed 1:1 line is included for comparison. Right) N_2O yield, or the proportion of denitrification products as N_2O, was calculated by dividing the average rate of N_2O production by the average total DeN rate. Observations are not independent so no statistical tests were performed. Symbols are the same as in the left panel.

Effects of site properties

The larger lakes in our dataset (surface area > 45 ha) had significantly higher rates of amended total DeN measured in center sediments compared to smaller lakes and ponds. We did not see a significant difference in amended N_2O rates or yields (Figure 3.3). In contrast, mixing regime appeared to be important for amended N_2O rate and yields, with both significantly higher in the center sediments of polymictic sites compared to seasonally stratified sites (Figure 3.4). There was no difference in amended total DeN rates measured in center sediments between seasonally stratified and polymictic sites.

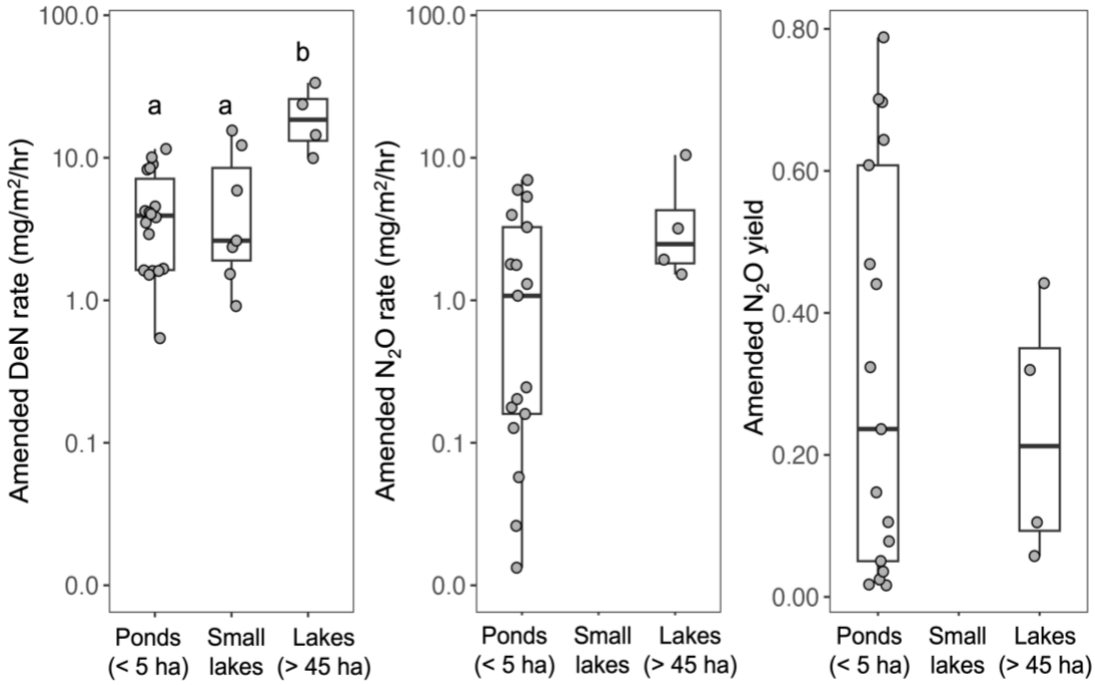

Figure 3.3. Amended total denitrification rate (DeN), N_2O production and N_2O yield vs. site type.
Site type (pond, small lake, larger lake) determined by surface area. Only sediments collected from the center of each site are included. Letters denote significant differences ($p < 0.05$). No N_2O data were collected when small lakes were sampled in 2022, and there were no significant differences between ponds and large lakes in amended N_2O rates or yields. Rates are displayed on a log-10 scale.

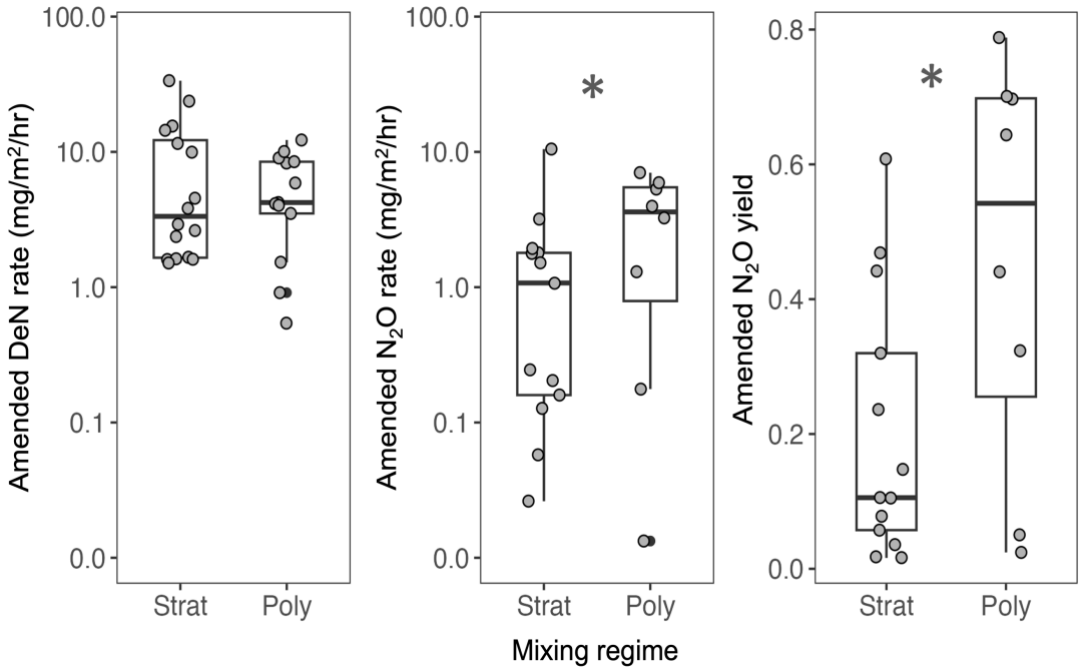

Figure 3.4. Amended total denitrification rate (DeN), N_2O production and N_2O yield in seasonally stratified (Strat) and polymictic (Poly) sites.
Only sediments collected from the center of each site are included. Asterisks indicate a significant difference ($p < 0.05$). Rates are displayed on a log-10 scale.

Edge sediments supported significantly higher rates of amended DeN (marginal R^2 = 0.30; conditional R^2 = 0.51) and N_2O production (marginal R^2 = 0.26; conditional R^2 = 0.43) compared to sediments collected from the center of each site (Figure 3.5). This pattern held when considering only those sites with paired observations from both edge and middle sediments and when all sites were considered. Including sampling location drove an overall effect of depth; removing edge sediments removed any effect of depth on amended DeN and N_2O rates despite a wide range of center sediment depths (60 cm – 10 m). Amended N_2O yield was not significantly different between center and edge sediments. The water overlying edge had lower specific conductivity ($p < 0.05$) compared to water overlying center sediments, and there were no differences in NO_3^- or NH_4^+ concentrations. At the time of sampling, the water overlying edge sediments was also warmer ($p < 0.1$) and had higher DO concentrations ($p < 0.05$), though these differences could change overnight. Additionally, edge sediments had significantly lower percent organic matter ($p < 0.05$).

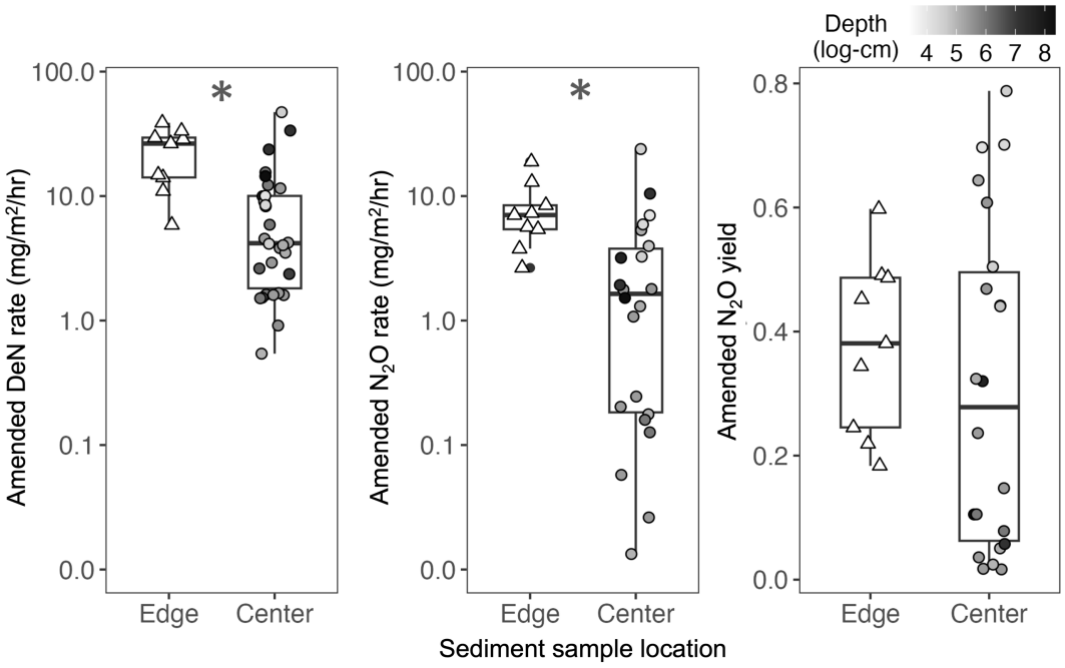

Figure 3.5. Within-site variation in total amended denitrification rate, N_2O production and N_2O yield.
Edge sediments were ≤ 30 cm deep; center sediments ranged from 60 cm to 10 m deep. Sample depth is indicated by symbol color, expressed on a log scale. Asterisks indicate a significant difference between edge and center sediments. Rates are displayed on a log-10 scale.

Models that included both center and edge sediments showed rates of amended total DeN were negatively related to TP concentrations and overlying water specific conductance (Table 3.3; Figure 3.6). Total P was the only significant predictor in the optimum MV model and in all models within two AICc units ($p < 0.05$). There remained a large amount of unexplained variation with the optimum model accounting for ~18% of amended total DeN variance. These same patterns emerged when modeling was repeated with only those sites with associated N_2O data (results not shown), confirming that the subset of sites used to model N_2O rates are representative of broader total DeN in our study. Focusing on center sediments, only the significant negative relationship between amended total DeN and TP concentrations persisted (Table 3.3), and TP was the only significant predictor in all models within two AICc units ($p < 0.05$). Conductivity had no effect on center sediment amended total DeN rates, suggesting that the effect across all sites was driven by low conductivity values and high rates in edge sediments as well as exceptionally high conductivity values in a few center sediments.

Table 3.3. Parameter estimates from the optimum multivariate mixed model for total denitrification rate (Total DeN), rate of N_2O production (N_2O rate), and the proportion of DeN products as N_2O (N_2O yield).

	Parameter estimates									
	TP* µg/L	Cond* µS/cm	DO* µg/L	NO_3^-* µg/L	NH_4^+* µg/L	Sed OM %	Temp c	n	Marg. R^2	Cond. R^2
Center & edge										
Total DeN*	**-0.51**	-0.35						35	0.18	0.18
N_2O rate*	-0.85		0.39					27	0.18	0.18
N_2O yield			0.05					27	0.14	0.14
Center										
Total DeN*	**-0.53**							27	0.17	0.82
N_2O rate*	(-0.87)							19	0.14	0.50
N_2O yield			(0.05)					19	0.13	0.14

All predictors included in the full model are listed. Parameter estimates are included for all predictors that appeared in the optimum model; bold values were significant ($p < 0.05$); non-bold values were significant at $p < 0.1$; values in parentheses were not significant ($p > 0.1$). Models were performed on pooled center and edge sediments and on only center sediments. Asterisks indicate log transformed values. Number of observations (n), the marginal R^2 (Marg. R^2), and conditional R^2 (Cond. R^2) are listed. TP: total phosphorus; Cond: specific conductance; DO: dissolved oxygen; NO_3^- = nitrate; NH_4^+ = ammonium; Sed OM = sediment organic matter; Temp = overlying water temperature at the time of sampling

Rates of amended N_2O production were best captured by a model with a negative effect of TP concentration and positive effect of dissolved oxygen (Table 3.3; Figure 3.7). These predictors were marginally significant ($p < 0.1$). A large fraction of the variation in N_2O remained unexplained, as the optimum model only accounted for 18% of the variance. Dissolved oxygen was also the only predictor in the optimum model for amended N_2O yield (Table 3.3; Figure 3.8). Increasing oxygen in overlying waters appears to increase N_2O production, indicating diminished DeN efficiency. Nonetheless, the effects of oxygen relied on the inclusion of edge sediments, which tended to have higher dissolved oxygen concentrations. Models of center sediment amended N_2O rates and yields had no significant predictors.

Site NO_3^- concentration had no effect on amended total DeN rates, rates of N_2O production, or N_2O yields in MV models. However, binning NO_3^- concentrations gave some support to our hypothesis that NO_3^- concentration influences DeN and N_2O production. BV assessments of all sample locations (Figure 3.9) and only center sediments (Figure 3.10) showed amended total DeN and N_2O rates increased from the low to medium to high NO_3^- categories,

though the significance varied and considerable within-category variation exists. Patterns across amended N_2O yields were less consistent.

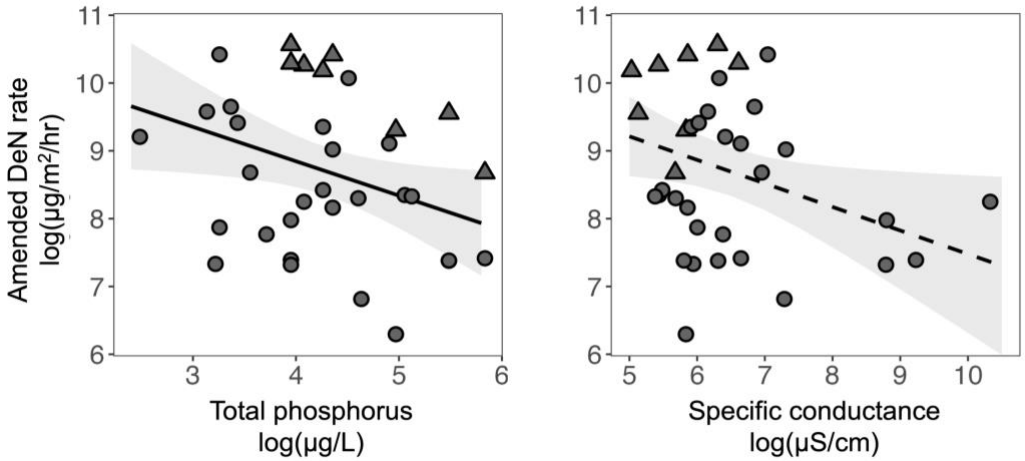

Figure 3.6. Significant predictors of amended total denitrification (DeN) rates.
Rates of amended DeN vs. total phosphorus (TP) concentration and specific conductance, an indicator of road salt inputs. In both panels, circles represent center sediments; triangles represent edge sediments. The trendline represents output from multivariate modeling of amended total DeN (solid line indicates p-value < 0.05; dashed line indicates p-value < 0.1); line shading represents the 95% confidence interval. All values log transformed prior to modeling, and N_2O rates converted to µg/L to facilitate log transformation. Full model output is presented in Table 3.3.

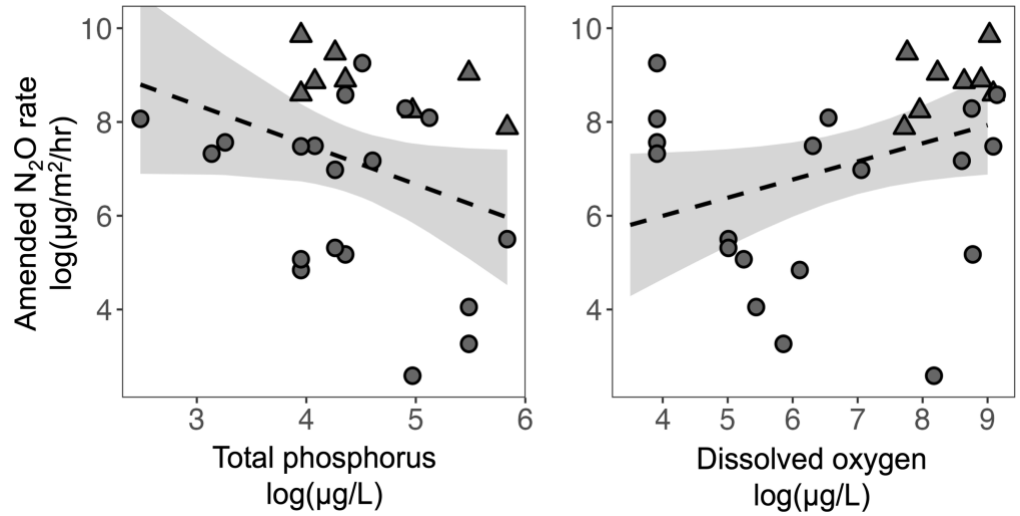

Figure 3.7. Best predictors of amended N_2O rates.
Amended N_2O rates vs. site total phosphorus concentration and dissolved oxygen concentration in overlying water. Total phosphorus was averaged from summer monitoring records. Dissolved oxygen was measured in the water column at the time of sampling, with hypolimnion readings paired with center sediments (circles) and surface readings paired with edge sediments (triangles). The trendline represents multivariate model output (dashed lines indicate p < 0.1); line shading represents the 95% confidence interval. All values log transformed prior to modeling, and N_2O rates converted to µg/L to facilitate log transformation. Full model output is presented in Table 3.3.

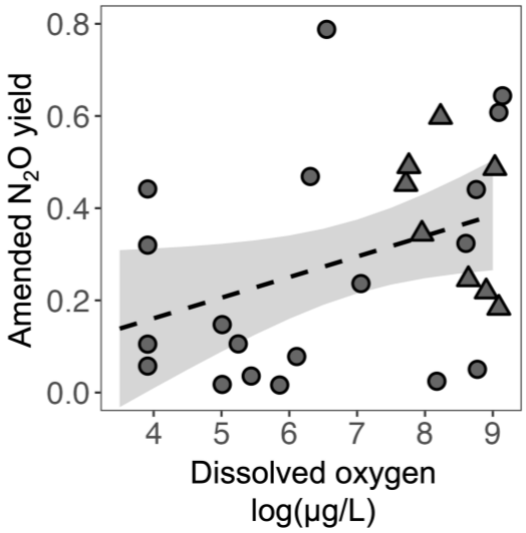

Figure 3.8. Amended N_2O yield vs. site dissolved oxygen concentration.
Amended N_2O yields is the fraction of denitrification products released as N_2O. Dissolved oxygen was measured in the water column at the time of sampling, with hypolimnion readings paired with center sediments (circles) and surface readings paired with edge sediments (triangles). The trendline represents multivariate model output ($p < 0.1$); line shading represents the 95% confidence interval. Full model output can be viewed in Table 3.3.

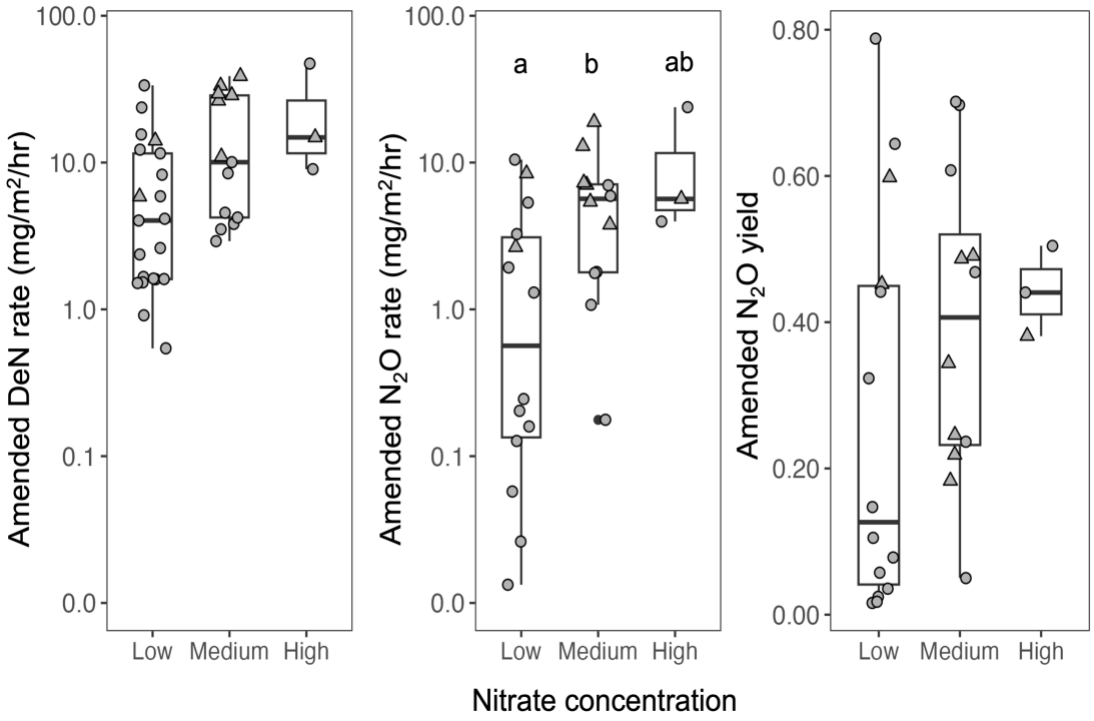

Figure 3.9. Amended total denitrification rate (DeN), N_2O production, and N_2O yield vs. nitrate.
Nitrate concentrations measured in water overlying sediments were classified as low (< 10 µg/L), medium (10 – 50 µg/L), and high (> 500 µg/L). In all panels, circles represent center sediments;

triangles represent edge sediments. Letters denote significant differences ($p < 0.05$). Rates are displayed on a log-10 scale.

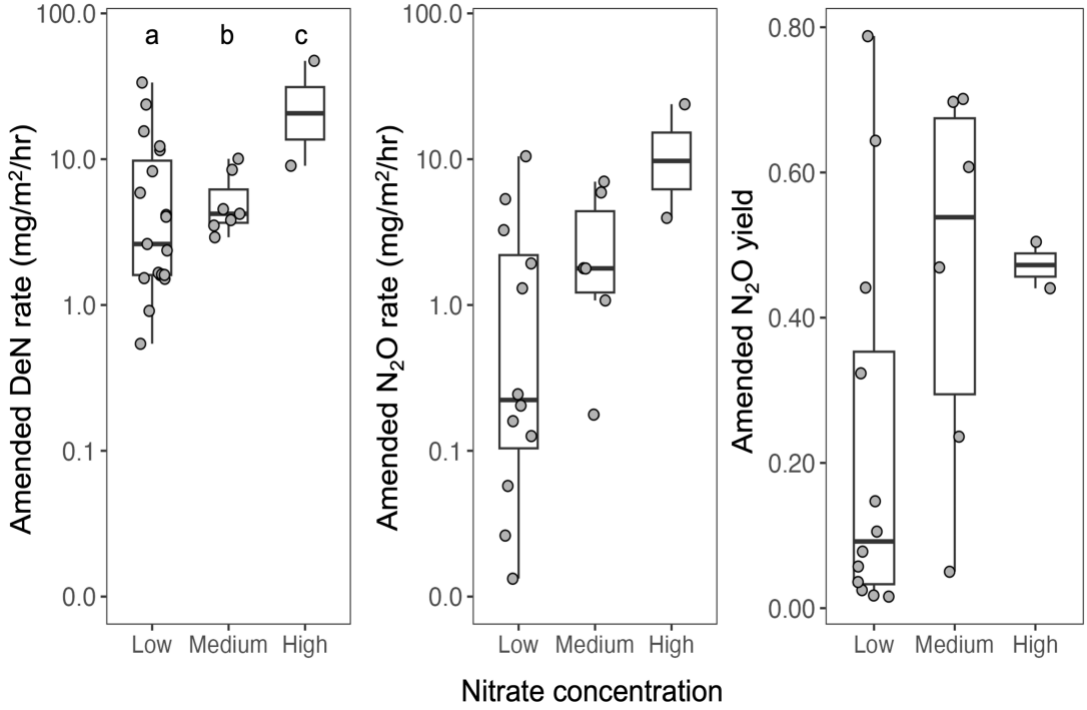

Figure 3.10. Amended total denitrification rate (DeN), N_2O production and N_2O yield vs. nitrate in center sediments.
Nitrate concentrations measured in water overlying sediments were classified as low (< 10 µg/L), medium (10 – 50 µg/L), and high (> 500 µg/L). Only sediments collected from the center of each site are included. In all panels, circles represent center sediments; triangles represent edge sediments. Letters denote significant differences ($p < 0.05$). Rates are displayed on a log-10 scale.

Discussion

Total denitrification

Our findings confirm that urban sediments have the potential to support high rates of N removal via denitrification (Hohman et al., 2021). Comparing our findings to previous work in urban sediments shows general agreement but emphasizes the substantial variation in total DeN rates. While we observed rates as high as 8.5 µg N g^{-1} hr^{-1} (Table S3.2), our mean potential DeN was 1.2 µg N g^{-1} hr^{-1} which was similar to other studies using DEA in urban systems. Bettez and Groffman (2012) reported an average amended DeN of 1.07 µg N g^{-1} hr^{-1} in urban wet ponds while Larson and Grimm (2012) reported 0.1 – 2.8 µg N g^{-1} hr^{-1} in urban lakes and ponds. Blaszczak et al. (2018) found substantially higher potential DeN in stormwater ponds across cities (0.42 – 37.6 µg N g^{-1} hr^{-1}), positing that the difference could be due to omitting acetylene

in their incubations. However, Ginger et al. (2017) applied acetylene inhibition to measure denitrification potentials in shallow lakes across land use types and found some of the highest areal rates in the aquatic literature. Areal DeN rates spanned 14 – 978 mg N m^{-2} hr^{-1} (mean 412) from urban lakes in MSP, which were generally higher than rates in non-urban lakes (2 – 461 mg N m^{-2} hr^{-1}) (Ginger et al., 2017). These values are notably higher than potential areal DeN in our study: 0.5 – 47.2 mg N m^{-2} hr^{-1}, but it is unknown how these values compare to the per mass values reported by Blaszczak et al. (2018). Additionally, Hohman (2021) reported average N_2 fluxes from 0.72 – 1.46 mg N m^{-2} hr^{-1} in stormwater pond sediment cores amended with NO_3^- (no acetylene). The large degree of variation among studies employing similar methodology may be attributable to the inherent heterogeneity in denitrification rates or the dynamic and varied nature of urban ecosystems.

We were able to attribute only a fraction of the variation in DeN in our study to sediment and site properties. Overall, sample location (e.g., edge or center) alone accounted for 30% of the variation in amended total DeN while MV models captured only 19%. Contrary to our expectations, amended total DeN in study sediments was unaffected by ambient NO_3^- and oxygen concentrations. Amended total DeN was negatively associated with both site TP and conductivity. Below we explore the potential mechanisms driving these associations.

Effects of nitrate on denitrification

Despite finding no effect of ambient NO_3^- concentrations, NO_3^- availability is undoubtedly an important regulator of amended total DeN rates in our study systems (Hohman et al., 2021; Piña-Ochoa & Álvarez-Cobelas, 2006; S. Seitzinger et al., 2006). The substantial increase in total DeN between unamended incubations and those amended with NO_3^- points to limitation of DeN by NO_3^- availability, though some of this response could be due to the carbon addition. Further, the notably high unamended DeN rates in Bell Pond were associated with uncommonly high NO_3^- concentrations. Most tellingly, amended total DeN increased steadily in sites with higher NO_3^- categorizations, though considerable variation in rates at low (i.e., below detection) NO_3^- concentrations exists. Study sites low in NO_3^- suggests coupled nitrification-denitrification could be important in these sediments (Seitzinger et al., 2006).

Most N that enters study sites is organic (Finlay et al., 2024) and needs to be mineralized and oxidized into NO_3^- before it can be removed via DeN. Evidence for coupled nitrification-

denitrification is abundant in aquatic sediments and is driven by NO_3^- availability and redox conditions (S. Seitzinger et al., 2006). We expect the proximity of nitrification to sites of denitrification may account for some of the elevated amended total DeN in edge sediments as they tended to have higher overlying dissolved oxygen content and therefore presumably relatively high rates of nitrification. Many of the variables discussed below may regulate DeN by altering NO_3^- availability, including its production via nitrification.

Effects of chloride on denitrification

Site conductivity, a reliable proxy for chloride contamination via road salt in our study sites, emerged as an important predictor of DeN. This negative relationship was driven by four observations in three sites (one site sampled in both 2019 and 2022), which were highly impacted by chloride (conductivity: 6500 – 30600 µS/cm; est. Cl^-: 2.3 – 10.6 mg/L). Removing the four highest chloride observations eliminated the effect of conductivity despite the conductivity of remaining observations spanning an order of magnitude (~150 – 1500 µS/cm; est. Cl^-: 0.02 – 0.5 mg/L).

The lack of DeN response across most conductivity values in our study suggests some degree of salt tolerance in denitrifier communities in inland urban lentic ecosystems. Studies in estuarine environments have demonstrated that denitrifiers possess the ability to resist or rapidly adapt to large changes in salinity (Lee & Francis, 2017; Santoro, 2009). Our findings lend evidence that inland denitrifiers are also flexible. Nonetheless, Wang et al. (2014) found that denitrifier activity in an inland stream can be inhibited by compounding urban stressors such as chloride and heavy metals. Additionally, we collected samples during a period when chloride concentrations are expected to be at their minimum in MSP. Therefore, our findings are relevant only to baseline chloride concentrations and do not reflect responses to peak salinity. Hale and Groffman (2006) measured denitrification potentials under peak salinities (Cl^- raised to 2 ppt) from Baltimore streams with a history of road salt and found that rates did not change. Future work should address whether our study sediments are similarly resilient to salinity when chloride peaks.

The highest conductivity values in our data, which drove the negative correlation between chloride and DeN, could exceed some threshold of denitrifier chloride or pollutant tolerance. The four extreme baseline conductivity values exceeded spring peak conductivities

measured in other study sites (max 4000 µS/cm where spring data were available) and exceeded peak salinities in the Hale and Groffman work described above (2006). This degree of salinization may directly interfere with denitrifiers by inducing osmotic stress (Velasco et al., 2018). Additionally, site conductivity could be an indicator of not only road salt inputs but also inputs of other urban pollutants that co-occur with road salt. Sites most strongly impacted by road salts tend to drain catchments with greater road densities and pavement cover (Novotny et al., 2008). These land cover types are also associated with higher heavy metals, hydrocarbons, and other pollutants known to inhibit microbial growth and function (Simpson et al., 2022). Prior research on the effects of heavy metals on denitrifiers are mixed (Blaszczak et al., 2018; S. Y. Wang et al., 2014), and additional work on the effects of urban pollutants on microbially-mediated ecosystem functions is needed.

Elevated sodium ions that accompany road salt inputs may inhibit DeN indirectly by displacing NH_4^+ from sediments and reducing rates of nitrification (Herbert et al., 2015; Laanbroek & Bollmann, 2007; Novotny et al., 2008). Ion displacement is expected to be most impactful for DeN in sediments at oxic-anoxic interfaces where DeN is linked to NH_4^+ via aerobic nitrification (Duan & Kaushal, 2015). Two sites with the highest observed conductivity values (HarMar and StBizW) had some of the highest NH_4^+ concentrations in overlying water. However, these sediments were frequently exposed to reducing conditions including at the time of sampling, so DeN in these sediments is less likely coupled to nitrification. By reducing nitrification, ion exchange may exacerbate NO_3^- limitation, though the extent of the effects of ion displacement on DeN observed in incubations is unclear.

Another mechanism underlying the relationship between DeN and conductivity is prolonged limitation of DeN reactants in bottom waters in sites with particularly high conductivities. Chloride may be an indicator of this reactant limitation or directly contribute to it. The persistence of elevated chloride throughout the summer may indicate longer residence times, lower storm volumes, and reduced bottom water flushing, consequences of site morphology and hydrology (Herb, 2017). These effects could compound with reduced mixing frequency driven by strong salt-induced density gradients to reduce delivery of DeN substrates as well as inhibit nitrification by prolonging anoxia and reducing nitrate supply. Taken together, these conditions would severely limit the availability of reactants in center sediments and reduce the abundance or

function of denitrifiers. We do not see strong support for this hypothesis as removing edge sediments from the analysis removes the effect of conductivity on amended total DeN. Further, we did not see an effect of site mixing regime on amended DeN rates. While mixing classifications were based on water column monitoring and would capture an effect of high chloride, these systems are highly dynamic and a more formal assessment of mixing frequency is needed. Chloride effects on mixing remains a primary hypothesis in need of more study.

Regardless of the mechanism, it appears that sites that retain high quantities of road salts—one potential benefit stormwater ponds could provide in northern climates—may be limited in their capacity to remove N via denitrification but uncertainties remain. Better understanding the relationship between DeN and chloride pollution can inform decision-making around what functions to prioritize and how to manage sites to accomplish diverse water quality goals (Koch et al., 2014).

Reduced denitrification under elevated total phosphorus

We found that sites enriched in P had a reduced ability to remove N via DeN. This finding aligns with a recent assessment of N and P retention in over 5,000 global lakes (Wu et al, 2022). While higher P concentrations can promote DeN activity in some lakes, there are limits to the stimulatory effects of P on DeN. As P enrichment and eutrophication worsened, N depletion mechanisms (including sedimentation and DeN) were inhibited (Wu et al., 2022). This work focused on larger lakes (median surface area ~100 ha). Our findings suggest that eutrophication can worsen DeN capacities in smaller lentic systems as well. It is unclear whether the potential mechanisms driving this relationship between TP and DeN would also be similar among diverse lentic systems.

Sites with high total P may experience reduced total-DeN potentials due to heightened competition for N when P is abundant. Denitrifiers compete for NO_3^- with algae, macrophytes, and others in the benthic community (Piña-Ochoa & Álvarez-Cobelas, 2006; Risgaard-Peterson, 2003). Veraart et al. (2011) found that uptake by floating and submerged plants, not denitrification, was responsible for a majority of water column NO_3^- reductions in a microcosm experiment. Racchetti et al. (2017) found that competition between denitrifiers and macrophytes was alleviated by high NO_3^- availability in the water column, which was generally low in our study sites. NO_3^- limitation of amended total DeN in high TP sites may be exacerbated by

reduced macrophyte cover and stronger anoxic conditions that prevent NO_3^- production via nitrification.

Total P is a broad indicator of lentic ecosystem trophic status, and its negative correlation with total amended DeN may be capturing an effect of dominant plant communities. Lentic ecosystems dominated by submerged macrophytes tend to have lower TP compared to those dominated by phytoplankton or floating macrophytes, primarily duckweed. We did not collect data on plant community cover or biomass, but field observations suggest that study sites follow this general trend. Further, prior work in MSP confirms that stormwater ponds with duckweed had significantly higher TP concentrations than those without duckweed (Rabaey & Cotner, 2022) as duckweed facilitates anoxic sediment P release. We posit that submerged and floating macrophytes may have differential effects on total amended DeN with macrophytes associated with higher and floating macrophytes associated with lower DeN through effects on sediment oxygen exposure and reactant availability.

At lower TP concentrations, systems are more likely to be dominated by macrophytes. Radial oxygen loss from roots adds oxygen to sediments, creating conditions that allow for aerobic nitrification to produce NO_3^- in close proximity to interstitial anoxic sites where it can be rapidly denitrified (Christensen & Sørensen, 1986). Rooted macrophytes may also increase C available for denitrification by facilitating the sedimentation of organic matter and directly providing labile C to sediments (Christensen & Sørensen, 1986). Additionally, by attenuating wave action macrophytes may increase retention of all DeN reactants in sediments and increase DeN reaction times (Benoy & Kalff, 1999; Saunders & Kalff, 2001). Indeed, prior work in lentic systems observed higher DeN in sediments with macrophytes (Christensen & Sørensen, 1986; Ginger et al., 2017; Saunders & Kalff, 2001). Similarly, Benelli et al (2020) observed a 10-fold increase in nitrification and DeN in the presence of macrophytes compared to bare sediments. The effect of macrophytes was only observed under eutrophic conditions with authors citing reduced competition between macrophytes and denitrifiers as a contributing factor. Further, variation among macrophytes in how deeply roots extend into sediments, the degree that they release oxygen or C from roots, their growth rate, and their nutrient requirements results in meaningful species-to-species differences in how they shape nitrifier and denitrifier communities and function (Benelli et al., 2020; Gordon et al., 2020; Wu et al., 2021).

At higher TP concentrations, study sites were dominated by floating plants like duckweed, which form thick surface mats that can shade out macrophytes. If, as discussed above, macrophytes enhance DeN, the loss of rooted macrophytes would itself diminish DeN abilities. The loss of macrophytes also reduces water column oxygen, and duckweed mats may further strengthen anoxia by inhibiting gaseous exchange with the atmosphere (Rabaey & Cotner, 2022). Prolonged anoxic conditions can reduce DeN by preventing nitrification and the production of NO_3^- in systems that may already have limited NO_3^-.

Taken together, we see evidence that urban lentic ecosystems with low TP concentrations have a greater capacity to remove N, perhaps driven by differences in the dominant plant community. This finding aligns with Ginger et al. (2017), who concluded that increased denitrification associated with macrophyte cover drives reductions in N in clear water (low TP) compared to turbid (high TP) lakes. Additionally, recent stormwater pond research in MSP has identified that duckweed-dominated sites may represent a unique "type" of stormwater pond whose characteristics and functional capacities deviate from ponds dominated by macrophytes or phytoplankton (Rabaey & Cotner, 2022). In particular, they are characterized by poorer water quality and depleted oxygen. Our results contribute to this emerging understanding, finding that duckweed-dominated systems have a reduced capacity to permanently remove N. A diminished capacity to denitrify means a greater fraction of N may remain in the system.

A reduced ability to remove N via denitrification in high TP lentic ecosystems could mean more N available for primary productivity. In other words, reduced DeN could generate a feedback that contributes to stabilizing a eutrophic state. This would depend on the degree that N limits primary production in study systems, but N limitation or co-limitation by N and P are not uncommon in MSP lakes (Bratt et al., 2020). Whether reduced DeN results in more bioavailable N would also depend on the ability of a system to convert abundant yet less bioavailable organic-N into forms available for uptake. As a result, future research should consider the role of N mineralization and nitrification for providing bioavailable N in urban lentic systems.

Denitrification efficiency

Our findings suggest that urban waters have the capacity to be sources of N_2O to the atmosphere with denitrification efficiency varying substantially among sites and sediments. Rates of N_2O production in our study were higher than those reported in Blaszczak et al. (2018).

They reported amended N_2O production ranging from 0 to 1.7 µg N g^{-1} hr^{-1} compared to 0 – 3.7 µg N g^{-1} hr^{-1} (mean 1.24) in our study sediments. N_2O also comprised a small fraction of total amended DeN products, averaging 4% and reaching a maximum of 39% across all sites. Our estimates of amended N_2O yields in MSP were far higher, averaging 33% (maximum of 79%).

Amended rates of N_2O production increased alongside total amended DeN, which is consistent with other findings (Beaulieu et al., 2011; Blaszczak et al., 2018). Total amended DeN alone explained more variation in N_2O production than the top MV model (78% compared to just 18%). As a result, we expect the same mechanisms discussed above for amended total DeN to also influence amended N_2O rates. In support of this, TP concentration was a meaningful predictor of amended N_2O rates in our study. We found no evidence that systems with high potential total amended DeN are inherently less efficient as amended N_2O yield did not appear to worsen as rates of amended total DeN increased. We found support for our hypothesis that dissolved oxygen regulates amended N_2O yields but found no evidence that NO_3^- affects N_2O yields.

Effects of site properties on N_2O

Oxygen appears to reduce denitrification efficiency in urban sediments, increasing the fraction of denitrification products emitted as N_2O. Not only was site dissolved oxygen an important predictor of amended N_2O rates and yields, sites classified as polymictic also had higher amended N_2O rates and yields. N_2O-reductases are the most oxygen-sensitive of the denitrifying enzymes and may be inhibited at lower oxygen concentrations compared to the other enzymes, resulting in N_2O production and release (Beaulieu et al., 2011; Knowles, 1982; Wrage et al., 2001). Our findings suggest that oxygen may block the transcription and/or function of N_2O-reductases in study sites with recent or more frequent sediment oxygen exposure and that this inhibition persists even in anoxic incubations.

Nitrate can also suppress the activity of N_2O-reductases, and denitrifiers may preferentially reduce NO_3^- over N_2O when NO_3^- and sufficient C are available (Bakken et al., 2012; Firestone et al., 1979). An effect of NO_3^- concentrations on N_2O yields has not consistently been observed (Beaulieu et al., 2011; DelVecchia et al., 2023; Liu et al., 2018; McCrackin & Elser, 2010; Weier et al., 1993), and we did not see an effect of NO_3^- concentration on amended N_2O yields. Results from Bell pond were especially interesting, where the highest NO_3^-

concentrations and some of the highest total DeN rates in amended and unamended incubations were accompanied by no measurable N_2O production. In other words, total-DeN under the highest NO_3^- concentration in our dataset was 100% efficient. Measures of overlying water concentrations may not capture NO_3^- availability in pore waters, especially if denitrification is coupled to nitrification. Additionally, Bakken et al. (2012) emphasizes that denitrifying microbial strains vary in their sensitivity to oxygen, NO_3^-, and other environmental factors. Some of the unexplained variation in amended N_2O production (and total DeN) in our study may be due to differences in denitrifier community composition. Additional work to characterize denitrifier community structure across urban sediments is needed.

There is still uncertainty regarding whether conditions that promote high rates of N removal via DeN simultaneously reduce DeN efficiency in urban lentic systems. The only variable to significantly affect amended N_2O yield, dissolved oxygen, was never a significant predictor of total amended DeN in our study sediments but could be contributing to the elevated activities in edge sediments, particularly if DeN is coupled with nitrification. If so, there may be a potential tradeoff between N removal and N_2O production but we cannot make that conclusion based on these findings alone. More work is needed to identify and compare drivers of both DeN and N_2O rates.

We expect that the observed range of potential N_2O yields captures actual variation in DeN efficiency across urban sediments, but whether N_2O yields as high 79% would be realized as actual emissions from sites is unlikely. Field surveys of N_2O emissions from small lentic ecosystems, including stormwater ponds, frequently report low or below detection values (Bauduin et al., 2024; Rabaey & Cotner, 2022). Beaulieu et al. (2011), measuring $\delta^{15}N_2$ and $\delta^{15}N_2O$ after a ^{15}N-tracer addition, found the greatest N_2O emissions in urban streams compared to other land use types but overall <1% of denitrified N was released as N_2O. As with total DeN estimates, estimates of N_2O production and N_2O yield from amended incubations represent an upper-bound when ample reactants are available. We also acknowledge methodological reasons why even these upper-bound N_2O production or yields could be high. NO_3^- can suppress N_2O-reductase, meaning NO_3^- amendments in our incubations may amplify N_2O release and, therefore, yields. N_2O production may also be higher than those measured using other methods due to shaking incubation bottles prior to sampling headspace gases, which releases N_2O from

porewaters when it may otherwise have been further denitrified. We expect the effects of both limitations to be consistent across samples and would not affect overall relationships observed.

Intra-site variability in denitrification

Consistent with the heterogeneous nature of DeN, we saw high within-site spatial variation in DeN even in systems where less than two meters separate edge and center sediments (Saunders & Kalff, 2001). Consistent with previous work, edge sediments had significantly higher potential total-DeN compared to center sediments (Bruesewitz et al., 2012; Grantz et al., 2012; Saunders & Kalff, 2001). Edge habitats integrate the characteristics discussed above that support high DeN. Specifically, reactants are delivered to edge sediment pore waters with frequent wind and wave action augmented by macrophytes, inputs from riparian areas, and/or high rates of nitrification (Bruesewitz et al., 2012; Cook et al., 2006; Kuwae et al., 2006). While we did not observe significant differences in NO_3^- and NH_4^+ concentrations overlying edge and center sediments and edge sediments had lower percent organic matter compared to center sediments, these values do not reflect reactant availability in pore waters or carbon degradability. Any potential adverse effects of high chloride or other pollutants are expected to be most prevalent in deeper regions, which is confirmed in our data. In addition, the higher temperatures we observed in shallow regions can increase microbial activities, including nitrification and DeN (Saunders & Kalff, 2001). These findings underscore the importance of incorporating spatial variation into assessments of the denitrification and N removal capabilities of ecosystems.

Inter-site variability in denitrification

Large lakes had significantly higher amended total DeN rates compared to smaller lakes and ponds. This was contrary to expectations, but reflects nuanced denitrifying conditions in small lentic systems. Many sites receive high inputs of N from their watersheds but most are in organic forms inaccessible to denitrifiers and while they may be shallow, they frequently experience persistent anoxia (Finlay et al., 2024; Holgerson et al., 2022; Janke et al., 2022). Together these conditions would result in NO_3^- limitation of DeN as the aerobic conditions required to convert organic N to NO_3^- via nitrification are not supported. Others have found DeN to be NO_3^- limited in stormwater ponds for these reasons (Goeckner et al., 2024; Hohman et al., 2021) As a result, sediment oxygen exposure and mixing patterns may be important determinants of N removal capacity in small lentic systems. We did not see an effect of the mixing regime on

amended total DeN, but high-frequency monitoring of these dynamic sites could better capture mixing frequency and duration.

Conclusions

We observed the highest rates of amended DeN in systems with low TP concentrations and conductivity values (i.e., road salt inputs), as well as in edge sediments and in center sediments from the largest systems sampled. In other words, center sediments from small, eutrophic and chloride-impacted systems were less capable of removing N via DeN. Numerous potentially interacting mechanisms may underpin these findings and are detailed above.

One shared possibility that we think is particularly likely is that amended DeN rates in our study were limited by the interacting effects of mixing, sediment oxygen exposure, and reactant availability. Elevated TP concentrations and road salt inputs are associated with reduced mixing and stronger bottom water anoxia. Smaller lentic systems may experience more prolonged bottom water anoxia and infrequent mixing compared to edge sediments or center sediments in larger systems. In our systems where NO_3^- is scarce and organic N is abundant, persistent anoxia inhibits aerobic nitrification and limits DeN reactant availability. Mixing regime and dissolved oxygen concentrations in overlying water had no effect on amended DeN rates in our study, but these variables may not capture sediment oxygen and mixing regimes in these dynamic and variable systems.

Nevertheless, measures of sediment oxygen exposure emerged as important determinants of N_2O yields. We found the greatest N_2O yield from sediments with higher dissolved oxygen concentrations in overlying water and from sediments collected from sites designated as polymictic. Given this finding, clarifying the role of sediment oxygen exposure for urban lentic system DeN rates and efficiencies should be prioritized. Until then, our findings suggest that efforts to maintain clear water, or lower TP, states in smaller urban lentic ecosystems will benefit their ability to remove N.

Works cited

Bakken, L. R., Bergaust, L., Liu, B., & Frostegard, A. (2012). Regulation of denitrification at the cellular level: A clue to the understanding of N2O emissions from soils. *Philosophical Transactions of the Royal Society B: Biological Sciences, 367,* 1226–1234. https://doi.org/10.1098/rstb.2011.0321

Bartoń, K. (2022). *MuMIn: Multi-Model Inference.* (Version 1.46.0) [R]. https://CRAN.R-project.org/package=MuMIn

Bauduin, T., Gypens, N., & Borges, A. V. (2024). Seasonal and spatial variations of greenhouse gas (CO_2, CH_4 and N_2O) emissions from urban ponds in Brussels. *Water Research, 253,* 121257. https://doi.org/10.1016/j.watres.2024.121257

Beaulieu, J. J., Tank, J. L., Hamilton, S. K., Wollheim, W. M., Hall, R. O., Mulholland, P. J., Peterson, B. J., Ashkenas, L. R., Cooper, L. W., Dahm, C. N., Dodds, W. K., Grimm, N. B., Johnson, S. L., McDowell, W. H., Poole, G. C., Valett, H. M., Arango, C. P., Bernot, M. J., Burgin, A. J., … Thomas, S. M. (2011). Nitrous oxide emission from denitrification in stream and river networks. *Proceedings of the National Academy of Sciences of the United States of America, 108*(1), 214–219. https://doi.org/10.1073/pnas.1011464108

Benelli, S., Ribaudo, C., Bertrin, V., Bartoli, M., & Fano, E. A. (2020). Effects of macrophytes on potential nitrification and denitrification in oligotrophic lake sediments. *Aquatic Botany, 167,* 103287. https://doi.org/10.1016/j.aquabot.2020.103287

Benoy, G. A., & Kalff, J. (1999). Sediment accumulation and Pb burdens in submerged macrophyte beds. *Limnology and Oceanography*, *44*(4), 1081–1090. https://doi.org/10.4319/lo.1999.44.4.1081

Bernhardt, E. S., Band, L. E., Walsh, C. J., & Berke, P. E. (2008). Understanding, Managing, and Minimizing Urban Impacts on Surface Water Nitrogen Loading. *Annals of the New York Academy of Sciences, 1134*(1), 61–96. https://doi.org/10.1196/annals.1439.014

Bernhardt, E. S., Blaszczak, J. R., Ficken, C. D., Fork, M. L., Kaiser, K. E., & Seybold, E. C. (2017). Control Points in Ecosystems: Moving Beyond the Hot Spot Hot Moment Concept. *Ecosystems, 20,* 665-682. https://doi.org/10.1007/s10021-016-0103-y

Bettez, N. D., & Groffman, P. M. (2012). Denitrification Potential in Stormwater Control Structures and Natural Riparian Zones in an Urban Landscape. *Environmental Science and Technology*, *46,* 10909–10917.

Blaszczak, J. R., Bernhardt, E. S., Hall, S. J., Hobbie, S. E., Neill, C., Badgley, B. D., Rivers, E. N., Pataki, D. E., Steele, M. K., Heffernan, J. B., Groffman, P. M., & Morse, J. L. (2018). Sediment chemistry of urban stormwater ponds and controls on denitrification. *Ecosphere*, *9*(6), e02318. https://doi.org/10.1002/ecs2.2318

Bratt, A. R., Finlay, J. C., Welter, J. R., Vculek, B. A., & Van Allen, R. E. (2020). Co-limitation by N and P Characterizes Phytoplankton Communities Across Nutrient Availability and Land Use. *Ecosystems*, *23*(6), 1121–1137. https://doi.org/10.1007/s10021-019-00459-6

Bruesewitz, D. A., Tank, J. L., & Hamilton, S. K. (2012). Incorporating spatial variation of nitrification and denitrification rates into whole-lake nitrogen dynamics. *Journal of Geophysical Research*, *117*, 1–12. https://doi.org/10.1029/2012JG002006

Christensen, P. B., & Sørensen, J. (1986). Temporal Variation of Denitrification Activity in Plant-Covered, Littoral Sediment from Lake Hampen, Denmark. *Applied and Environmental Microbiology*, *51*(6), 1174–1179. https://doi.org/10.1128/aem.51.6.1174-1179.1986

Cook, P. L. M., Wenzhöfer, F., Rysgaard, S., Galaktionov, O. S., Meysman, F. J. R., Eyre, B. D., Cornwell, J., Huettel, M., & Glud, R. N. (2006). Quantification of denitrification in permeable sediments: Insights from a two-dimensional simulation analysis and experimental data. *Limnology and Oceanography: Methods*, *4*(9), 294–307. https://doi.org/10.4319/lom.2006.4.294

Davidson, E. A., & Seitzinger, S. (2006). The enigma of progress in denitrification research. *Ecological Applications*, *16*(6), 7. https://doi.org/10.1890/1051-0761(2006)016[2057:TEOPID]2.0.CO;2

Deemer, B. R., Harrison, J. A., & Whitling, E. W. (2011). Microbial dinitrogen and nitrous oxide production in a small eutrophic reservoir: An in situ approach to quantifying hypolimnetic process rates. *Limnology and Oceanography*, *56*(4), 1189–1199. https://doi.org/10.4319/lo.2011.56.4.1189

DelVecchia, A. G., Rhea, S., Aho, K. S., Stanley, E. H., Hotchkiss, E. R., Carter, A., & Bernhardt, E. S. (2023). Variability and drivers of CO_2 , CH_4 , and N_2 O concentrations in streams across the United States. *Limnology and Oceanography*, *68*(2), 394–408. https://doi.org/10.1002/lno.12281

Dodds, W. K., Burgin, A. J., Marcarelli, A. M., & Strauss, E. A. (2017). Nitrogen Transformations. In *Methods in Stream Ecology* (Issue 2010). Elsevier Inc. https://doi.org/10.1016/B978-0-12-813047-6.00010-3

Duan, S., & Kaushal, S. S. (2015). Salinization alters fluxes of bioreactive elements from stream ecosystems across land use. *Biogeosciences*, *12*(23), 7331–7347. https://doi.org/10.5194/bg-12-7331-2015

Dugan, H.A, Bartlett, S.L., Burke, S.M., Doubek, J.P., Krivak-Tetley, F.E., Skaff, N.K., Summers, J.C., Farrell, K.J., McCullough, I.M., Morales-Williams, A.M., Roberts, D.C., Ouyang, Z., Scordo, F., Hanson, P.C., Weathers, K.C. (2017). Salting our freshwater lakes. *Proceedings of the National Academy of Sciences*, *114*(17), 4453-4458. www.pnas.org/cgi/doi/10.1073/pnas.1620211114

Elser, J. J., Bracken, M. E. S., Cleland, E. E., Gruner, D. S., Harpole, W. S., Hillebrand, H., Ngai, J. T., Seabloom, E. W., Shurin, J. B., & Smith, J. E. (2007). Global analysis of nitrogen and phosphorus limitation of primary producers in freshwater, marine and terrestrial ecosystems. *Ecology Letters*, *10*(12), 1135–1142. https://doi.org/10.1111/j.1461-0248.2007.01113.x

Fieberg, J. (2024). *Statistics for Ecologists: A Frequentist and Bayesian Treatment of Modern Regression Models*. University of Minnesota Libraries Publishing. https://doi.org/10.24926/9781959870029

Finlay, J. C., Janke, B. D., Trojan, M., Wilson, B., & Marek-Sparts, M. (2024). *Leveraging Minnesota's Stormwater Data for Improved Modeling and Management of Water Quality in Cities; Final Report*. Retrieved from the University Digital Conservancy, https://hdl.handle.net/11299/259975

Firestone, M. K., Smith, M. S., Firestone, R. B., & Tiedje, J. M. (1979). The Influence of Nitrate, Nitrite, and Oxygen on the Composition of the Gaseous Products of Denitrification in Soil. *Soil Science Society of America Journal*, *43*(6), 1140–1144. https://doi.org/10.2136/sssaj1979.03615995004300060016x

Fork, M. L., & Heffernan, J. B. (2014). Direct and Indirect Effects of Dissolved Organic Matter Source and Concentration on Denitrification in Northern Florida Rivers. *Ecosystems*, *17*(1), 14–28. https://doi.org/10.1007/s10021-013-9705-9

Galloway, J. N., Townsend, A. R., Erisman, J. W., Bekunda, M., Cai, Z., Freney, J. R., Martinelli, L. a, Seitzinger, S. P., & Sutton, M. a. (2008). Transformation of the Nitrogen Cycle: Recent Trends, Questions, and Potential Solutions. *Science*, *320*(May), 889–892. https://doi.org/10.1126/science.1136674

Ginger, L. J., Zimmer, K. D., Herwig, B. R., Hanson, M. A., Hobbs, W. O., Small, G. E., & Cotner, J. B. (2017). Watershed vs. within-lake drivers of nitrogen: Phosphorus dynamics in shallow lakes. *Ecological Applications*, *27*(7), 2155–2169. https://doi.org/10.1002/eap.1599

Goeckner, A. H., Smyth, A. R., Holgerson, M. A., & Reisinger, A. J. (2024). Subtropical stormwater ponds are more frequently net nitrogen fixing compared to natural ponds. *Biogeochemistry*, *167*(8), 1007–1024. https://doi.org/10.1007/s10533-024-01153-z

Gordon, B. A., Lenhart, C., & LaPara, T. M. (2020). A comparison of nitrate removal and denitrifying bacteria populations among three wetland plant communities. *Journal of Environmental Quality*, *49*(1), 210–219. https://doi.org/10.1002/jeq2.20004

Grantz, E. M., Kogo, A., & Scott, J. T. (2012). Partitioning whole-lake denitrification using in situ dinitrogen gas accumulation and intact sediment core experiments. *Limnology and Oceanography*, *57*(4), 925–935. https://doi.org/10.4319/lo.2012.57.4.0925

Groffman, P. M., Altabet, M. A., Böhlke, J. K., Butterbach-bahl, K., David, M. B., Firestone, M. K., Giblin, A. E., Kana, T. M., Nielsen, L. P., Voytek, M. A., Groffman, P. M., Altabet, M. A., Bohlke, J. K., Butterbach-bahl, K., David, M. B., Firestone, M. K., Giblin, A. E., Kana, T. M., Nielsen, L. P., & Voytek, M. A. (2006). Methods for Measuring Denitrification: Diverse Approaches to a Difficult Problem. *Ecological Applications*, *16*(6), 2091–2122. https://doi.org/10.1890/1051-0761(2006)016[2091:MFMDDA]2.0.CO;2

Hale, R. L., & Groffman, P. M. (2006). Chloride Effects on Nitrogen Dynamics in Forested and Suburban Stream Debris Dams. *Journal of Environment Quality*, *35*(6), 2425. https://doi.org/10.2134/jeq2006.0164

Hall, S. J., Learned, J., Ruddell, B., Larson, K. L., Cavender-Bares, J., Bettez, N., Groffman, P. M., Grove, J. M., Heffernan, J. B., Hobbie, S. E., Morse, J. L., Neill, C., Nelson, K. C., O'Neil-Dunne, J. P. M., Ogden, L., Pataki, D. E., Pearse, W. D., Polsky, C., Chowdhury, R. R., … Trammell, T. L. E. (2016). Convergence of microclimate in residential landscapes across diverse cities in the United States. *Landscape Ecology*, *31*(1), 101–117. https://doi.org/10.1007/s10980-015-0297-y

Heiri, O., Lotter, A. F., & Lemcke, G. (2001). Loss on ignition as a method for estimating organic and carbonate content in sediments: Reproducibility and comparability of results. *Journal of Paleolimnology*, *25*, 101–110.

Herb, W., Janke, B., Heinz, S. (2017). *Study of De-icing Salt Accumulation and Transport Through a Watershed; Final report*. Minnesota Department of Transportation.

Herbert, E. R., Boon, P., Burgin, A. J., Neubauer, S. C., Franklin, R. B., Ardon, M., Hopfensperger, K. N., Lamers, L. P. M., Gell, P., & Langley, J. A. (2015). A global perspective on wetland salinization: Ecological consequences of a growing threat to freshwater wetlands. *Ecosphere*, *6*(10), 1–43. https://doi.org/10.1890/ES14-00534.1

Hobbie, S. E., Finlay, J. C., Janke, B. D., Nidzgorski, D. A., Millet, D. B., & Baker, L. A. (2017). Contrasting nitrogen and phosphorus budgets in urban watersheds and implications for managing urban water pollution. *Proceedings of the National Academy of Sciences*, *114*(16), 4177-4182. https://doi.org/10.1073/pnas.1618536114

Hohman, S. P., Smyth, A. R., Bean, E. Z., & Reisinger, A. J. (2021). Internal nitrogen dynamics in stormwater pond sediments are influenced by pond age and inorganic nitrogen availability. *Biogeochemistry*, *156*(2), 255–278. https://doi.org/10.1007/s10533-021-00843-2

Holgerson, M.A., Richardson, D.C., Roith, J., Bortolotti, L.E., Finlay, K., Hornbach, D.J., Gurung, K., Ness, A., Andersen, M.R., Bansal, S., Finlay, J.C., Cianci-Gaskill, J.A., Hahn, S., Janke, B.D., McDonald, C., Mesman, J.P., North, R.L., Roberts, C.O., Sweetman, J.N., Webb, J.R. (2022). Classifying Mixing Regimes in Ponds and Shallow Lakes. *Water Resources Research, 58*(7). https://agupubs.onlinelibrary.wiley.com/doi/10.1029/2022WR032522

Janke, B. D., Finlay, J. C., & Hobbie, S. E. (2017). Trees and Streets as Drivers of Urban Stormwater Nutrient Pollution. *Environmental Science and Technology*. https://doi.org/10.1021/acs.est.7b02225

Janke, B. D., Finlay, J. C., Taguchi, V. J., & Gulliver, J. S. (2022). Hydrologic processes regulate nutrient retention in stormwater detention ponds. *Science of the Total Environment*, *823*, 153722. https://doi.org/10.1016/j.scitotenv.2022.153722

Kim, S. Y., & Koretsky, C. (2013). Effects of road salt deicers on sediment biogeochemistry. *Biogeochemistry*, *112*(1–3), 343–358. https://doi.org/10.1007/s10533-012-9728-x

Knowles, R. (1982). Denitrification. *Microbiological Reviews*, *46*(1), 43–70.

Koch, B. J., Febria, C. M., Gevrey, M., Wainger, L. A., & Palmer, M. A. (2014). Nitrogen Removal by Stormwater Management Structures: A Data Synthesis. *Journal of the American Water Resources Association*, *50*(6), 1594–1607. https://doi.org/10.1111/jawr.12223

Kuwae, T., Kamio, K., Inoue, T., Miyoshi, E., & Uchiyama, Y. (2006). Oxygen exchange flux between sediment and water in an intertidal sandflat, measured in situ by the eddy-correlation method. *Marine Ecology Progress Series*, *307*, 59–68. https://doi.org/10.3354/meps307059

Laanbroek, H., & Bollmann, A. (2007). *Nitrification in Inland Waters*. In Ward, B.B., Arp, D.J., & Klotz, M.G. (Eds.), *Nitrification* (385–403). ASM Press. 10.1128/9781555817145.ch15

Larson, E. K., & Grimm, N. B. (2012). Small-scale and extensive hydrogeomorphic modification and water redistribution in a desert city and implications for regional nitrogen removal. *Urban Ecosystems*, *15*(1), 71–85. https://doi.org/10.1007/s11252-011-0208-1

Laverman, A. M., Canavan, R. W., Slomp, C. P., & Cappellen, P. V. (2007). Potential nitrate removal in a coastal freshwater sediment (Haringvliet Lake, The Netherlands) and response to salinization. *Water Research*, *41*(14), 3061–3068. https://doi.org/10.1016/j.watres.2007.04.002

Lee, J. A., & Francis, C. A. (2017). Deep nirS amplicon sequencing of San Francisco Bay sediments enables prediction of geography and environmental conditions from denitrifying community composition. *Environmental Microbiology*, *19*(12), 4897–4912. https://doi.org/10.1111/1462-2920.13920

Lenth, R. V. (2024). *emmeans: Estimated Marginal Means, aka Least-Squares Means.* (Version 1.10.0) [R]. https://CRAN.R-project.org/package=emmeans

Liu, W., Jiang, X., Zhang, Q., Li, F., & Liu, G. (2018). Has Submerged Vegetation Loss Altered Sediment Denitrification, N_2O Production, and Denitrifying Microbial Communities in Subtropical Lakes? *Global Biogeochemical Cycles*, *32*(8), 1195–1207. https://doi.org/10.1029/2018GB005978

McCrackin, M. L., & Elser, J. J. (2010). Atmospheric nitrogen deposition influences denitrification and nitrous oxide production in lakes. *Ecology*, *91*(2), 528–539. http://www.jstor.org/stable/25661078

MN DNR. (n.d.). *Twin Cities Metropolitan Area Normals, Means, and Extremes (1981-2010)*. Minnesota Dept. of Natural Resources. https://www.dnr.state.mn.us/climate/twin_cities/normals.html

Mosier, A. C., & Francis, C. A. (2010). Denitrifier abundance and activity across the San Francisco Bay estuary. *Environmental Microbiology Reports*, *2*(5), 667–676. https://doi.org/10.1111/j.1758-2229.2010.00156.x

Novotny, E. V., Murphy, D., & Stefan, H. G. (2008). Increase of urban lake salinity by road deicing salt. *Science of the Total Environment*, *406*(1–2), 131–144. https://doi.org/10.1016/j.scitotenv.2008.07.037

Piña-Ochoa, E., & Álvarez-Cobelas, M. (2006). Denitrification in Aquatic Environments: A Cross-system Analysis. *Biogeochemistry*, *81*(1), 111–130. https://doi.org/10.1007/s10533-006-9033-7

Rabaey, J., & Cotner, J. (2022). Pond greenhouse gas emissions controlled by duckweed coverage. *Frontiers in Environmental Science*, *10*, 889289. https://doi.org/10.3389/fenvs.2022.889289

Racchetti, E., Longhi, D., Ribaudo, C., Soana, E., & Bartoli, M. (2017). Nitrogen uptake and coupled nitrification–denitrification in riverine sediments with benthic microalgae and rooted macrophytes. *Aquatic Sciences*, *79*(3), 487–505. https://doi.org/10.1007/s00027-016-0512-1

Ravishankara, A. R., Daniel, J. S., & Portmann, R. W. (2009). Nitrous Oxide (N_2 O): The Dominant Ozone-Depleting Substance Emitted in the 21st Century. *Science*, *326*(5949), 123–125. https://doi.org/10.1126/science.1176985

Richardson, D. C., Holgerson, M. A., Farragher, M. J., Hoffman, K. K., King, K. B. S., Alfonso, M. B., Andersen, M. R., Cheruveil, K. S., Coleman, K. A., Farruggia, M. J., Fernandez, R. L., Hondula, K. L., López Moreira Mazacotte, G. A., Paul, K., Peierls, B. L., Rabaey, J. S., Sadro, S., Sánchez, M. L., Smyth, R. L., & Sweetman, J. N. (2022). A functional definition to distinguish ponds from lakes and wetlands. *Scientific Reports*, *12*(1), 10472. https://doi.org/10.1038/s41598-022-14569-0

Risgaard-Peterson, N. (2003). Coupled nitrification-denitrification in autotrophic and heterotrophic estuarine sediments: On the influence of benthic microalgae. *Limnology and Oceanography*, *48*(1), 93–105. https://doi.org/10.4319/lo.2003.48.1.0093

Robert Hamersley, M., Woebken, D., Boehrer, B., Schultze, M., Lavik, G., & Kuypers, M. M. M. (2009). Water column anammox and denitrification in a temperate permanently stratified lake (Lake Rassnitzer, Germany). *Systematic and Applied Microbiology*, *32*(8), 571–582. https://doi.org/10.1016/j.syapm.2009.07.009

Rysgaard, S., Risgaard-Petersen, N., Niels Peter, S., Kim, J., & Lars Peter, N. (1994). Oxygen regulation of nitrification and denitrification in sediments. *Limnology and Oceanography*, *39*(7), 1643–1652. https://doi.org/10.4319/lo.1994.39.7.1643

Rysgaard, S., Thastum, P., Dalsgaard, T., Christensen, P. B., Sloth, N. P., Estuaries, S., & Mar, N. (1999). Effects of Salinity on NH4 + Adsorption Capacity , Nitrification , and Denitrification in Danish Estuarine Sediments Stable. *Estuaries*, *21*(1), 21-30. http://www.jstor.org/stable/1352923

Santoro, A. E. (2009). Microbial nitrogen cycling at the saltwater–freshwater interface. *Hydrogeology Journal*, *18*(1), 187–202. https://doi.org/10.1007/s10040-009-0526-z

Saunders, D. L., & Kalff, J. (2001). Denitrification rates in the sediments of Lake Memphremagog, Canada–USA. *Water Research*, *35*(8), 1897–1904. https://doi.org/10.1016/S0043-1354(00)00479-6

Seitzinger, S., Harrison, J., Bohlke, J., Bouwman, A., Lowrance, R., Peterson, B., Tobias, C., & Van Drecht, G. (2006). Denitrification across landscapes and waterscapes: A synthesis. *Ecological Applications*, *16*(6), 2064–2090. https://doi.org/10.1890/1051-0761(2006)016[2064:DALAWA]2.0.CO;2

Seitzinger, S. P., Nixon, S. W., & Pilson, M. E. Q. (1984). Denitrification and nitrous oxide production in a coastal marine ecosystem. *Limnology and Oceanography*, *29*(1), 73–83. https://doi.org/10.4319/lo.1984.29.1.0073

Simpson, I. M., Winston, R. J., & Brooker, M. R. (2022). Effects of land use, climate, and imperviousness on urban stormwater quality: A meta-analysis. *Science of The Total Environment*, *809*, 152206. https://doi.org/10.1016/j.scitotenv.2021.152206

Song, K., Xenopoulos, M. A., Buttle, J. M., Marsalek, J., Wagner, N. D., Pick, F. R., & Frost, P. C. (2013). Thermal stratification patterns in urban ponds and their relationships with vertical nutrient gradients. *Journal of Environmental Management*, *127*, 317–323. https://doi.org/10.1016/j.jenvman.2013.05.052

Velasco, J., Gutiérrez-Cánovas, C., Botella-Cruz, M., Sánchez-Fernández, D., Arribas, P., Carbonell, J. A., Millán, A., & Pallarés, S. (2018). Effects of salinity changes on aquatic organisms in a multiple stressor context. *Philosophical Transactions of the Royal Society B: Biological Sciences*, *374*(1764), 20180011. https://doi.org/10.1098/RSTB.2018.0011

Veraart, A. J., De Bruijne, W. J. J., De Klein, J. J. M., Peeters, E. T. H. M., & Scheffer, M. (2011). Effects of aquatic vegetation type on denitrification. *Biogeochemistry*, *104*(1–3), 267–274. https://doi.org/10.1007/s10533-010-9500-z

Wang, G., Xia, X., Liu, S., Zhang, S., Yan, W., & McDowell, W. H. (2021). Distinctive Patterns and Controls of Nitrous Oxide Concentrations and Fluxes from Urban Inland Waters. *Environmental Science & Technology*, *55*(12), 8422–8431. https://doi.org/10.1021/acs.est.1c00647

Wang, S. Y., Bernhardt, E. S., & Wright, J. P. (2014). Urban stream denitrifier communities are linked to lower functional resistance to multiple stressors associated with urbanization. *Hydrobiologia*, *726*(1), 13–23. https://doi.org/10.1007/s10750-013-1747-7

Weier, K. L., Doran, J. W., Power, J. F., & Walters, D. T. (1993). Denitrification and the Dinitrogen/Nitrous Oxide Ratio as Affected by Soil Water, Available Carbon, and Nitrate. *Soil Science Society of America Journal*, *57*(1), 66. https://doi.org/10.2136/sssaj1993.03615995005700010013x

Wrage, N., Velthof, G. L., Beusichem, M. L. V., & Oenema, O. (2001). Role of nitrifier denitrification in the production of nitrous oxide. *Soil Biology & Biochemistry*, *33*, 1723–1732.

Wu, X., Probst, A., Barret, M., Payre-Suc, V., Camboulive, T., & Granouillac, F. (2021). Spatial variation of denitrification and key controlling factors in streams and ponds sediments from a critical zone (southwestern France). *Applied Geochemistry*, *131*, 105009. https://doi.org/10.1016/j.apgeochem.2021.105009

Wu, Z., Li, J., Sun, Y., Peñuelas, J., Huang, J., Sardans, J., Jiang, Q., Finlay, J.C., Britten, G.L., Follows, M.J., Gao, W., Qin, B., Ni, J., Huo, S., Liu, Y. (2022). Imbalance of global nutrient cycles exacerbated by the greater retention of phosphorus over nitrogen in lakes. *Nature Geosciences, 15*(6), 464-468. https://www.nature.com/articles/s41561-022-00958-7

Zuur, A. F., Ieno, E. N., Walker, N., Saveliev, A. A., & Smith, G. M. (2009). *Mixed effects models and extensions in ecology with R*. Springer New York. https://doi.org/10.1007/978-0-387-87458-6

Chapter 4: Urban street tree litterfall can be a key driver of stormwater nutrient concentrations and yields throughout the year

Summary

Street trees in urban environments can be important conduits for nutrients; they take up nutrients from soils and deposit them onto streets in the form of litter. These nutrients can rapidly enter stormwater in dissolved and particulate forms, contributing to eutrophication of receiving waters. Our goal was to quantify the contribution of street tree litterfall to stormwater phosphorus (P) and nitrogen (N) at the watershed scale. Using data from high-frequency street sweeping programs in the Minneapolis-St. Paul Metropolitan Area (MSP), we demonstrate that fractional canopy cover over the street is a powerful indicator of litterfall inputs to streets and can be used to predict street tree litterfall inputs of total N and P at the watershed scale. Comparing predicted litterfall total nutrient inputs to observed stormwater nutrient data from MSP watersheds revealed that litterfall inputs were a significant predictor of stormwater total N and P concentrations and yields across seasons. We further predicted that litter contributes an average of 60% of stormwater total P and 69% of stormwater total N yields during the snow-free season, with the greatest contributions in the spring and fall. Predicted contributions from litterfall ranged greatly between watersheds (~0 – 185% for total P and ~0 – 149% for total N) likely due to variation in land use and land cover metrics and nutrient retention with the stormwater network. These findings reveal the outsized effects of street trees on stormwater nutrient loading and suggest that targeting street litterfall may be a powerful tool to address excess nutrients in urban freshwaters.

Introduction

Urban waters—flowing and non-flowing, inland and coastal-—are some of cities' most vital features, providing essential services for human and ecological communities (Lowe et al., 2022). As city populations and footprints continue to grow, the number and importance of urban waters increases (Grimm et al., 2008). At the same time, these systems face numerous stressors from the urban environment.

Urban watersheds can export high levels of nitrogen (N) and phosphorus (P) to urban waters resulting in eutrophication. Eutrophication decreases water clarity, produces more

frequent and larger algal blooms, shifts aquatic plant communities and food webs, disrupts oxygen regimes, and limits recreation and other forms of use (Ansari & Gill, 2014). Nitrogen is of increasing concern in both coastal regions and inland areas, freshwaters are sensitive to P, and many systems can exhibit N and P co-limitation (Elser et al., 2007). Further, the nutrients that originate, flow through, and affect urban waters also have implications for downstream or connected systems at regional and global scales.

Considerable efforts have been made to understand and address eutrophication in urban waters and downstream. The Clean Water Act spurred interventions that targeted point-source pollution, successfully reducing nutrient concentrations and improving clarity in many urban waters (Stets et al., 2020; Topp et al., 2021). Nonpoint sources such as stormwater continue to affect water quality in cities' coastal and inland waters (Carle et al., 2005; Walsh et al., 2005). Efforts to reduce nutrient loading from stormwater are complicated by the heterogeneity and complexity of urban environments and stormwater networks, as well as the inherent differences of N and P sources and cycling. Previous work found that urban N and P differ in their primary sources, pathways, and controlling factors (Carle et al., 2005; Hobbie et al., 2017). What emerges from this complexity are different and sometimes competing management strategies. For example, encouraging infiltration of stormwater might increase P retention while exacerbating N export via groundwater (Hobbie et al., 2017).

One common conduit for both N and P to move from land to surface water are trees planted adjacent to roadways, hereafter street trees, which may offer opportunities for targeted and efficient nutrient removal from roads in watersheds where street trees are common. Street trees accumulate nutrients from soils and deposit them directly onto the landscape, including streets, as leaves, flowers, seeds, and other litterfall (Janke et al., 2017). In street gutters, stormwater or snowmelt enable rapid leaching and decomposition of organic matter (Hobbie et al., 2013; Kaushal & Belt, 2012). Given the imperviousness of streets, there are very few opportunities for infiltration or uptake, and mobilized nutrients and remaining litter are transported through stormwater infrastructure to receiving waters.

There is growing evidence that trees play a role in N and P loading to stormwater. Time series data of stormwater show pulses of N and P in the spring and fall, which correlate with phenological events like tree flowering and leaf drop (Janke et al., 2017). Material intercepted by

street sweeping also shows similar seasonal patterns as stormwater with pulses of organic matter, N, and P in the spring and fall (Hobbie et al., 2023; Kalinosky, 2015). Further, sweeper material often contains a high proportion of organic matter (Hobbie et al., 2023; Kalinosky, 2015; Sorenson, 2013). And swept material from residential settings, where canopy cover tends to be higher, had higher organic matter and TP relative to material from an industrial setting (Sorenson, 2013).

Explicitly incorporating street trees in assessments of stormwater nutrient dynamics confirms a relationship between canopy cover over streets and stormwater nutrient loading. In watershed-scale multivariate modeling, street canopy cover emerged as a primary predictor of N and P concentrations in stormwater (Janke et al., 2017). Kalinosky (2015) also found strong correlations between percent canopy cover and the concentrations and mass of N and P in material collected via street sweeping.

While percent canopy cover is a useful proxy for assessing the role of street trees in contributing nutrients to surface waters, it has limitations. First, there are uncertainties around the proportion of urban canopy litter that falls into streets versus yards, where nutrients may be processed and transported differently (Kalinosky, 2015; McDonnell et al., 1997). Second, using canopy cover as a predictor of stormwater nutrients does not disentangle trees' direct contributions from their indirect effects on non-tree or soil inputs. For example, higher canopy cover could increase stormwater nutrient concentrations directly through an increase in litter or indirectly through an increase in erosion from shaded, poorer quality turf grass (Bierman et al., 2009).

There is a need to directly quantify the contribution of street trees to N and P inputs to streets and stormwater. Theoretically, this can be achieved by collecting all litterfall deposited onto streets with sufficient frequency to minimize loss of material and nutrients to stormwater. Selbig et al. (2016) used this approach, removing all street detritus from a residential catchment with 17% street canopy cover in Madison, WI, from April to November. They observed substantial reductions of stormwater TP and TN exports in the cleaned catchment relative to a catchment that was not cleaned. They attributed 84% of stormwater TP and 74% of stormwater TN loads to the removed street debris, including litterfall, across the snow-free period and revealed nuances between seasons and nutrients. While this study added important support for

the role of street trees in urban nutrient dynamics, it could not separate the effects of litterfall from other material removed from streets (e.g. soils), nor could it explore the contribution of trees to stormwater nutrients across watersheds that vary in their tree canopy cover over streets.

To further refine our understanding of the relationship between street trees and stormwater nutrients, we leveraged high-frequency street sweeping data that differentiates coarse organic matter to estimate the mass of P and N inputs to streets and stormwater from street tree litterfall under differing canopy cover conditions throughout the year. We linked these predictions to comprehensive data on watershed-scale stormwater nutrient yields to quantify the fraction of nutrient loading coming from street trees. This analysis enabled us to 1) estimate the proportion of stormwater N and P exports that are contributed by street trees and are therefore available for relatively efficient removal (and prevention from entering stormwater) through street sweeping, 2) refine our understanding of how and when street trees affect stormwater nutrient concentrations and yields, and 3) explore the watershed characteristics that mediate the role of street trees in stormwater nutrient loading.

Methods

Study area and time periods

Street sweeping routes and stormwater watersheds were located in the Minneapolis-St Paul Metropolitan Area (MSP) in central Minnesota, USA. The climate of this region is typical of the Upper Midwest with large variation in temperature and precipitation throughout the year. This work spans the snow-free period (April 1 – October 31) when precipitation averages 27.1 inches, with June – August being the wettest months (Palecki et al., 2021). Season drives the phenology of street trees with flowering and leaf out occurring April – May with senescence and leaf drop occurring September – November. Street trees and street sweeping programs are managed by 113 individual municipalities (population > 1000) within the MSP, leading to a patchwork of objectives and management strategies across the region.

To understand how litterfall contributions to stormwater nutrients vary with season and tree phenology, we focus on three periods of active litterfall: summer (June 1 – August 31), fall+spring (September 1 – October 31 and April 1 – May 31), and snow-free (April 1 – October 31). We combined the spring and fall seasons to allow for realistic comparisons to observed

stormwater nutrient data. A portion of fall litter typically overwinters in streets, and its associated nutrients do not appear in stormwater until spring thaw and precipitation events (Bratt et al., 2017). By combining the spring and fall seasons, we prevent overestimating nutrient contributions from spring litterfall and underestimating contributions from fall litterfall.

Street sweeping dataset

Data on the N and P concentrations and loads in swept materials from four cities were used to estimate the amount of P and N that the over-street canopy deposits onto streets as litterfall (Hobbie 2023). Samples from street sweepers were collected from 2010 to 2012 from four sweeping routes in Prior Lake, MN and from 24 additional routes in Forest Lake, Minneapolis, and Roseville, MN in 2019 (Hobbie et al., 2023). All streets on study routes were curbed.

Details of the collection, preparation, and analysis of street sweeping samples have been published in Kalinosky (2015) and Hobbie (2023). To summarize, a sample of the material collected by a street sweeper during regular street sweeping operations was collected within 24 hours of the conclusion of a sweeping event. To ensure a representative sample, samples were collected after the swept material was dumped (and therefore mixed) and compared against visual estimates of the fraction of soil and plant components in the larger pile. Samples were separated into fine (< 2 mm) and coarse (≥ 2 mm) fractions using a sieve. The coarse fraction was added to deionized water and agitated to isolate floating (i.e., organic) material and remove adhered soil particles. The coarse and fine fractions were analyzed for total P (TP) and N (TN).

Inputs of TN and TP from the street canopy via litterfall appear mainly in the coarse fraction, the focus of this work. Kalinosky et al. (2015) reported significant positive relationships between the average percent canopy cover over the street and the coarse fraction loads but not with the fine fraction loads. We acknowledge that the fine fraction might have contained some nutrients that originated from the coarse fraction and street trees, as litterfall in streets can be ground into fines by physical disturbance such as vehicle traffic or by weathering. To assess the likelihood of significant litterfall contributions to the fine fraction, we compared C:N ratios of the fine and coarse organic fractions and found a significant difference across all months (coarse $\bar{x}$ = 28.4 ± se 0.44, n = 574; fine $\bar{x}$ = 51.2 ± se 1.56, n = 562; t-test $\alpha < 0.05$). This suggests the fine fraction was mainly soil-derived. However, it is also possible that fines from

litterfall were more processed than intact, coarse litter (i.e., had leached more N). Adding an estimate of fine organic matter into our analyses did not substantially alter our results. Given these considerations, we use only data from the coarse organic fraction here.

Methods used to derive percent canopy cover over the street for each sweeping route are detailed in Janke et al. 2017 and Hobbie et al. 2023. Briefly, shapefiles from the Twin Cities Metropolitan Area (same as MSP in our study) 1-Meter Urban Tree Canopy Cover Classification (Knight et al., 2017) and the Metro Regional Centerlines Collaborative Local Centerlines (MRCC Collaborative, 2018) were overlain to isolate canopy cover directly overhanging streets and calculate the total area of overhanging canopy and total street area. We then divided the total overhanging canopy area by total street area and multiplied by 100 to produce percent street canopy cover.

Selecting street sweeping routes and estimating cumulative masses of N and P

We selected sweeping routes with the longest records and most frequent sweeping to ensure that the cumulative material collected from street sweeping events reasonably reflected contributions from litterfall into streets. We first selected sweeping routes with observations that spanned each time period of interest. A route's first and last observation had to fall within the range of start and end dates for a given period to limit underestimating cumulative masses of N and P (Table 4.1). We next selected routes with relatively frequent sweeping so that we could assume minimal material was removed from streets via wash-off into storm drains in between sweeping events. We determined that routes with an average sweeping frequency of 17 days or fewer captured the widest range of street canopy cover scenarios with the most frequent sweeping possible (Table 4.2). We calculated average sweeping frequencies by averaging the number of days between each sweeping event for each period. We acknowledge that some leaching and particulate transport likely occurred between sweepings and, as a result, our cumulative masses of litterfall nutrients are likely conservative (*see* Prediction uncertainties in SI).

To calculate the cumulative mass of TN and TP from the coarse organic fraction of each qualifying route, we summed all loads over each period. Total cumulative loads from multiple years, when available, were averaged by period.

Table 4.1. Date ranges for each study period.

Study period	Start date	Start date allowance	End date	End date allowance
Spring	April 1	March 21 – May 5	May 31	May 17 – May 31
Summer	June 1	June 1 – June 12	Aug 31	Aug 20 – Aug 31
Fall	Sept 1	Sept 1 – Sept 15	Oct 31	Oct 17 – Nov 14
Snow-free	April 1	March 21 – May 5	Oct 31	Oct 17 – Nov 14

To be included in this work, street sweeping routes and stormwater monitoring stations had to have a first and last observation within the allowed ranges. Data had to qualify for both the spring and fall periods to be included in the Fall+Spring period.

Table 4.2. Street sweeping routes that meet selection criteria for each study period model, ordered by fractional street canopy cover.

			Summer models				Fall+Spring models				Snow-free models			
City	Route ID	Frac street canopy cover	Ave sweep freq	No. sweep events	Mass TP	Mass TN	Ave sweep freq	No. sweep events	Mass TP	Mass TN	Ave sweep freq	No. sweep events	Mass TP	Mass TN
Prior Lake	L2	0	17	6	0.00	0.17	12	16	0.10	0.73	16	18	0.10	0.90
Prior Lake	L4	1	7	14	0.03	0.47	21	8	0.09	0.88	8	34	0.12	1.32
Prior Lake	M2	6	13	8	0.06	0.63	12	14	0.29	1.93	14	20	0.34	2.56
Forest Lake	F2	6	16	6	0.02	0.36								
Forest Lake	SH	7	14	7	0.02	0.27								
Forest Lake	SRC1	7	16	6	0.05	0.60								
Forest Lake	F3	8	14	7	0.03	0.32								
Prior Lake	M4	12	7	13	0.14	1.54	20	7	0.39	2.90	7	33	0.53	4.44
Forest Lake	F1	17	14	7	0.07	0.79								
Prior Lake	H4	19	7	13	0.16	1.40	20	8	0.72	5.21	8	33	0.88	6.61

Ave sweep freq = average sweeping frequency in days; No. sweep events = number of individual street sweeping events; Mass TP = Mass of total phosphorus in coarse organic fraction (kg/curb-km); Mass TN = Mass of total nitrogen in coarse organic fraction (kg/curb-km); Empty cells indicate a route not included in that period's model.

Stormwater dataset

We assembled stormwater event volume data and event TP, TN, dissolved inorganic NO_3^- and NO_2^- (NOx), and Total Kjeldahl N (TKN) concentration data measured from watershed outflows by MSP watershed management organizations. These observed stormwater data do not include coarse particulate organic matter, which may be derived from street tree litter. A subset of watersheds with extensive data and subsurface drainage (i.e., no stream channels) was selected for study (Table S4.1; *see* Finlay et al., 2023 for details). These watersheds have separate sanitary sewer and stormwater infrastructure, no septic systems, and their streets are curbed. Watershed attributes known or predicted to influence stormwater nutrient dynamics were

provided by monitoring agencies or calculated using publicly available spatial datasets. A full list of watershed attributes may be found in Finlay et al. (2024) but include land use and land cover metrics (e.g. fractional residential, industrial, undeveloped, waterbody, and total impervious surface covers), indicators of the degree of urbanization (e.g., population density, road density, development age), and estimates of soil infiltration capacity and erodibility. Most relevant to this work are estimates of street canopy cover, which were derived using 2015 data from the Twin Cities Metropolitan Area 1-Meter Urban Tree Canopy Cover Classification (Knight et al., 2017) and Twin Cities Metro Area Road Surface Area (Marek-Sparts, 2023) shapefiles and in a manner similar to estimates of street canopy cover over sweeping routes (Hobbie et al., 2023; Janke et al., 2017).

Concentrations designated as below detection, or censored, were adjusted using β-substitution (Ganser & Hewett, 2010). β-substitution was found to result in bias far lower than standard substitution methods for censored data, which have been shown to distort signals and lead to erroneous conclusions (Ganser & Hewett, 2010; Helsel & Helsel, 2012). Following the procedure outlined in Ganser & Hewett (2010), we calculated a common limit of detection for each nutrient, then generated a unique beta-correction factor for each nutrient at each monitoring station. Censored values were corrected using these beta-factors and used alongside uncensored observations in calculations and analyses.

When TN concentration was not directly reported, it was calculated as the sum of NOx and TKN concentrations. The Como 3 monitoring station was missing NOx concentrations meaning its TN concentrations and yields are slightly underestimated (NOx concentrations comprised on average 19% ± se 0.17 of TN concentrations in stations with both values reported).

Stormwater nutrient loads were either directly reported by an organization or calculated by multiplying total event volume and event mean concentration. When calculating loads, we estimated missing concentrations from known storm events by averaging a monitoring station's event concentrations three weeks before and after the missing date with all of a station's observations from that month (Janke et al., 2017). These estimated concentrations were only used to calculate loads, not when working directly with stormwater concentrations. Watershed stormwater nutrient yields were calculated by dividing loads by a station's watershed area. For each qualifying watershed, we calculated average stormwater TP and TN concentrations and

cumulative stormwater TP and TN yields for each period. When multiple years from a station qualified, mean concentrations and cumulative yields were averaged to account for year to year variation.

Selecting stormwater watersheds

To ensure concentration and yield data were representative of each time period (summer, fall+spring, and snow-free), we selected only monitoring stations whose first and last observation fell within the start and end dates for each period (Table 4.1). The allowable date range for the first spring observation was extended due to delayed onset of monitoring in some watersheds, resulting in some watersheds missing a fraction of spring nutrient export. We do not expect these missing data to affect our findings as watersheds with delayed spring monitoring also happen to have some of the highest TP and TN yields. We selected stormwater data from 2013 – 2017 to match the street canopy cover estimates from 2015. Qualifying watersheds and their monitoring periods are listed in Table 4.2. The range of average fractional canopy cover over the street in qualifying watersheds (~0 – 35%) was representative of the broader MSP (~0 – 45%).

Building and applying sweeping models

To ultimately predict street litterfall contributions to stormwater N and P for all watersheds for which we had estimates of stormwater nutrient export, but not measurements of litterfall TN and TP, we constructed simple linear regression models relating proportional canopy cover over the street to cumulative loads of TP and TN in the swept coarse fraction for each of the three time periods for the street sweeping routes reported in Hobbie et al. (2023). We explored the inclusion of sweeping frequency in these models, which others found to be an important predictor for TP and TN loads (Hobbie et al., 2023; Kalinosky, 2015). Our multivariate models affirmed that sweeping frequency had a significant influence on cumulative TP and TN loads in the swept coarse fraction over a given time period, but AIC model selection did not show a significant difference between models with and without sweeping frequency. Therefore, we omitted sweeping frequency as a predictor here. This allowed our models to be more readily applied to watersheds that spanned multiple municipalities and, therefore, sweeping programs.

We used these models to predict street litterfall contributions to nutrient yields for watersheds lacking measurements of litterfall inputs to streets. By inputting average proportional

canopy cover over all streets and the total curb distance for each stormwater watershed, we calculated a predicted TP and TN litterfall input for each period at the watershed scale ($Pred_{Mass}$, *kg N or P km*$^{-2}$) (Eqn. 1, where *m* is the slope and *b* is the y-intercept). These values represent our best estimate of the total nutrients that trees adjacent to streets deposited onto streets in a watershed.

We amended these total estimates to account for any nutrients that would have been removed by typical street sweeping operations, which occurred once between mid-March and mid-April and again in early to mid-October in study watersheds. We again built simple linear regression models relating percentage canopy cover over the street to the March and October coarse organic TP and TN loads (Figure S4.1; Table S4.2). For these models, we selected only those routes that were swept least frequently (≥ 18 days) to best reflect the amount of material recovered during typical sweeping. Using these models, we predicted the amount of material removed by typical street sweeping (once in the spring and once in the fall) from each watershed given its total curb distance and average street canopy cover. We corrected the fall+spring and snow-free estimates of street tree nutrient inputs by subtracting the material typically removed by sweeping events in the spring and fall.

$$Mass_{pred} = \frac{(m * average\ percent\ canopy\ cover\ over\ street + b) * curb\ distance,km}{watershed\ area,km^2} \quad \text{Equation 1}$$

We divided the predicted litterfall TP and TN ($Mass_{Pred}$) delivered to streets by the observed cumulative TP and TN stormwater yields (*observed cumulative stormwater yield, kg N or P km*$^{-2}$) for each watershed across each period, to calculate the proportional contribution of street trees to stormwater P and N exports ($Prop_{Pred}$) (Eqn. 2). These proportions were then related to watershed characteristics to explore variables that influence or mediate the connection between street trees and stormwater.

$$Prop_{pred} = \frac{Mass_{pred}}{observed\ cumulative\ stormwater\ yield} \quad \text{Equation 2}$$

Statistical analyses

We assessed relationships between inputs from street tree litterfall and observed stormwater nutrient concentrations and yields using bivariate linear regression models (R Core Team, 2021; $\alpha = 0.05$). Stormwater nutrient concentrations reflect nutrient inputs to streets and

other connected impervious surfaces. Yields are a function of both concentration and runoff volume, which is closely linked to the intensity of stormwater drainage, indicated by street density. Thus, variation in yields is highly influenced by differences in watershed structure as well as factors that affect concentration, so may be expected to have a more complex relationship to canopy inputs (Janke et al., 2017).

To explore how watershed characteristics mediate the relationship between street litter and stormwater, we related the predicted proportion of stormwater nutrients associated with street litter (or $Prop_{Pred}$) to watershed attributes for each period of interest using bivariate linear regression models (R Core Team, 2021; $\alpha = 0.05$). We selected predictor variables based on those we hypothesized would be important given previous work and our understanding of the urban stormwater system. Predictors were: watershed development age, population density, road density, erodibility, fractional land use and land cover categories (lawn, impervious surface, rooftop, surface water, industrial, residential, urban, undeveloped). We additionally used bivariate linear regression to assess how predicted proportion of stormwater nutrients associated with street litter compared to cumulative stormwater total suspended solid yield, a measure of erosional inputs, for each period of interest averaged across years. Variables used to derive predicted proportions were not assessed (fractional canopy cover over the street, road length, and watershed area).

Results & Discussion

Our work expands understanding of the relationship between street trees and stormwater nutrients by using street canopy cover to estimate street tree litterfall inputs at the watershed scale and quantifying the fraction of stormwater nutrient yields that can be attributed to street tree litterfall. This novel approach confirms that street trees have a direct and significant effect on stormwater nutrient concentrations and that litterfall contributes a substantial fraction of N and P to stormwater, especially in watersheds with high street canopy cover. Our findings suggest that stormwater networks likely retain some fraction of litterfall nutrients and emphasize that street trees can be an important focal point for managing excess N and P in cities and urban surface waters.

Percent street canopy cover strongly predicts litterfall inputs of TP and TN to streets.

Across street-sweeping routes, cumulative TP and TN in the coarse organic fraction recovered via street sweeping were strongly predicted by street canopy cover across all periods. Relationships were strongest for the snow-free period, followed by the fall+spring period, and the summer period (Figure 4.1). Model slopes for the fall+spring period were greater than those in the summer period, reflecting the greater mass of TP and TN recovered during these seasons. The intercepts of these relationships were at or near zero, supporting our assumption that most of the litter represented in these models was associated with canopy cover adjacent to and over the street. However, we acknowledge that non-tree litter, for example grass clippings, might have contributed some material or may account for some variation during the summer period.

Predictions of total litterfall inputs from the fall+spring and snow-free periods were corrected to account for the amount of litter removed during typical spring and fall street sweepings (Figure S4.2). We estimated that typical biannual street sweeping removes an average of 29% of TP and 27% of TN from the snow-free estimates and 36% of TP and 36% of TN from the fall+spring estimates of litterfall N and P inputs to streets (all se ± <0.02). Correcting for material removed by typical street sweeping resulted in predictions of net litterfall TP and TN inputs to streets available for downstream transport at the watershed scale.

Street trees have direct effects on stormwater TN and TP concentrations and yields via litterfall inputs.

Predicted litterfall inputs to streets were a significant predictor of mean stormwater TP and TN concentrations across all study periods (simple linear regression, p-value < 0.05, Figure 4.2). Janke et al. (2017) found similarly strong correlations using percent street canopy cover as a predictor of stormwater concentrations in MSP, though it was unclear whether the strength of this effect was due to direct effects through litterfall inputs or indirect effects on turf quality erosional inputs. Our use of predicted litterfall inputs as a predictor confirms that street trees have a direct effect on stormwater through litterfall inputs to streets or that predicted litterfall inputs are correlated with any indirect effects of street trees on stormwater nutrient concentrations.

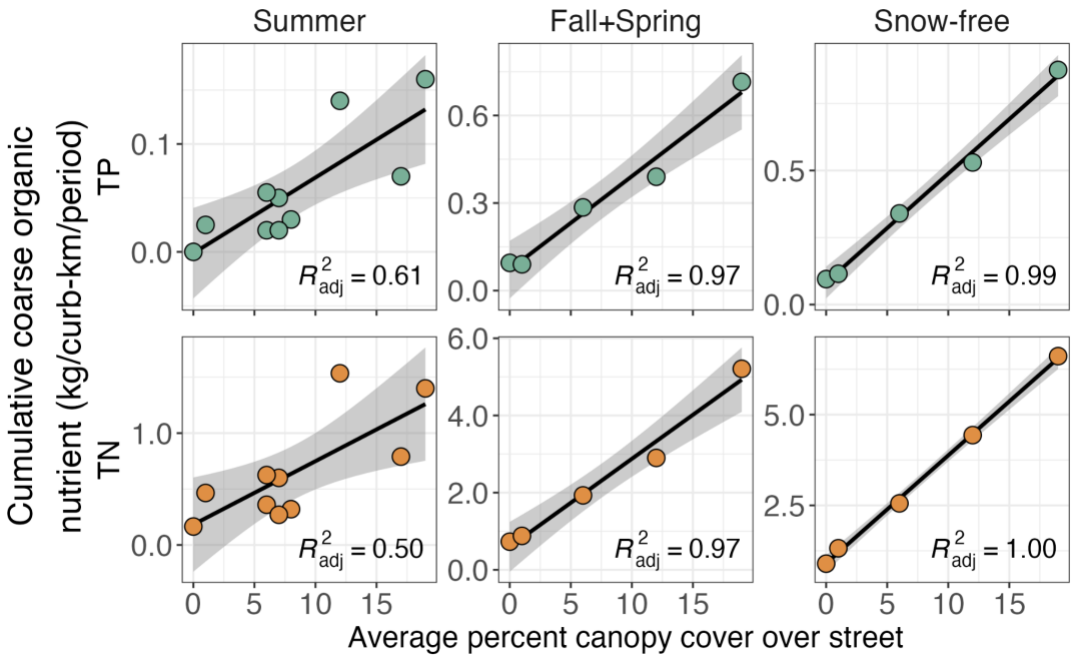

Figure 4.1. Average cumulative TP (top row) and TN (bottom row) in the coarse litter fraction vs average percent canopy cover over the street.
Only frequently swept routes are included (average sweeping frequency ≤ 17 days). Columns represent the summer (June 1 - August 31), fall+spring (September 1 - October 31 and April 1 - May 31), and snow-free (April 1 - October 31) periods. Grey shading indicates the 95% confidence interval. All models have a p-value < 0.05.

Street trees were especially important determinants of stormwater TP concentrations across the snow-free period. Predicted litterfall inputs were more strongly correlated with stormwater TP concentrations (adj-R^2 = 0.51) compared to TN (adj-R^2 = 0.36). The fall+spring period appeared to drive the relationship for TP, showing a markedly stronger correlation (adj-R^2 = 0.52) compared to the summer period (adj-R^2 = 0.10). This was not the case for TN, which showed similar relationships with litterfall inputs during the fall+spring (adj-R^2 = 0.28) and summer periods (adj-R^2 = 0.21). This aligns with previous work that found canopy cover tended to have a greater influence on stormwater P compared to N, particularly in the fall (Bratt et al. 2017; Janke et al., 2017; Selbig, 2016).

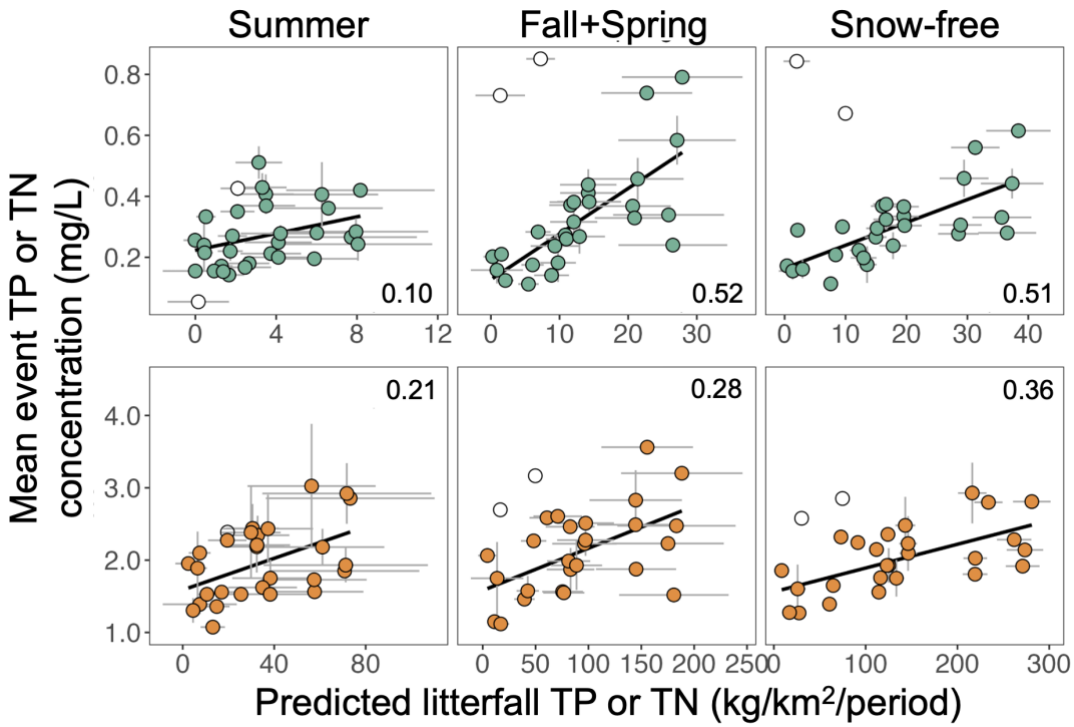

Figure 4.2. Predicted mass of litterfall TP (top row) and TN (bottom row) inputs to streets on a watershed area basis vs observed mean stormwater TP and TN concentrations for each period.
Horizontal error bars represent the 95% confidence interval around each prediction. Vertical error bars represent the standard error around each mean, calculated when data from multiple years were available. Open points are watersheds (B-Dale and MLK) that were excluded from regression analyses due to especially high erosional inputs. Solid trend line indicates p-value < 0.05. Values on plots are the adjusted R^2 for that model.

Stronger relationships between litterfall inputs and TP concentrations may be due to P being more readily lost from litterfall to stormwater compared to N. Nutrient loss from litterfall is dictated by the microbial community (e.g., metabolic and nutrient requirements), litter characteristics (e.g. ratio of carbon to nutrients and soluble vs. insoluble nutrient forms), physical processes (e.g., fragmentation), and the solubility of N and P. These factors culminate in notable differences between N and P, with P being more readily lost from litterfall via leaching and decomposition, likely because it can be stored as inorganic P in vacuoles within leaves (Hobbie et al., 2013). Similarly, P is more readily lost from non-tree litter, such as grass clippings, which may account for some of the additional variation in summer TP concentrations (Timmons et al., 1970). Other sources (e.g., wet and dry deposition, chemical fertilizers) and retention pathways (discussed below) that tend to be more prevalent for TN compared to TP in our study area may

also drive additional variation in the relationships between litterfall TN inputs and stormwater TN concentrations (Hobbie et al., 2017; Janke et al., 2017; Selbig, 2016).

Litterfall inputs were positively correlated with stormwater nutrient yields, though these relationships were weaker compared to those for concentrations (Figure 4.3). This was expected; stormwater nutrient yields respond to variables that affect nutrient concentrations (as litterfall inputs do here) but are especially sensitive to variables that affect runoff volumes. Street density, for example, is often correlated with stormwater nutrient yields (Hobbie et al., 2017; Janke et al., 2014; Y.-Y. Yang & Lusk, 2018) and shows positive trends with TP (though p-value < 0.1; adj-R^2 = 0.16) and TN yields (p-value < 0.05; adj-R^2 = 0.26) in our dataset during the snow-free season. The fact that predicted litterfall inputs emerge as a driver of yields despite the often overwhelming importance of variables affecting runoff volumes is a reflection of their outsized effects on stormwater nutrient concentrations. A comprehensive assessment of the drivers of stormwater N and P concentrations and yields is the focus of ongoing research in MSP and may provide additional insight into the importance of litterfall and street trees relative to other nutrient sources and landscape variables.

Street tree litterfall contributes a substantial proportion of stormwater TP and TN exports throughout the year.

We estimated the proportion of stormwater nutrient exports from litterfall inputs to streets at the watershed scale by relating the predicted mass of litterfall TP and TN to observed stormwater nutrient yields (Eqn. 2). Predicted litterfall inputs of TP and TN to streets accounted for a majority of stormwater nutrient yields during the snow-free season (Figure 4.4). We predicted that net litterfall contributed on average 18 kg/km^2 of TP (se ± 3.4, n = 18) and 138 kg/km^2 of TN (se ± 26, n = 17) to streets during the snow-free period, comprising on average 60% (se ± 12%) of observed stormwater TP and 69% (se ± 12%) of stormwater TN yields. Selbig (2016) may be the only other work that quantified litterfall effects on stormwater nutrient export at the watershed scale. They attributed reductions of 84% and 74% in TP and TN loads, respectively, to the removal of street litterfall and other debris. These values represent a single watershed with moderate street canopy cover (17%), and are in line with our predictions of litterfall contributions to stormwater nutrients.

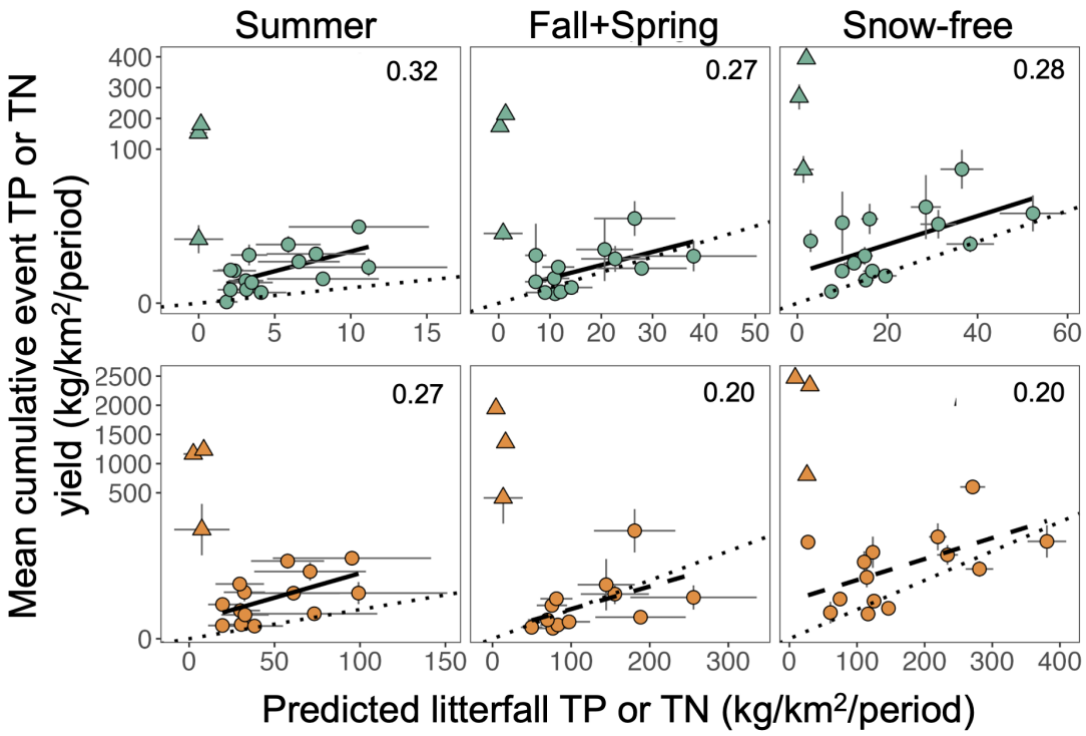

Figure 4.3. Predicted mass of litterfall TP (top row) and TN (bottom row) inputs to streets on a watershed area basis vs observed mean stormwater TP and TN yields for each period.
Dotted line is the 1:1 line. Horizontal error bars represent the 95% confidence interval around each prediction. Vertical error bars represent the standard error around each mean, calculated when data from multiple years were available. Triangles indicate watersheds (MLK, Dickerman Park, and Franklin) that were excluded from regression analyses because they represent vastly different land use from all others in our dataset. Solid trendline indicates p-value < 0.05, dashed trendline indicates p-value < 0.10. Values on plots are the adjusted R^2 for that model.

Litterfall nutrient contributions to stormwater occurred primarily during the fall+spring period. We predict litterfall inputs contributed on average 14 kg/km^2 of TP (se ± 2.7, n = 16) and 100 kg/km^2 of TN (se ± 19, n = 15) to streets in the fall and spring, comprising on average 89% (se ± 16%) of observed stormwater TP and 115% (se ± 22%) of observed stormwater TN yields during this period (Figure 4.2). This aligns with the phenology of tree litter drop and mirrors seasonal trends observed in previous work (Janke et al., 2017; Kalinosky, 2015; Selbig, 2016). We were unable to reliably assess differences between the fall and spring seasons due to nutrients from litterfall deposited onto streets in the fall not reaching stormwater outflows until spring. Prior work has observed the highest mass of litterfall TP and TN in the fall (Hobbie et al., 2023; Selbig, 2016; Kalinosky, 2015). We expect spring is still an important period for litterfall

inputs to stormwater as spring litter (e.g., flowers) appears to more readily leach nutrients compared to fall litter (e.g., leaves) (Hill et al., 2022).

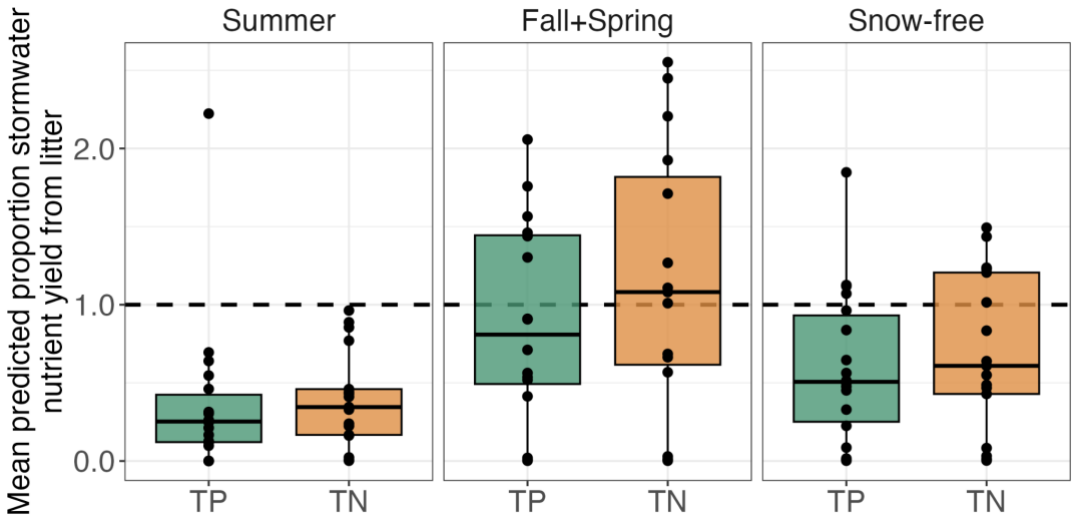

Figure 4.4. Mean proportion of stormwater TP and TN yields associated with street litterfall.
Proportions are calculated by dividing the predicted net litterfall mass of TP and TN by observed cumulative stormwater P and N yields from select Twin Cities watersheds. Dashed line highlights a proportion of 1.0.

We found that street tree litterfall may be an important source of nutrients in the summer, however the magnitude of litterfall inputs was lower compared to those deposited in other seasons. We predicted litterfall inputs contributed on average 4 kg/km^2 of TP (se ± 0.8, n = 18) and 42 kg/km^2 of TN (se ± 7.2, n = 17), comprising 37% (se ± 12%) of observed stormwater TP and 40% (se ± 8%) of observed stormwater TN yields. Similarly, Selbig (2016) found that removing street debris reduced summer TP exports by 36%, but saw no significant change in summer TN export. Trees can drop flowers and leaves during the summer months, and storms and organisms that inhabit street trees can also dislodge leaves into streets.

The relatively predictable timing and location of street tree litterfall inputs to stormwater present a unique opportunity to quantify inputs from a single source on the watershed scale. Inputs from other, more diffuse sources are challenging to capture, leaving few opportunities to compare litterfall inputs to other sources of stormwater TN and TP. Prior efforts to identify sources of stormwater P and N have measured rates of nutrient release from urban features (e.g., lawns, roofs, or pavement) into runoff or estimated contributions from known sources (e.g.,

atmospheric deposition). Accurately scaling these estimates to the watershed and relating them to watershed TP and TN export is challenging given the spatial and temporal heterogeneity of the urban environment. Stable isotopes have been used to partition sources of nitrate-N in stormwater at the watershed scale; isotope methods for P source identification are less established and to our knowledge have yet to be applied to urban stormwater (Glibert et al., 2019). Atmospheric deposition and N fertilizer are consistently identified as contributing the greatest proportion of stormwater nitrate-N exports, though estimates vary widely between studies and across study catchments (Jani et al., 2020; Kaushal et al., 2011; Y. Y. Yang & Toor, 2016). Estimates of source contributions to stormwater nitrate are rarely related to TN exports and therefore lack important context, especially when stormwater can be dominated by other N forms. For example, in MSP on average 77% of stormwater TN (IQR 70% – 83%) is organic-N (Finlay et al., 2023). Yang and Toor (2016), working in residential catchments in Florida, USA, were one exception; they reported ~17 – 25% of stormwater TN from atmospheric deposition, ~6% – 25% from chemical fertilizer, and ~3% – 13% from organic- and soil-derived nitrate. Reported estimates of source inputs to stormwater vary widely across catchments and studies, regardless of method, and our findings are no different.

We observed considerable variation in the predicted proportional litterfall contributions to stormwater TN and TP exports across watersheds. We expected some of this variation to be driven by watershed attributes (e.g., street density) known to affect the stormwater nutrient yields from which proportions were derived (Eqn. 2). However, no watershed attributes were significantly correlated with the proportion of stormwater yields from predicted litterfall inputs (simple linear regression, $\alpha = 0.05$). The lack of expected relationships reflects the heterogeneity of urban watersheds and complex, often covarying, interactions between landscape attributes. There are indications that the proportional inputs from litterfall may shift with changes in street canopy cover. Because our predictions are derived from street canopy cover (Eqn. 1 and 2), these relationships are discussed qualitatively.

Sources and transport of stormwater nutrients may shift with differences in watershed street canopy cover and land use

Litterfall inputs may contribute a greater fraction of stormwater nutrient yields as street canopy cover increases, indicated by the convergence of trend lines in Figure 4.5. Stormwater TP

and TN yields remained high in watersheds with low litterfall inputs. This is most apparent in watersheds with fractional street canopy cover less than 1% (represented with triangles in Fig 4) but persists when those watersheds are excluded. This trend suggests alternative nutrient sources or transport dynamics at low canopy cover and a shift toward litterfall as street tree cover, and landscape features that covary with street trees, increase.

Watersheds with low street canopy cover tended to have higher impervious surface area and road densities, characteristics associated with high runoff volumes and nutrient inputs from erosion and deposition. A high degree of imperviousness and road cover limits water infiltration and interception by vegetation, resulting in higher runoff volumes, peak storm flows, and storm velocities that more effectively move soils and particulate matter, which contain N and P, from the landscape into stormwater and through stormwater networks to outlets (Janke et al., 2014; Miguntanna et al., 2013; Simpson et al., 2022). These erosional inputs join N and P inputs from deposition and, in the case of N, vehicle fossil fuel combustion—both also associated with high imperviousness and road cover—to increase stormwater nutrient concentrations and yields (Bettez et al., 2013; Simpson et al., 2022). These mechanisms are likely driving the persistently high TN and TP yields at low street canopy cover. In support of this, we observed that watersheds with low predicted proportions of stormwater TN and, especially, TP yields from litterfall had significantly higher stormwater yields of total suspended solids, an indicator of erosional inputs (Figure 4.6).

As street canopy cover increases, mature trees and the lawns and vegetation that tend to accompany them replace impervious surfaces, reducing stormwater volumes and altering nutrient sources. Permeable surfaces such as lawns can reduce stormwater yields by encouraging infiltration and storage of stormwater and nutrients in soils or plant tissues (Simpson et al., 2022). Decreased stormwater flows also increase residence time of nutrients in the watershed, increasing opportunities for uptake or removal via biogeochemical processes (Hale et al., 2014). There is evidence that adding trees to permeable surfaces further enhances stormwater volume and nutrient reductions. Tree canopies may intercept and direct precipitation away from impervious surfaces to soils, and deep tree roots may encourage infiltration. Trees can also store water in their tissues and transpire it to the atmosphere (Berland et al., 2017). These effects of trees on runoff volumes are often studied at the tree scale with uncertainties around how they

scale to the watershed (Baker et al., 2021). However, Janke et al. (2017) found that increasing street canopy cover reduced nutrient yields via stormwater volume reductions but only at low street densities. Increasing tree cover and permeable surfaces may reduce runoff volumes and nutrient inputs from some sources and pathways, such as erosion and overland flow, while activating or increasing inputs from other sources, such as from litterfall (Simpson et al., 2022).

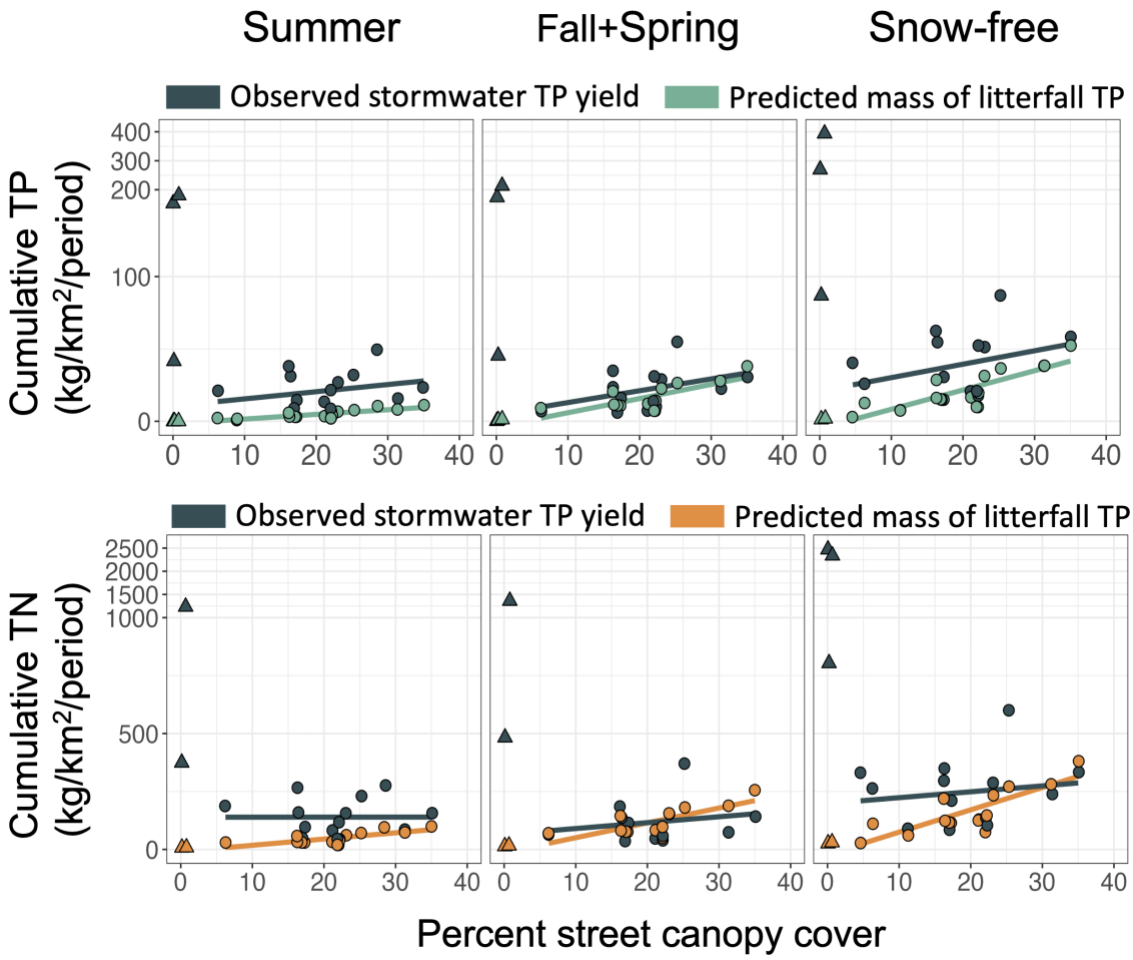

Figure 4.5. Predicted net mass of litterfall inputs of TP and TN to streets in select Twin Cities stormwater and observed stormwater nutrient vs street canopy cover (averaged by watershed) for each period of interest.
Both predicted net mass of litterfall inputs and stormwater nutrient yields are on a watershed area basis. Note the compressed y-axis. The summer (June 1 - August 31), fall+spring (September 1 - October 31 and April 1 - May 31), and snow-free (April 1 - October 31) periods are shown. Three watersheds represented by triangles (MLK, Dickerman Park, Franklin) are substantively different from all others (dominated by impervious surface cover and non-residential land use) and are omitted from trendlines. No statistical output for predicted litterfall and canopy cover relationships are shown as these variables are not independent. None of the relationships between percent street canopy cover and observed stormwater yield were significant ($p > 0.05$).

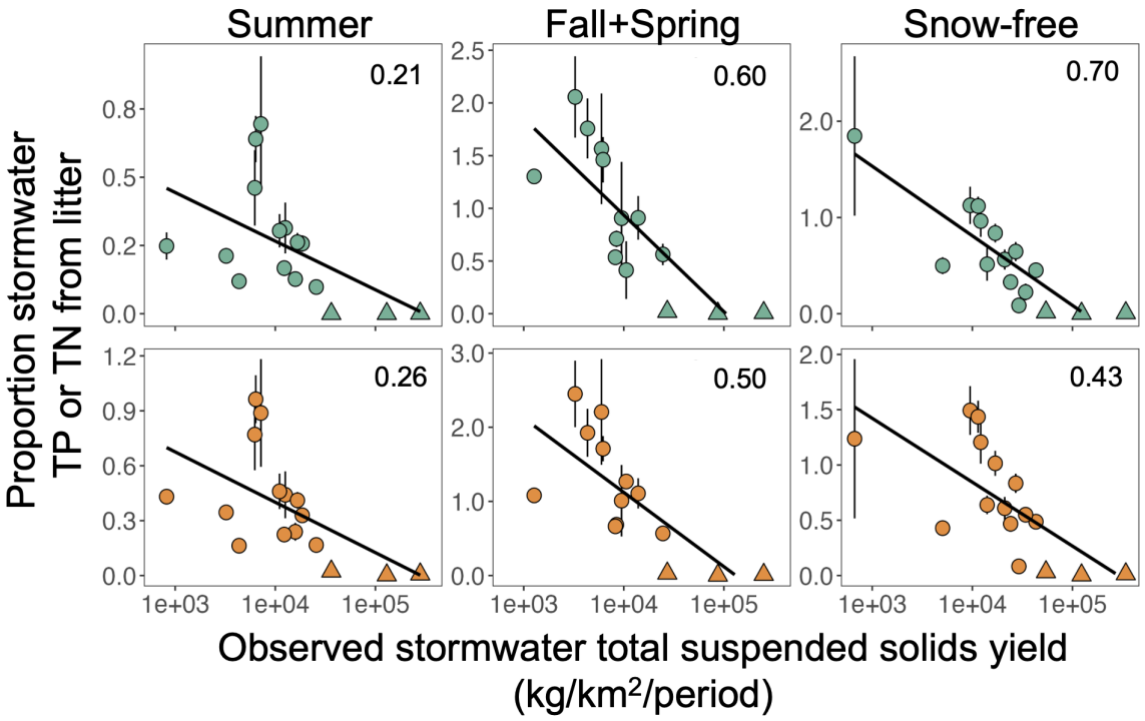

Figure 4.6. Predicted mean proportion of stormwater TP (top row) and TN (bottom row) yields associated with street litterfall vs. mean observed stormwater total suspended solids yields.
Total suspended solids yields have been log-transformed. Vertical error bars represent the standard error around each mean, calculated when data from multiple years were available. Solid trend lines indicate p-value < 0.05. Three watersheds (MLK, Dickerman Park, Franklin; indicated with triangles) had higher impervious surface cover and non-residential land use compared to all others. Values on plots are the adjusted R^2 for that model.

We caution, however, that urban watersheds do fall along a simple gradient from high imperviousness to high canopy cover; variation in land use and land cover characteristics exist across canopy cover values. This complexity challenges our ability to identify patterns, particularly for stormwater nutrient yields. Future work to collect and incorporate nutrient yield data from additional watersheds across land use types would improve our ability to capture and understand interactions between key watershed characteristics such as street canopy cover and street density.

Nutrient retention may mediate the effect of street trees on stormwater nutrient loading.

Predicted litterfall inputs that exceeded observed stormwater nutrient yields (i.e. predicted proportions >1.0) likely resulted from watershed nutrient retention or underestimation of stormwater nutrient yields. Watershed nutrient retention, or the removal of nutrients from stormwater upstream of outflows, would reduce stormwater nutrient yields relative to nutrient inputs. There are numerous opportunities for N and P retention within the stormwater networks of our study watersheds. Stormwater networks can include surface waters, wetlands, and stormwater infrastructure like ponds and sumps that can trap and bury N and P in their sediments (Janke et al., 2022; Kloiber, 2006), as well as connections to groundwater where N and P may be lost via infiltration (Janke et al., 2014). Any sites within stormwater networks that support anoxic conditions (e.g., those with high moisture) may support high rates of N removal via denitrification (Bettez & Groffman, 2012; Blaszczak et al., 2018). Urban watersheds tend to more readily retain N compared to P as there are fewer retention mechanisms for P (Hobbie et al., 2017), which may explain why we attributed greater proportions of stormwater TN to litterfall compared to TP (Figure 4.4). P lacks a transformation pathway analogous to denitrification (Djodjic, 2004). Further, the prevalence of particulate forms of P facilitates retention in soils outside the stormwater network, but P in stormwater has few opportunities to interact with soils (Hobbie et al., 2017). Nutrient retention is undoubtedly occuring in our study watersheds, and future work to incorporate the presence and distribution of retention sites will better reflect controls on nutrient transport in stormwater.

Underestimation of nutrient exports in stormwater could also have led to predicted litterfall inputs that exceeded stormwater nutrient yields. Stormwater monitoring captures nutrients that can be measured from water samples; it does not include nutrients that exit watersheds in coarse organic material (Bannerman et al., 1993; Selbig, 2016, Chapman et al., 2024). Nutrients remaining in coarse material are less bioavailable (until released during decomposition or consumption processes) but can still be transported through stormwater networks, joining dissolved forms of N and P as exports of nutrients to surface waters. Our predicted masses reflect all N and P in litterfall regardless of pending transformations, but we relate these to observed stormwater N and P yield data that may be missing a substantial fraction of N and P remaining in litter. Compared to N, P is more readily lost from litterfall (Hobbie et

al., 2013), suggesting that a smaller fraction of the predicted litterfall TP inputs would exit the watershed as unaccounted for coarse organic material. We are unsure of the extent to which the omission of coarse litter undercounts exported nutrients and, therefore, how it affects our predicted proportions of litterfall inputs.

It is unlikely that overpredicting litterfall inputs to streets inflated predicted proportions of stormwater from litterfall inputs. A full discussion of prediction uncertainties can be found in the supplemental materials. Here, we highlight that we are most likely underestimating litterfall N and P inputs to stormwater due to incomplete capture of litterfall nutrients. The average sweeping frequency for qualifying routes was 12 days, with the highest frequency being 7 days (Table 4.1). During years when street sweeping data were collected, there were on average three days between precipitation events for the summer, fall+spring, and snow-free periods (results not shown, data source: Minnesota Department of Natural Resources). Rain events undoubtedly facilitated nutrient and litter loss to stormwater between sweeping intervals, lowering the amount of measured coarse litterfall N and P in our models, and resulting in underestimating litterfall N and P inputs. Given the rapid loss of P from litter, we may be especially underestimating litterfall P (Hobbie et al., 2013).

Conclusions

We found 1) canopy cover is a powerful indicator of litterfall inputs to streets, 2) in watersheds with >5% canopy cover, litterfall has strong positive effects on stormwater TP and TN nutrient concentrations which translate to positive (though less strong) effects on stormwater TP and TN yields, 3) street tree litterfall inputs of TP and TN comprise a substantial fraction of stormwater nutrient yields throughout the year but especially in the fall+spring period, 4) litterfall may comprise a greater proportion of stormwater TN and TP yields in watersheds with high canopy cover, and 5) litterfall nutrient inputs to streets can exceed watershed nutrient exports, suggesting nutrient retention in stormwater networks or coarse litter.

Given that the effects of street trees on stormwater are substantial, seasonally predictable, and similar for N and P, we conclude that street trees may be a powerful focal point for managing excess nutrients in cities. Others have shown that more frequent street sweeping has immense potential for reducing litterfall N and P inputs to stormwater (Hobbie et al., 2023;

Kalinosky, 2015; Selbig, 2016). Our results underscore this, showing that over 70% of litterfall TN and TP in streets during the snow-free period remains after typical biannual street sweeping. Our work contributes to a growing set of resources useful for those developing street sweeping programs, or other community-based street litter removal programs, aimed at maximizing nutrient export reduction while minimizing costs and burdens to the community. Our models can be used to estimate net litterfall TP and TN inputs to streets for other north-temperate cities where street canopy cover data are available, thereby highlighting areas where reductions via sweeping may be most effective.

Finally, though street trees present an important opportunity to reduce nutrient loading to stormwater, inputs from litterfall do not represent new sources of N and P to the watershed. Reducing allochthonous N and P inputs to urban watersheds and closing urban nutrient cycles, which includes keeping litterfall nutrients on the landscape, are essential to truly addressing excess nutrient loading to cities.

Works cited

Ansari, A. A., & Gill, S. S. (Eds.). (2014). *Eutrophication: Causes, Consequences and Control: Volume 2*. Springer Netherlands. https://doi.org/10.1007/978-94-007-7814-6

Baker, H. J., Hutchins, M. G., & Miller, J. D. (2021). How robust is the evidence for beneficial hydrological effects of urban tree planting? *Hydrological Sciences Journal*, *66*(8), 1306–1320. https://doi.org/10.1080/02626667.2021.1922692

Bannerman, R. T., Owens, D. W., Dodds, R. B., & Hornewer, N. J. (1993). Sources of Pollutants in Wisconsin Stormwater. *Water Science and Technology*, *28*(3–5), 241–259. https://doi.org/10.2166/wst.1993.0426

Berland, A., Shiflett, S. A., Shuster, W. D., Garmestani, A. S., Goddard, H. C., Herrmann, D. L., & Hopton, M. E. (2017). The role of trees in urban stormwater management. *Landscape and Urban Planning*, *162*, 167–177. https://doi.org/10.1016/j.landurbplan.2017.02.017

Bettez, N. D., & Groffman, P. M. (2012). Denitrification Potential in Stormwater Control Structures and Natural Riparian Zones in an Urban Landscape. *Environmental Science and Technology*, *46*, 10909–10917. dx.doi.org/10.1021/es301409z

Bettez, N. D., Marino, R., Howarth, R. W., & Davidson, E. A. (2013). Roads as nitrogen deposition hot spots. *Biogeochemistry*, *114*(1–3), 149–163. https://doi.org/10.1007/s10533-013-9847-z

Bierman, P. M., Horgan, B. P., Rosen, C. J., Hollman, A. B., & Pagliari, P. H. (2009). Phosphorus Runoff from Turfgrass as Affected by Phosphorus Fertilization and Clipping Management. *Journal of Environmental Quality*, *39*(1), 282–292. https://doi.org/10.2134/jeq2008.0505

Blaszczak, J. R., Bernhardt, E. S., Hall, S. J., Hobbie, S. E., Neill, C., Badgley, B. D., Rivers, E. N., Pataki, D. E., Steele, M. K., Heffernan, J. B., Groffman, P. M., & Morse, J. L. (2018). Sediment chemistry of urban stormwater ponds and controls on denitrification. *Ecosphere*, *9*(6), e02318. https://doi.org/10.1002/ecs2.2318

Bratt, A. R., Finlay, J. C., Hobbie, S. E., Janke, B. D., Worm, A. C., & Kemmitt, K. L. (2017). Contribution of Leaf Litter to Nutrient Export during Winter Months in an Urban Residential Watershed. *Environmental Science and Policy*. https://doi.org/10.1021/acs.est.6b06299

Carle, M. V., Halpin, P. N., & Stow, C. A. (2005). Patterns of watershed urbanization and impacts on water quality. *Journal of the American Water Resources Association*, *41*(3), 693–708. https://doi.org/10.1111/j.1752-1688.2005.tb03764.x

Chapman, J.A., Baker, L. M., Finlay, J.C., Wilson, G.L., Pietsch, A.J., Hoffman, K. (2024). *Investigation of coarse Organic Matter and Gross Solids Loading in Minnesota Urban Stormwater*; *Final Report*. https://hdl.handle.net/11299/261453

Djodjic, F., Börling, K., Bergström, L. (2004). Phosphorus Leaching in Relation to Soil Type and Soil Phosphorus Content. *J. Environ. Qual.*, *33*, 678–684. https://doi.org/10.2134/jeq2004.6780

Elser, J. J., Bracken, M. E. S., Cleland, E. E., Gruner, D. S., Harpole, W. S., Hillebrand, H., Ngai, J. T., Seabloom, E. W., Shurin, J. B., & Smith, J. E. (2007). Global analysis of nitrogen and phosphorus limitation of primary producers in freshwater, marine and terrestrial ecosystems. *Ecology Letters*, *10*(12), 1135–1142. https://doi.org/10.1111/j.1461-0248.2007.01113.x

Finlay, J. C., Janke, B. D., Trojan, M., Wilson, B., & Marek-Sparts, M. (2024). *Leveraging Minnesota's Stormwater Data for Improved Modeling and Management of Water Quality in Cities; Final Report*. Retrieved from the University Digital Conservancy, https://hdl.handle.net/11299/259975

Ganser, G. H., & Hewett, P. (2010). An Accurate Substitution Method for Analyzing Censored Data. *Journal of Occupational and Environmental Hygiene*, *7*(4), 233–244. https://doi.org/10.1080/15459621003609713

Glibert, P. M., Middelburg, J. J., McClelland, J. W., & Jake Vander Zanden, M. (2019). Stable isotope tracers: Enriching our perspectives and questions on sources, fates, rates, and pathways of major elements in aquatic systems. *Limnology and Oceanography*, *64*(3), 950–981. https://doi.org/10.1002/lno.11087

Grimm, N. B., Faeth, S. H., Golubiewski, N. E., Redman, C. L., Wu, J., Bai, X., & Briggs, J. M. (2008). Global Change and the Ecology of Cities. *Science*, *319*(5864), 756-760. https://doi.org/10.1126/science.1150195

Hale, R. L., Turnbull, L., Earl, S., Grimm, N., Riha, K., Michalski, G., Lohse, K. A., & Childers, D. (2014). Sources and Transport of Nitrogen in Arid Urban Watersheds. *Environmental Science & Technology*, *48*(11), 6211-6219. dx.doi.org/10.1021/es501039t

Helsel, D. R., & Helsel, D. R. (2012). *Statistics for censored environmental data using Minitab and R* (2nd ed). Wiley.

Hill, S.K., Hale, R.L, Grinath, J.B., Folk, B.T., Nielson, R., Reinhardt, K. (2022). Looking beyond leaves: variation in nutrient leaching potential of seasonal litterfall among different species within an urban forest. *Urban Ecosystems, 25*(2), 1097-1109. https://link.springer.com/10.1007/s11252-022-01217-8

Hobbie, S. E., Baker, L. A., Buyarski, C., Nidzgorski, D., & Finlay, J. C. (2013). Decomposition of tree leaf litter on pavement: Implications for urban water quality. *Urban Ecosystems, 17*(2), 369–385. https://doi.org/10.1007/s11252-013-0329-9

Hobbie, S. E., Finlay, J. C., Janke, B. D., Nidzgorski, D. A., Millet, D. B., & Baker, L. A. (2017). Contrasting nitrogen and phosphorus budgets in urban watersheds and implications for managing urban water pollution. *Proceedings of the National Academy of Sciences*, 1–6. https://doi.org/10.1073/pnas.1618536114

Hobbie, S. E., King, R. A., Belo, T., Kalinosky, P., Baker, L. A., Finlay, J. C., Buyarski, C. A., & Bintner, R. (2023). Sources of variation in nutrient loads collected through street sweeping in the Minneapolis-St. Paul Metropolitan Area, Minnesota, USA. *Science of The Total Environment, 905*, 166934. https://doi.org/10.1016/j.scitotenv.2023.166934

Jani, J., Yang, Y.-Y., Lusk, M. G., & Toor, G. S. (2020). Composition of nitrogen in urban residential stormwater runoff: Concentrations, loads, and source characterization of nitrate and organic nitrogen. *PLOS ONE*, *15*(2), e0229715. https://doi.org/10.1371/journal.pone.0229715

Janke, B. D., Finlay, J. C., & Hobbie, S. E. (2017). Trees and Streets as Drivers of Urban Stormwater Nutrient Pollution. *Environmental Science and Technology*, *51*(17), 9569–9579. https://doi.org/10.1021/acs.est.7b02225

Janke, B. D., Finlay, J. C., Hobbie, S. E., Baker, L. A., Sterner, R. W., Nidzgorski, D., & Wilson, B. N. (2014). Contrasting influences of stormflow and baseflow pathways on nitrogen and phosphorus export from an urban watershed. *Biogeochemistry*, *121*(1), 209–228. https://doi.org/10.1007/s10533-013-9926-1

Janke, B. D., Finlay, J. C., Taguchi, V. J., & Gulliver, J. S. (2022). Hydrologic processes regulate nutrient retention in stormwater detention ponds. *Science of the Total Environment, 823*, 153722. https://doi.org/10.1016/j.scitotenv.2022.153722

Kalinosky, P. M. (2015). *Quantifying solids and nutrient recovered through street sweeping in a suburban watershed*. [Master's thesis, University of Minnesota]. https://hdl.handle.net/11299/172600

Kaushal, S. S., & Belt, K. T. (2012). The urban watershed continuum: Evolving spatial and temporal dimensions. *Urban Ecosystems*, *15*(2), 409–435. https://doi.org/10.1007/s11252-012-0226-7

Kaushal, S. S., Groffman, P. M., Band, L. E., Elliott, E. M., Shields, C. A., & Kendall, C. (2011). Tracking Nonpoint Source Nitrogen Pollution in Human-Impacted Watersheds. *Environmental Science & Technology*, *45*(19), 8225–8232. https://doi.org/10.1021/es200779e

Kloiber, S. M. (2006). Estimating Nonpoint Source Pollution for the Twin Cities Metropolitan Area Using Landscape Variables. *Water, Air, and Soil Pollution*, *172*(1–4), 313–335. https://doi.org/10.1007/s11270-006-9083-4

Knight, J. F., Rampi, L. P., & Host, T. K. (2017). *2015 Twin Cities Metropolitan Area Urban Tree Canopy Assessment* [dataset]. University Digital Conservancy. https://doi.org/10.13020/D6C016

Lowe, E. C., Steven, R., Morris, R. L., Parris, K. M., Aguiar, A. C., Webb, C. E., Bugnot, A. B., Dafforn, K. A., Connolly, R. M., & Mayer Pinto, M. (2022). Supporting urban ecosystem services across terrestrial, marine and freshwater realms. *Science of The Total Environment*, *817*, 152689. https://doi.org/10.1016/j.scitotenv.2021.152689

Marek-Sparts, M. (2023). *Twin Cities Metro Area Road Surface Area, 2022* [dataset]. https://doi.org/10.13020/6a0a-3f38

McDonnell, M. J., Pickett, S. T. A., Groffman, P., Bohlen, P., Pouyat, R., Zipperer, W. C., Parmelee, R. W., Carreiro, M. M., & Medley, K. (1997). Ecosystem processes along an urban to rural gradient. *Urban Ecosystems*, *1*, 21–36. https://doi.org/10.1023/A:1014359024275

Miguntanna, N. P., Liu, A., Egodawatta, P., & Goonetilleke, A. (2013). Characterizing nutrients wash-off for effective urban stormwater treatment design. *Journal of Environmental Management*, *120*, 61–67. https://doi.org/10.1016/j.jenvman.2013.02.027

MRCC Collaborative. (2018). *Metro Regional Centerlines Collaborative Local Centerlines.* [dataset]. Metropolitan Council, Minnesota Geospatial Commons, St. Paul, MN.

R Core Team. (2021). *R: A language and environment for statistical computing* (Version 4.1.2) [R]. R Foundation for Statistical Computing. https://www.R-project.org/

Palecki, M., Durre, I., & Lawrimore, J. (2021). *U.S. Climate Normals 2020: U.S. Hourly Climate Normals (1991-2020) [U of M St Paul, MN US station, Summary of monthly normals]. NOAA National Centers for Environmental Information* (gov. noaa.ncdc:C01620) [dataset]. https://www.ncei.noaa.gov/access/search/data-search/

Selbig, W. R. (2016). Evaluation of leaf removal as a means to reduce nutrient concentrations and loads in urban stormwater. *Science of The Total Environment*, *571*, 124–133. https://doi.org/10.1016/j.scitotenv.2016.07.003

Simpson, I. M., Winston, R. J., & Brooker, M. R. (2022). Effects of land use, climate, and imperviousness on urban stormwater quality: A meta-analysis. *Science of The Total Environment*, *809*, 152206. https://doi.org/10.1016/j.scitotenv.2021.152206

Sorenson, J. R. (2013). Potential Reductions of Street Solids and Phosphorus in Urban Watersheds from Street Cleaning, Cambridge, Massachusetts, 2009–11. *U.S. Geological Survey Scientific Investigations Report 2012–5292*. http://pubs.usgs.gov/sir/2012/5292/.

Stets, E. G., Sprague, L. A., Oelsner, G. P., Johnson, H. M., Murphy, J. C., Ryberg, K., Vecchia, A. V., Zuellig, R. E., Falcone, J. A., & Riskin, M. L. (2020). Landscape Drivers of Dynamic Change in Water Quality of U.S. Rivers. *Environmental Science & Technology*, *54*(7), 4336–4343. https://doi.org/10.1021/acs.est.9b05344

Timmons, D. R., Holt, R. F., & Latterell, J. J. (1970). Leaching of Crop Residues as a Source of Nutrients in Surface Runoff Water. *Water Resources Research*, *6*(5), 1367–1375. https://doi.org/10.1029/WR006i005p01367

Topp, S. N., Pavelsky, T. M., Stanley, E. H., Yang, X., Griffin, C. G., & Ross, M. R. V. (2021). Multi-decadal improvement in US Lake water clarity. *Environmental Research Letters*, *16*(5), 055025. https://doi.org/10.1088/1748-9326/abf002

Walsh, C. J., Roy, A. H., Feminella, J. W., Cottingham, P. D., Groffman, P. M., & Ii, R. P. M. (2005). The urban stream syndrome: Current knowledge and the search for a cure. *Journal of the North American Benthological Society*, *24*(3).

Yang, Y. Y., & Toor, G. S. (2016). δ15N and δ18O Reveal the Sources of Nitrate-Nitrogen in Urban Residential Stormwater Runoff. *Environmental Science and Technology*, *50*(6), 2881–2889. https://doi.org/10.1021/acs.est.5b05353

Yang, Y.-Y., & Lusk, M. G. (2018). Nutrients in Urban Stormwater Runoff: Current State of the Science and Potential Mitigation Options. *Current Pollution Reports*, *4*(2), 112–127. https://doi.org/10.1007/s40726-018-0087-7

Appendix 1: Chapter 2 Supplemental Materials

Table S2.1. Study site physical attributes and key sediment properties.

				Site properties						Sediment properties			
	Site ID	mo.	yr.	Age (years)	Size (ac)	Max depth (ft)	Site DO (mg/L)	Site temp (C)	Anoxic factor	OM %	C:N	C:P	Total-P (ug/L)
Ponds	Alam	7	2022	>70	2.89	7.4	0.04	16.8	0.78 (5)	20.1	18.9	231.8	1303.0
	Almq	8	2022	>70	9.36	5.8	3.68	23.2	0.00 (1)	17.0	10.3	142.1	1383.6
	BizN	8	2021	30	0.46	11.5	0.08	21.4	0.01 (4)	25.7	17.6	226.3	1534.7
	BizW	7	2021	30	0.38	13.0	3.81	25.8	0.01 (2)	22.9	25.5	254.0	1474.0
	BrOk	8	2022	>70	15.50	8.9	0.33	20.1	--	24.7	13.1	60.2	6182.4
	CentPrk	7	2021	>70	0.27	0.8	0.12	24.1	1.00 (1)	14.9	16.6	189.4	763.0
	Char	7	2022	41	2.29	4.8	0.15	22.0	0.63 (3)	16.7	14.3	252.6	952.0
	HrMr	8	2021	20	0.16	7.9	0.02	21.2	0.26 (3)	31.2	47.4	360.4	1249.1
	Larp	7	2021	3	0.16	4.9	0.21	22.3	0.21 (1)	17.6	32.9	143.5	1181.5
	MryInd	7	2021	3	0.60	4.9	0.23	24.4	0.52 (2)	7.2	26.9	87.0	888.7
	PnOak	8	2021	1	0.37	1.0	10.57	24.2	0.00 (1)	1.1	14.8	17.2	434.8
	ResCircE	7	2021	12	0.02	2.5	0.09	20.9	1.00 (1)	29.0	26.6	326.2	1336.1
	ResCircW	7	2021	12	0.04	2.5	0.09	20.9	1.00 (1)	10.0	15.2	170.4	674.1
	ResWds	8	2021	4	0.04	1.5	13.4	29.8	0.00 (1)	7.6	18.0	123.4	718.1
	SemNw	7	2021	1	0.15	2.5	7.47	18.8	0.00 (1)	3.4	20.2	19.6	685.3
	SemOld	7	2021	30	0.23	1.6	0.12	18.8	0.10 (1)	10.6	26.3	66.8	723.0
	TRckN	7	2022	5	0.20	2.5	0.31	24.9	0.00 (1)	4.4	24.1	144.4	516.8
	TRckS	8	2021	5	0.33	5.6	0.73	22.8	0.01 (3)	9.7	17.6	132.5	1001.8
	VonHan	8	2022	30	0.74	9.8	0.03	16.6	0.19 (1)	7.6	21.9	169.7	705.0
Lakes	Como	6	2021	>70	68.00	15.0	0.01	18.1	0.40 (7)	29.7	18.9	128.0	3425.7
	Elmo	9	2022	>70	256.82	140.0	0.25	5.6	0.50 (1)	16.4	21.1	470.8	759.7
	Joha	8	2022	>70	197.51	43.0	0.0	9.3	0.34 (1)	29.6	13.1	285.1	1431.9
	Jose	8	2022	>70	105.33	44.0	0.0	10.7	0.21 (1)	50.0	15.2	365.5	1774.8
	Sqr	9	2022	>70	203.05	68.0	0.0	7.4	0.32 (10)	24.0	12.1	128.2	2434.5

Sampling month (mo.) and year (yr.)
Age = estimated site age in 2022; DO = bottom water dissolved oxygen at the time of sampling; Site temp = bottom water temperature at the time of sampling; OM = organic matter; C = carbon; N = nitrogen; P = phosphorus; Anoxic factor = index from 0 – 1 (number of monitoring years that inform calculations) with high values indicating more frequent sediment anoxia.

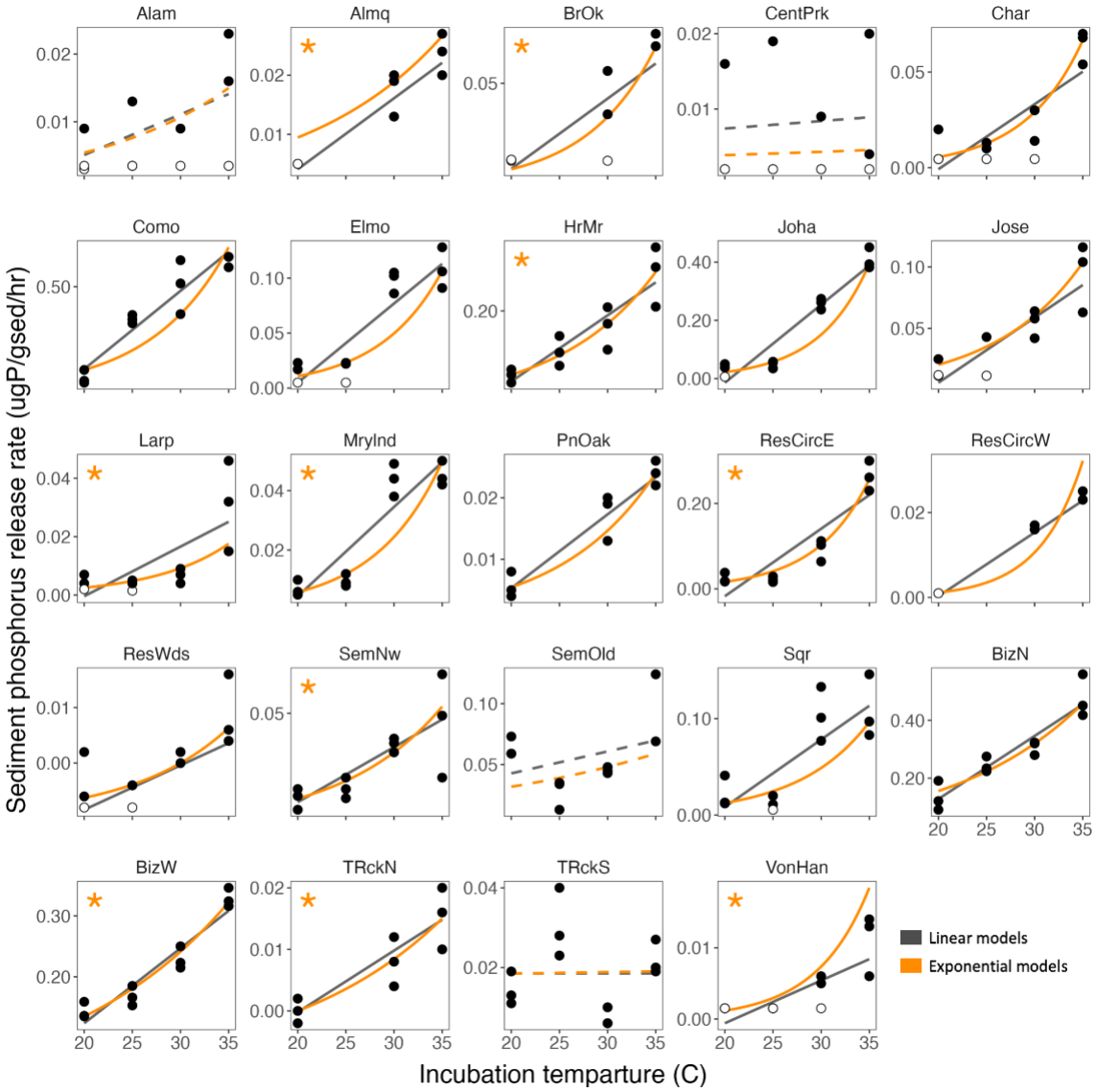

Figure S2.1. Sediment phosphorus release rates vs incubation temperature
Sediment phosphorus (P) release rates measured at the conclusion of incubations (72 hours or 120 hours) vs. incubation temperature for each study site. Each point represents a bottle replicate. Open symbols indicate concentrations below the detection limit. Black lines indicate linear models, orange lines indicate exponential models. Exponential models fit using ATS. Solid lines indicate a significant relationship ($p < 0.05$); dotted lines indicate insignificant relationship ($p > 0.05$). Asterisks indicate sites where the adj-R^2 of the exponential model was greater than the adj-R^2 of the linear model.

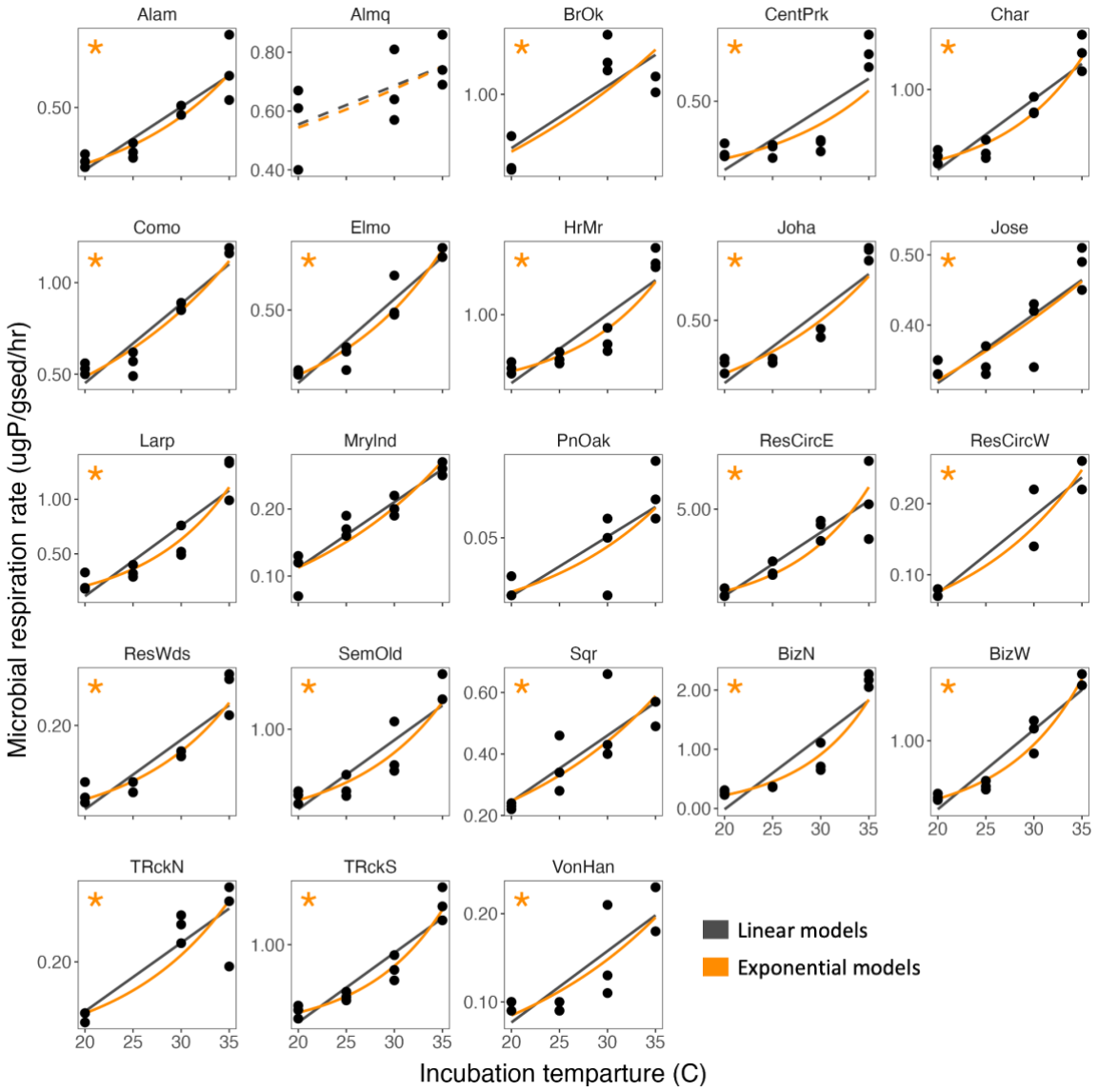

Figure S2.2. Microbial respiration rates vs incubation temperature
Microbial respiration rates, measured as the accumulation of CO_2 and CH_4 at the conclusion of incubations (72 hours or 120 hours), vs. incubation temperature for each study site. Each point represents a bottle replicate. Black lines indicate linear models, orange lines indicate exponential models. Solid lines indicate a significant relationship ($p < 0.05$); dotted lines indicate insignificant relationship ($p > 0.05$). Asterisks indicate sites where the adj-R^2 of the exponential model was greater than the adj-R^2 of the linear model.

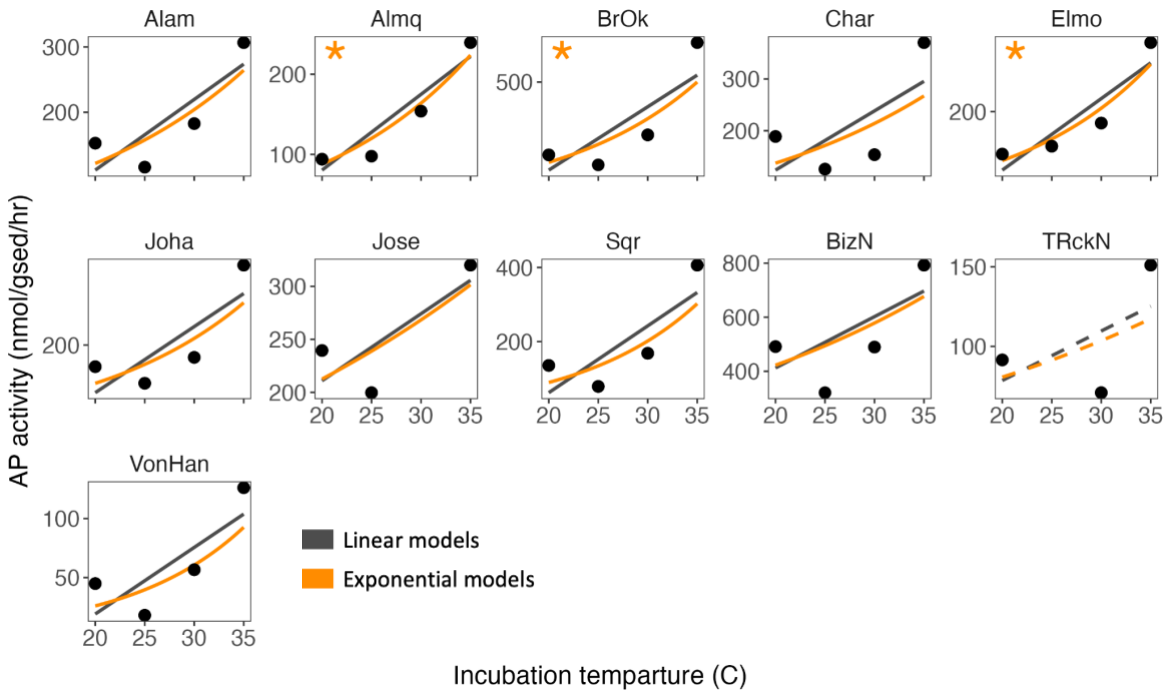

Figure S2.3. Acid phosphatase activity vs incubation temperature

Acid phosphatase (AP) activity, measured in enzyme activity assays, vs. incubation temperature for each study site. Solid lines indicate a significant relationship ($p < 0.05$); dotted lines indicate insignificant relationship ($p > 0.05$). Asterisks indicate sites where the adj-R^2 of the exponential model was greater than the adj-R^2 of the linear model.

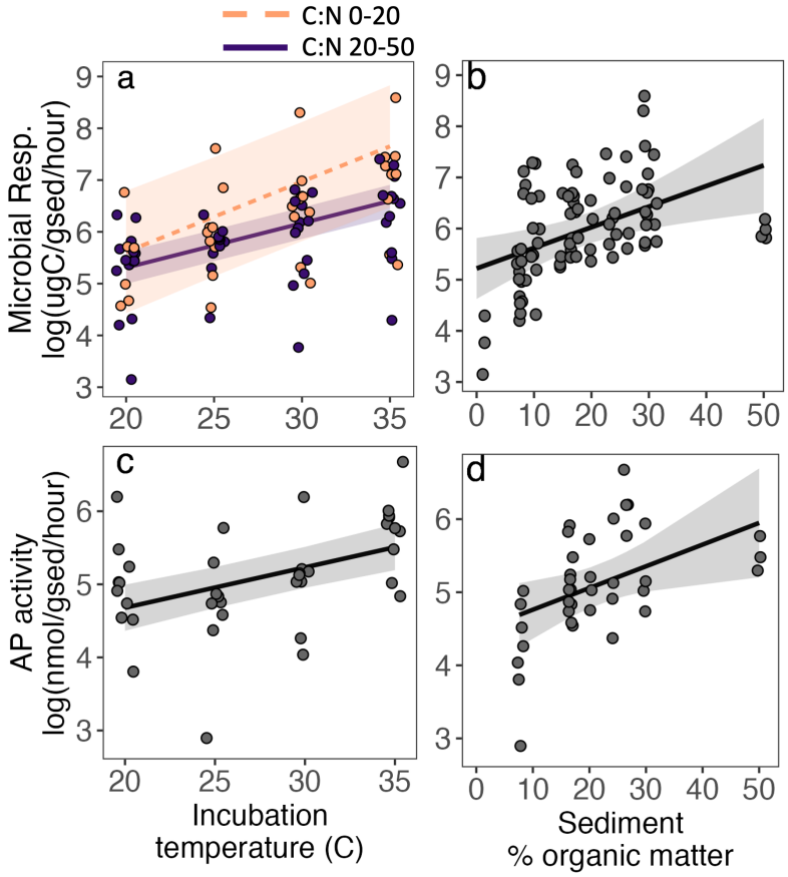

Figure S2.4. Drivers of microbial respiration rates and phosphatase enzyme activity
Sediment microbial respiration rates (a, b) and acid phosphatase activities (c, d) vs. each of the significant predictors ($p < 0.05$) that appeared in the optimum multivariate mixed-effects models. Panel (a) includes the significant interaction between incubation temperature and sediment C:N ratio, which was modeled as a continuous variable but is binned for visualization. Shading represents the 95% confidence interval. Models included observations from all sites (i.e., lakes and ponds) with site as a random intercept. Model output can be viewed in the main text in table 2.2.

Appendix 2: Chapter 3 Supplemental Materials

Table S3.1. Key site and sample properties.

Site	Site type	Surface area ha	Sample date	Sample year	Sample location	Sample depth cm	Mix. Reg	Dom. Plant	Ave TP µg/L	Cond. µS/cm	Est. Cl^- µg/L	DO µg/L	NO_3^- µg/L	MV mod.
Ala	pond	1.2	Sep-5	2019	Edge	30	Strat	Dckwd	241	169	36.5	3700	*1.97*	y
					Center	225				550	168.3	300	*1.97*	y
			Oct-6	2022	Center	225				332	92.9	180	*3.08*	y
Almq	pond	3.8	Aug-22	2022	Center	177	Poly	Phyt	157	230	57.6	3680	10.71	y
Arrow	pond	0.1	Oct-6	2022	Center	175	Poly	Mix	100	294	79.7	5400	*5.23*	y
Bell	pond	0.04	Oct-6	2019	Edge	30	Poly	Phyt	66	308	84.6	9900	1530.80	
					Center	94				317	87.7	6800	4191.30	
			Oct-5	2022	Center	94		Mix	168	217	53.1	650	*4.94*	y
BlkHwk	lake	18.8	Aug-22	2022	Center	372	Poly	Mix	31	413	120.9	960	*4.24*	y
BrOak	lake	6.3	Aug-22	2022	Center	271	Poly	Macr	103	1463	484.2	330	*4.29*	y
Carlson	lake	5.3	Aug-22	2022	Center	610	Strat	Mix	26	405	118.1	390	*3.27*	y
ClevRose	pond	0.9	Sep-5	2019	Edge	30	Poly	Mix	144	342	96.3	2800	11.15	y
					Center	152				342	96.3	3500	*4.72*	y
ColPk	pond	0.6	Oct-4	2022	Center	120	Poly	Mix	135	768	243.7	6300	609.52	y
Elmo	lake	103.9	Sep-12	2022	Center	4267	Strat	Phyt	23	430	126.8	0	--	y
Fish	lake	12.3	Aug-22	2022	Center	1030	Strat	Mix	41	591	182.5	220	*7.46*	y
GrpBim	pond	1.2	Sep-22	2019	Edge	30	Poly	Phyt	78	351	99.4	7300	31.26	y
					Center	170				350	99.1	6400	33.01	y
			Oct-4	2022	Center	170				1496	495.6	9300	*1.99*	y
HarMar	pond	0.1	Sep-22	2019	Edge	30	Strat	Macr	59	228	56.9	5600	14.51	y
					Center	240				30600	10565.6	500	17.10	y
Hay	lake	9.3	Aug-22	2022	Center	302	Poly	Mix	25	381	109.8	1120	*3.17*	y
HmDepN	pond	0.2	Oct-6	2019	Edge	30	Strat	Phyt	52	744	235.4	8800	50.07	y
					Center	240				6630	2272.0	8800	31.19	y
Joh	lake	85.8	Aug-29	2022	Center	1311	Strat	Phyt	26	1144.5	374.0	0	0.00	y
Jose	lake	47.0	Aug-29	2022	Center	1341	Strat	Phyt	91	559.3	171.5	0	0.00	y
LeMay	lake	14.8	Aug-22	2022	Center	442	Strat	Mix	29	942	303.9	170	6.63	y
MarStps	pond	0.1	Sep-22	2019	Edge	30	Strat	Mix	71	153	30.9	2300	20.91	y
					Center	220				370	106.0	100	*0.59*	y
			Oct-4	2022	Center	220				241	61.4	1110	11.63	y
North	lake	8.3	Aug-22	2022	Center	415	Poly	Phyt	35	1047	340.3	360	*7.72*	y
SemNew	pond	0.1	Oct-5	2022	Center	60	Poly	Phyt	--	348	98.4	2130	11.12	
Square	lake	82.2	Sep-12	2022	Center	2073	Strat	Phyt	12	611.9	189.7	0	--	y
StBizW	pond	0.2	Oct-6	2019	Edge	30	Strat	Phyt	52	545	166.6	8300	25.48	y
					Center	396				10210	3510.7	400	*9.77*	y
			Oct-5	2022	Center	396				6560	2247.8	140	*9.77*	y
VillaPk	pond	0.8	Oct-6	2022	Center	75	Poly	Mix	--	1157	378.3	--	38.07	
WmSt	pond	0.3	Sep-22	2019	Edge	30	Strat	Dckwd	342	292	79.0	2200	0.00	y
					Center	225				770	244.4	100	0.00	y

"Dom. Plant" indicates rough estimates of dominant plant type: Dckwd = duckweed or other floating macrophytes, Phyt = algae and phytoplankton, Mix = no clear dominant type and often a mix of macrophytes and duckweed or algae, Macr = submerged macrophytes. Average total phosphorus concentrations (Ave TP) is a site-level variable calculated from monitoring records. The remaining variables reflect conditions as inferred from sampling of water overlying sediments at the time of sediment sampling. Surface water values are paired with edge sediments and bottom water values with center

sediments. Specific conductance (Cond.) was used to estimate chloride concentrations (Est. Cl^-). DO indicates dissolved oxygen. NO_3^- indicates nitrate concentrations, and any value below 10 ug/L (italicized) is below detection. A "y" in the "MV mod." column indicates those observations that were included in multivariate models.

Table S3.2. Summary of total denitrification rates, rates of N_2O production, and N_2O yields on a per mass basis

Amend-ments	Variable	Sample location	n	Mean	Median	Stnd Dev	Min	Max
C+N	Total-DeN	All	39	1.21	0.55	2.02	0.07	8.46
		Center	30	1.31	0.48	2.24	0.07	8.46
		Edge	9	0.88	0.57	0.99	0.11	3.39
C+N	N2O-rate	All	31	0.35	0.15	0.70	0.00	3.74
		Center	22	0.34	0.13	0.78	0.00	3.74
		Edge	9	0.36	0.16	0.51	0.05	1.66
C+N	N2O-yield	All	31	0.33	0.32	0.23	0.02	0.79
		Center	22	0.31	0.28	0.26	0.02	0.79
		Edge	9	0.38	0.38	0.14	0.18	0.60
None	Total-DeN	All	39	0.030	0.000	0.140	0.000	0.880
		Center	30	0.030	0.000	0.160	0.000	0.880
		Edge	9	0.030	0.000	0.080	0.000	0.240
None	N2O-rate	All	31	0.000	0.000	0.010	0.000	0.030
		Center	22	0.000	0.000	0.000	0.000	0.000
		Edge	9	0.000	0.000	0.010	0.000	0.030
None	N2O-yield	All	31	0.02	0.00	0.09	0.00	0.50
		Center	22	0.02	0.00	0.11	0.00	0.50
		Edge	9	0.02	0.00	0.05	0.00	0.14

Total denitrification rates (Total-DeN) and N_2O rates (N_2O-rate) are expressed on a per mass basis (µg N g dry $sediment^{-1}$ hr^{-1}). N_2O yields (N_2O-yield) are the proportion of Total-DeN products released as N_2O, calculated as N_2O-rate divided by Total-DeN. Summaries of amended (C+N) and unamended incubations are shown. Summaries were performed on all observations as well as each sample location: sediments collected from the center of each site and sediments collected along the edge (≤ 30 cm deep).

Appendix 3: Chapter 4 Supplemental Materials

Table S4.1. Minneapolis-St. Paul metropolitan area stormwater monitoring stations (or "watersheds") that meet selection criteria for inclusion in total phosphorus (TP) and total nitrogen (TN) concentration and yield analyses, ordered by fractional street canopy cover.

	TP concentration			TN concentration			TN yield			TN yield			Frac street					
Watershed	Sum-mer	Fall+ Spring	Snow-free	Sum-mer	Fall+ Spring	Snow-free	Sum-mer	Fall+ Spring	Snow-free	Sum-mer	Fall+ Spring	Snow-free	canopy cover	Area (km^2)	Devel. Age (years)	Road density (km/km^2)	Frac Imp.	Frac Res.
Dickerman Park	x	x	x	x	x	x	x	x	x	x	x	x	0.0	0.00	60	6.7	0.7	0.0
Franklin	x	x	x	x	x	x	x	x	x	x	x	x	0.2	0.00	89	19.3	0.7	0.0
MLK	x	x	x	x	x	x	x	x	x	x	x	x	0.7	0.00	82	19.6	0.7	0.0
MS 1	x	x	x	x	x	x			x			x	4.6	5.30	21	8.3	0.4	0.2
Site 9 Lyndale	x	x	x	x	x	x							4.7	0.10	61	7.2	0.8	0.1
Hampden	x	x	x	x	x	x	x	x	x	x	x	x	6.2	0.00	104	28.0	0.5	0.7
Site 7 Park	x	x	x	x	x	x							6.9	0.10	89	26.0	0.7	0.4
Winter Inf	x			x									8.0	0.10	88	9.2	0.7	0.1
24th/Elm N	x			x									8.1	0.00	59	11.5	0.8	0.0
24th/Elm S.	x			x									8.4	0.00	48	8.0	0.7	0.0
Powers Trees		x	x		x	x							8.5	0.10	29	11.8	0.3	1.0
Wakefield L. outfall	x						x						9.0	0.10	44	14.8	0.4	0.4
Hidden Falls	x	x	x	x	x	x							11.3	1.00	63	2.7	0.7	0.1
MS 2	x	x	x	x	x	x			x			x	11.3	29.80	26	9.7	0.4	0.6
Greeley St.	x	x	x										12.5	0.10	59	15.7	0.5	0.8
Hillcrest Knoll	x			x									15.4	0.20	70	22.1	0.5	0.6
Parkers L.	x	x	x	x	x	x							15.8	0.80	38	7.9	0.5	0.5
William St.		x	x		x	x							16.0	0.20	53	8.9	0.4	0.9
St Albans	x	x	x	x	x	x	x	x	x	x	x	x	16.2	0.10	92	26.0	0.6	0.7
Trout Brook E.	x	x	x	x	x	x	x	x	x	x	x	x	16.3	3.30	72	14.6	0.5	0.6
Trout Brook Outlet	x	x	x	x	x	x	x	x	x	x	x	x	17.0	31.70	82	13.3	0.5	0.5
St. Anthony Park	x	x	x	x	x	x	x	x	x	x	x	x	17.3	13.80	90	12.9	0.6	0.3
Colby West Trib.	x			x									18.5	1.60	36	10.4	0.3	0.9
Maryland Pond	x	x	x	x	x	x							18.8	0.10	99	23.1	0.5	0.6
St Paul Park	x			x									19.1	8.00	60	5.2	0.5	0.3
Site 4 PP	x	x	x	x	x	x							21.0	11.20	102	22.0	0.6	0.6
Trout Brook W.	x	x	x	x	x	x	x	x	x	x	x	x	21.1	21.00	78	11.9	0.4	0.6
Central Ravine		x	x		x	x							21.5	14.70	36	8.6	0.4	0.6
Site 10 SA	x	x	x	x	x	x							21.8	3.40	65	12.3	0.4	0.6
Upper Villa Inlet	x			x			x	x	x	x			22.0	1.30	65	6.8	0.4	0.7
B-Dale Outlet	x	x	x	x	x	x	x	x	x	x	x	x	22.1	1.30	65	6.8	0.4	0.7
Como 3	x	x	x	x	x	x	x	x	x	x	x	x	22.2	2.10	101	13.3	0.4	0.3
Site 6 UMN	x	x	x	x	x	x							22.6	3.10	91	13.1	0.6	0.3
Phalen Creek	x	x	x	x	x	x	x	x	x	x	x	x	23.1	5.80	107	20.5	0.5	0.6
Site 11 CHF	x	x	x	x	x	x							23.3	8.10	68	10.8	0.6	0.4
East Kittsondale	x	x	x	x	x	x	x	x	x	x	x	x	25.2	4.50	99	21.9	0.5	0.7
Golf Course P. inlet	x	x	x	x	x	x							29.9	0.60	86	18.2	0.4	0.8
Site 1 NE	x	x	x	x	x	x							30.2	8.50	79	14.9	0.5	0.5
Arlington-Hamline	x	x	x	x	x	x	x	x	x	x	x	x	31.3	0.20	96	18.7	0.4	0.8
Como 7	x	x	x	x	x	x							31.4	1.20	90	18.2	0.4	0.7
Mooney Lake 2	x	x	x	x	x	x							31.8	0.60	46	9.9	0.3	0.9
Site 6 Aldrich	x	x	x	x	x	x							33.2	0.00	104	17.4	0.6	1.0
Newport	x	x	x	x	x	x							33.2	5.80	38	3.6	0.4	0.4
Beacon	x	x	x	x	x	x	x	x	x	x	x	x	35.0	0.60	106	22.9	0.5	0.9
Parkers Lake S.	x	x	x	x	x	x							36.1	1.00	55	8.4	0.3	0.9
Site 8a Pershing	x	x	x	x	x	x							67.4	0.00	47	--	0.3	0.0
Victoria							x			x			28.5	0.10	103	26.4	0.4	1.0
No. | Mean	43	38	38	41	37	37	18	16	18	17	15	17	19.2	4.1	71.1	14.1	0.5	0.5
Standard deviation													12.1	7.3	24.5	6.6	0.1	0.3
Minimum													0.0	0.0	21.0	2.7	0.3	0.0
Maximum													67.0	32.0	107.0	28.0	0.8	1.0

TP = Total phosphorus; TN = Total nitrogen; Frac = Fractional; Imp = Impervious surface; Res = Residential; Devel Age = Development age from 2024

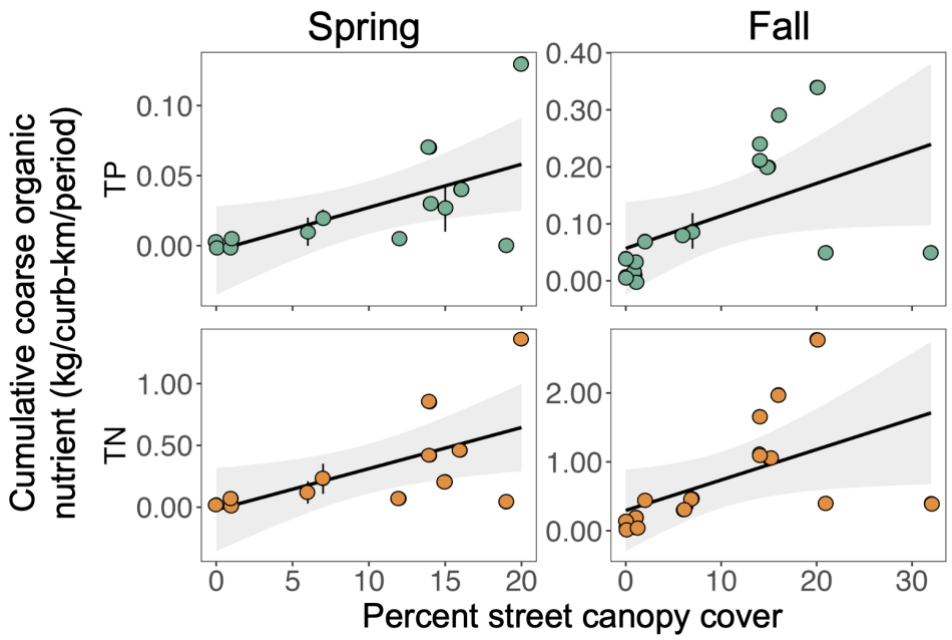

Figure S4.1. Typical street sweeping models.
Models used to estimate the mass of litterfall nutrients removed from streets during typical street sweeping based on the average percent canopy cover over the street for a given watershed. The average mass of TP and TN in the coarse litter fraction were recovered during spring and fall street sweeping events selected to reflect biannual street sweeping that typically occurs in each study region (Spring: March 1 - April 30; Fall: October 1 - November 30). Only infrequently swept routes were included (sweeping frequency ≥ 18 days). Grey shading indicates the 95% confidence interval. Error bars represent standard error around the mean, calculated when data from multiple years were available. Model output is included in Table S4.2.

Table S4.2. Model output for typical sweeping models.

Response Var.	Period	Intercept	Slope	Adj-R^2	p-value
TP	Spring	-0.004	0.003	0.32	0.03
TP	Fall	0.057	0.006	0.19	0.06
TN	Spring	-0.021	0.033	0.33	0.02
TN	Fall	0.294	0.044	0.22	0.05

Response variables (Var.) are total phosphorus (TP) and total nitrogen (TN) in kg/curb-km. Models are simple linear regressions relating the average mass of TP and TN in the coarse litter fraction to the average percent canopy cover over the street for each route. Models can be viewed in Figure S4.1.

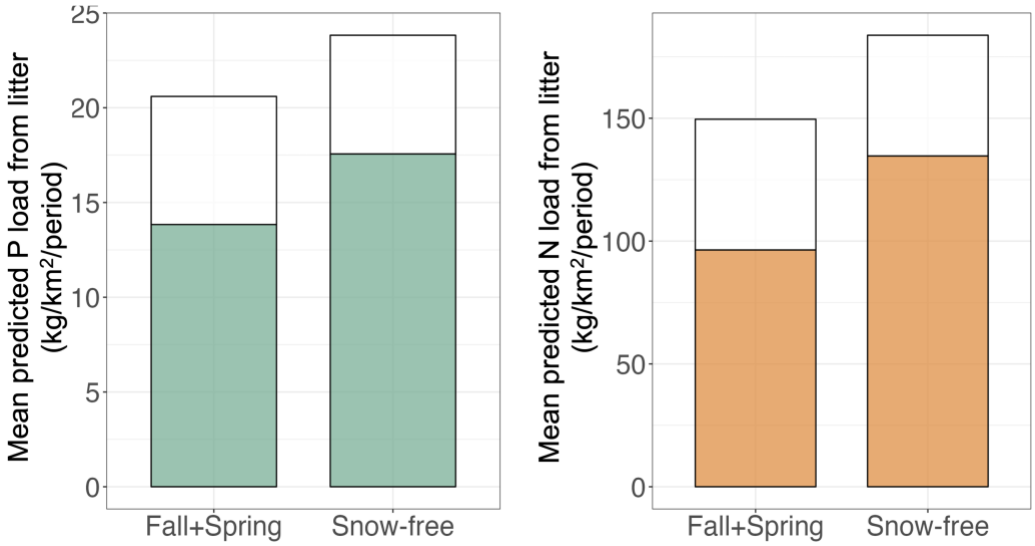

Figure S4.2. Reductions in litter-associated nutrient load due to typical spring and fall street sweeping.
The full height of the bar represents the total predicted TP and TN from litterfall, averaged for all watersheds. The bottom portion of each bar represents average nutrients that remain after typical street sweeping.

Prediction uncertainties

Predicted litterfall N and P inputs were derived from models built using street sweeping data. We assume that sweeping events were sufficiently frequent to intercept litterfall nutrients that typically enter stormwater. Here we consider methodological limitations that could have affected our results, namely whether litterfall was lost to stormwater prior to being captured by sweeping, leading to an underprediction of litterfall inputs, and whether sweepers captured litterfall that would not typically enter stormwater, leading to an overprediction of litterfall inputs.

It is most likely that we are underestimating litterfall N and P inputs to stormwater due to incomplete capture of litterfall nutrients. The average sweeping frequency for qualifying routes was 12 days, with the highest frequency being 7 days (Table 2). During the years when street sweeping data were collected, over 85% of measurable precipitation events (>0.01 inches) in MSP occurred within 7 days of a prior rain event, and over 95% of events occurred within 12 days. On average, there were about three days between precipitation events for the summer, fall+spring, and snow-free periods (results not shown, data source: Minnesota Department of Natural Resources). Rain events undoubtedly facilitated nutrient and litter loss to stormwater

between sweeping intervals, lowering the amount of measured coarse litterfall N and P in our models, and resulting in underestimating litterfall N and P inputs. Given the rapid loss of P in street gutters even within 24 hours, we may be especially underestimating litterfall P (Hobbie et al. 2013).

Our predictions of litterfall inputs are unlikely to be overestimates, which could result if sweepers and our subsequent models captured litterfall typically removed from streets prior to interacting with stormwater. We accounted for the primary way litterfall is removed from streets, municipal street sweeping in the spring and fall. Litterfall could also be removed from streets via wind action, snow removal, clearing of street gutters by individuals or property managers, or maintenance of stormwater infrastructure (e.g., clearing catch basins). For each, we expect no major effect on our findings: the frequency of sweeping events in our study would likely still allow for typical wind removal, a substantial amount of litterfall has been observed to remain in streets throughout the winter despite active snow removal, and private or municipal maintenance of stormwater infrastructure is often infrequent and irregular.

We finally considered whether our assumption of a continued linear relationship when extrapolating beyond the highest street canopy cover represented in our models could lead to overpredicting litterfall inputs. Recent work using the same MSP street sweeping dataset observed saturating relationships between street canopy cover and the total mass of P and N in swept material (Hobbie et al., 2023). The discrepancy between these findings and our models is likely caused by differences in data selection. The goals of our work necessitated stricter sweeping route selection criteria and a focus on the coarse litter fraction, while the Hobbie et al. (2023) work incorporates all sweeping routes and fractions. Further, the relationships in Hobbie et al. (2023) begin to saturate prior to the highest street canopy value represented in our models (~15%), which suggests that we would have seen saturation if it were present in our data. We are therefore confident that our models are sufficiently accurate to produce useful predictions of litterfall N and P inputs to streets.